

1N-39

027255

NASA Contractor Report 202336

Mechanical System Reliability and Cost Integration Using a Sequential Linear Approximation Method

Michael T. Kowal
Vanderbilt University
Nashville, Tennessee

April 1997

Prepared for
Lewis Research Center
Under Grant NAG3-1352



National Aeronautics and
Space Administration

ACKNOWLEDGEMENTS

The author wishes to express his gratitude for the technical and financial support through NASA under Grant NAG3-1352, Lewis Research Center, Dr. C. C. Chamis, Technical Advisor.

TABLE OF CONTENTS

	Page
LIST OF FIGURES.....	iv
LIST OF TABLES.....	v
Chapter	
I. MECHANICAL SYSTEM RELIABILITY AND COST INTEGRATION.....	1
Background.....	1
Research Objective.....	2
Terminology.....	2
Product Reliability Research.....	3
Product Costing and Design Research.....	6
Research Overview.....	8
II. ASSESSMENT OF MECHANICAL SYSTEM RELIABILITY MODELS.....	11
Introduction.....	11
Analytical Reliability Models.....	11
System Hazard Rates.....	15
The Uniform Failure Rate Model.....	18
Dependent and Independent Failure Modes.....	19
Limitations on the Application of Uniform Failure Rate Models to System Reliability Estimation.....	28
Implications of Analytical Reliability Methods on the Reliability-Cost Trade-Off Methodology.....	36
III. EXTENSION OF FIRST-ORDER RELIABILITY METHODS TO MECHANICAL SYSTEM DESIGN.....	39
Introduction.....	39
First-Order Reliability Method Concepts.....	40
Linking FORM, Primitive Variables, and Analytical Reliability Models.....	43
First-Order Reliability Method Modeling Strategies for Mechanical Limit States.....	46
Validation of First-Order Reliability Method Modeling Strategies.....	49
Implications of FORM for the Reliability-Cost Trade-Off Methodology.....	54

IV. PHYSICS-BASED RELIABILITY MODELING.....	56
Introduction.....	56
Review of Physics-Based Failure Rate Reliability Prediction Techniques.....	57
Linking Physics Failure Rate Methods and Traditional Reliability Techniques.....	58
Assumptions Made in Deriving Physics Failure Rate Techniques.....	64
Implications of Physics-Based Methods for the Reliability-Cost Trade-Off Methodology.....	66
V. INTEGRATED PRODUCT DESIGN: A SEQUENTIAL LINEAR APPROXIMATION METHOD.....	69
Introduction.....	69
Defining Product Cost and Reliability Trade-Off Issues.....	70
Improving Product Reliability.....	72
Product Design Using Sequential Linear Approximation.....	73
Sequential Linear Approximation-Overview.....	76
Applying the Sequential Linear Approximation Method.....	80
Implications of the Sequential Linear Approximation Methodology.....	94
VI. CONCLUSIONS AND FUTURE RESEARCH.....	96
Conclusions.....	96
Future Research.....	98
Appendices	
A. COMPENDIUM OF MECHANICAL LIMIT STATES.....	99
B. MECHANICAL LIMIT STATES USED IN FIRST-ORDER RELIABILITY MODELS.....	152
REFERENCES.....	156

LIST OF FIGURES

Figure	Page
1. Two Failure Modes with Separate Aging Mechanisms.....	21
2. Combined and Individual Failure Mode PDF's.....	24
3. Hazard Rate for Individual and System Failure When Failure Resets All Failure Modes.....	25
4. Combined and Individual Failure Mode PDF's-O(0.1) Case.....	26
5. Combined and Individual Failure Mode Hazard Rates-O(0.1) Case.....	27
6. Hazard Rate-Normal Distribution (COV=0.10).....	30
7. Hazard Rate-Normal Distribution (COV=0.20).....	31
8. Hazard Rate-Normal Distribution (COV=0.30).....	31
9. Influence of Changes in Mean on Hazard Rates.....	33
10. Bi-Modal Time to Failure Distribution.....	34
11. Bi-Modal Distribution Hazard Rate.....	35
12. Sequential Linear Approximation Method.....	80

LIST OF TABLES

Table	Page
1. Limit State Kolmogorov-Smirnov Test Results.....	51
2. Monte Carlo and FORM Failure Probability Differences.....	53
3. Pump Shaft Initial Variable Parameters.....	81
4. Pump Shaft Permissibility Matrix.....	84
5. Most Probable Point Vector Values.....	85
6. Probability of Failure Sensitivities-First Iteration Results.....	88
7. Cost Sensitivities-First Iteration Results.....	89
8. Updated Most Probable Point Vector Values.....	92
9. Updated Pump Shaft Variable Parameters.....	93

CHAPTER I

MECHANICAL SYSTEM RELIABILITY AND COST INTEGRATION

Background

The development of new products is dependent on product designs that incorporate high levels of reliability along with a design configuration that meets predetermined levels of system life-cycle costs. Additional constraints on the product include explicit and implicit performance requirements. In response to the increasing awareness of product reliability and cost, numerous techniques have been advocated as methodologies best suited to address the need for improved reliability or cost estimates. Despite the availability of diverse approaches to product reliability and cost predictions, little work on integrating product cost and performance has been done.

The separation of reliability and cost prediction methods results in no direct linkage existing between variables affecting these two dominant product attributes. Techniques linking cost and reliability would provide engineers with information on the trade-off that exists between variables affecting product performance and cost, thereby permitting a rational design approach for complex mechanical systems.

Research Objective

The objective of the research is to develop a methodology to permit manufacturing cost and reliability trade-offs in a component design.

Terminology

We now define the following terminology that will be used:

A **mechanical system** is an organization of multiple subsystems, which in turn may be composed of multiple components, so as to be capable of performing a specified physical function.

Reliability is the probability that a component will perform in a satisfactory manner for a given period of time when used under specified operating conditions.

Primitive variables are the stochastically independent variables that define the behavior of a system. The variables are not only stochastically independent, but also independent in terms of their physical properties.

A **response surface** describes the behavior of a system as a function of several primitive variables.

A **failure mode** is a physically measurable system behavior that requires the termination of system use.

A **failure mechanism** is a predictable, physical deterioration in a system which if unrepaired results in failure of the system from a specific failure mode.

Analytical reliability models predict failures based on the system time to failure distribution.

Physics-based failure rate reliability methods predict system failure rates based on a historical system failure rate modified by correction factors that consider alternative primitive variable values.

Product Reliability Research

The development of reliability assessment and prediction methods has been a recent area of investigation. The reliability techniques currently used can be traced through two distinctive historical paths. The first developmental path evolved from an examination of the failure of mechanical systems and developed analytical reliability and physics-based failure rate techniques. The second developmental path considered the problems inherent in assessing structural reliability and developed first order reliability methods. We will briefly review each of these different evolutionary processes.

The initial interest in the study of reliability was undertaken to examine the question of machine maintenance. Khintchine¹ and Palm² attempted to use methods suggested by Erlang and Palm that had focused on the problems associated with telephone trunking problems.

At the same time Lotka suggested the use of renewal theory as a means of modeling equipment replacement problems.³ Other early authors who considered using renewal theory to model equipment replacement problems were Campbell⁴ and Feller.⁵

The study of extreme value theory was initiated by Weibull^{6 7} and Gumbel.⁸ Weibull was to propose the extreme value distribution named after him, as best describing the fatigue behavior of materials.

The advent of World War II increased interest in assessing and predicting mechanical system reliability. The realization that a high percentage of military equipment was never used, due to its being unserviceable, was a major impetus to examining reliability methods.⁹ The wartime experience led the Air Force to form an *ad hoc* Group on Reliability of Electronic Equipment in 1950. In 1951 both the Navy and Army began investigating equipment reliability issues. In order to coordinate these various investigations, the Department of Defense, in 1952, established the Advisory Group on Reliability of Electronic Equipment (AGREE).¹⁰ The first report from AGREE was published in 1957, and established minimum reliability requirements, testing procedures, and suggested requiring equipment suppliers demonstrate a confidence level for equipment reliability. The report suggested using mean time between failures as the equipment reliability measure.¹¹

The result of the initial AGREE report was to begin requiring reliability assessment and engineering in military applications. More importantly, it began a ongoing investigation of reliability methods by the Department of Defense (DOD) that has resulted in periodic reassessment of procedures for prediction and evaluation of reliability. Following the introduction of the AGREE report, the DOD reissued the report as a military standard, MIL-STD-781, which has been subsequently revised.¹²

In addition, the introduction of MIL-STD-785B: Reliability Programs for Systems and Equipment, mandated the integration of reliability planning and assessment in the engineering design and development of a product.¹³ Its aim was to allow for the earlier determination and detection of reliability problems.

The desire by the DOD to develop predictive methodologies led to the creation of physics-based failure rate models that allow for component reliability predictions depending on operating and design primitive variable values. The initial effort in developing physics-based failure rate models focused on models for electronic equipment and these efforts led to the release of MIL-HDBK-217. Recently, a similar approach has been proposed for use with mechanical components, beginning in 1990 with the release of the Handbook of Reliability Prediction Procedures for Mechanical Equipment.¹⁴

In the development of structural reliability methods, the initial interest focused on the development of engineering theory to accurately reflect the conditions existing in various structural elements. This initial interest in stress analysis understood that loading and strength were uncertain, but that the situation could be realistically modeled if upper and lower limits on load and strength respectively were considered.¹⁵ Given this approach to reliability, the engineering community strove to develop a set of design codes that set out the requirements for different structural designs, with the inclusion of appropriate safety factors to accommodate the diverse sources of uncertainty in the design.

Two problems hindered the development of probabilistic reliability techniques. First, the error in the mathematical models of engineering phenomenon is unknown. Second, with a system subjected to a wide variety of possible failure modes, using statistical methods to predict its reliability seemed infeasible.¹⁶

In 1967 Cornell proposed the second-moment approach to reliability assessment.¹⁷ Lind then proposed a way of relating the safety index suggested by Cornell to regular safety factors suggested in most building codes.¹⁸

Immediately following this work, the problem of invariance of the reliability index was uncovered by both Ditlevsen¹⁹ and Lind.²⁰ The invariance problem was finally resolved by Hasofer and Lind.²¹

The solution of the reliability problem using first-order methods for non-linear limit states is presented by Rackwitz and Fiessler.²² The authors present an algorithm to update estimates of the most probable point using a gradient search approach.

The determination of system reliability estimates for systems with 2 limit states was presented by Ditlevsen.²³ The case involving numerous limit states was solved by deriving upper and lower bounds by Cruse et al.²⁴

Thus, by the 1990's the underlying reliability concepts had been established for mechanical systems using analytical and physics-based failure rate reliability methods, and for structural systems using probabilistic methods. The extension of probabilistic methods to mechanical systems remained to be examined.

Product Costing and Design Research

Methods to determine product configuration and cost have evolved recently into several divergent areas. The design and costing methods currently in use can be identified as belonging to three distinctive approaches, namely design-based, time-based, and cost-based methods. All three methods have been recent areas of research interest.

In 1983 Boothroyd presented a report entitled "Design for Assembly"²⁵ which presented a method to evaluate competing product designs with respect to ease of assembly. The methodology focuses on reducing the number of parts used in a

component, with emphasis on simple assembly methods. An alternative approach to assessing assembly ease of design was proposed by Hitachi in 1983.²⁶ The Hitachi approach, known as 'Assemblability Evaluation Method', has been favored owing to its lower level of complexity as compared to the Boothroyd approach. Both methods focus exclusively on product design with respect to assembly, and do not consider product cost in assessing a proposed design configuration.

Time-based methods focus on reducing the product development time through the application of techniques such as concurrent engineering. The idea underlying concurrent engineering is that the majority of the product cost is determined in the concept stage of product development, and that sequential development processes increase product development time.²⁷ Time-based methods view time reduction as critical to the success of a product in the marketplace.²⁸

Cost-based methods, such as target costing, were developed to examine ways of incorporating final product cost into the product development process.²⁹ Such methods do not consider the impact of product performance on cost, but rather they seek to allocate product manufacturing costs to each assembly or component.

By the 1990's several competing methodologies exist to manage product development. The integration of product cost and reliability into a comprehensive and analytically rigorous framework remained to be examined.

Research Overview

In order to develop a design methodology that permits cost and reliability trade-offs, we must first examine existing reliability estimation techniques. In chapter 2 we review analytical reliability models as they are presently being used for mechanical systems. We examine the statistical concepts that form the foundations of this approach, and consider the limitations and shortcomings inherent in applying analytical reliability models. We shall demonstrate that four limitations of analytical reliability models preclude their use in assessing the impact of design changes on component reliability. First, analytical reliability methods do not consider the physical variables that define component behavior. We shall show that the absence of physical variables in analytical methods prevents assessment of changes in variables values on reliability. Second, analytical methods do not consider component operating conditions. Third, analytical methods are only applicable in the estimation of the reliability of systems that have attained a steady-state failure rate. We will demonstrate that many mechanical systems operate in a transient failure rate regime, for which the application of reliability estimates based on analytical methods is inappropriate. Fourth, analytical methods do not consider the impact of variance reduction on component reliability. We will examine how the absence of variance information in analytical methods prevents their use in assessing primitive variable variance changes on reliability.

Chapter 3 examines the extension of first-order reliability methods (FORM) to mechanical system design. Currently, the majority of applications of FORM have been in structural problems, with few mechanical phenomena being analyzed. We will

demonstrate methods to model specific mechanical limit states, and determine the validity of alternative limit state modeling strategies. We will show how the use of FORM provides one of two major elements of the proposed design paradigm by providing a means of calculating the reliability sensitivity to changes in the distributional parameters of the primitive variables. We will detailed how FORM techniques are a less restrictive means of assessing component reliability.

In chapter 4 we will examine the physics-based failure rate reliability estimation method. We will demonstrate that although physics-based methods provide a means of assessing the impact of changes in the primitive variable means, they have two major limitations. First, we will show that physics-based methods are only applicable for changes in the mean value of a primitive variable. Second, physics-based methods suffer from a large degree of uncertainty in their estimated based failure rates due to the small sample sizes used. We will demonstrate that these two limitations preclude the application of physics-based methods in the reliability-cost trade-off methodology.

Chapter 5 presents the proposed sequential linear approximation method for assessing component design. We will show how the proposed methodology incorporates two elements to assess component design, reliability and cost. The first principle element of the methodology is the utilization of FORM results to determine the reliability sensitivities to changes in primitive variable distributional parameters. The second element is a means of determining the manufacturing cost sensitivities to changes in the primitive variable distributional parameters. The method will demonstrate that the sensitivity of the cost to design changes is required to determine how the design should be modified. The

total product cost is not required to assess the component design. We will demonstrate how these two elements can be combined into an overall methodology to permit reliability-cost trade-off analysis. A sequential linear approximation methodology is presented to determine the product configuration with respect to either cost or reliability. An example problem is presented to demonstrate the application of the methodology.

Chapter 6 concludes by briefly reviewing the research findings and identifies areas for further research. We will review how the proposed design methodology utilizes FORM and costing information to provide engineers with an effective means of addressing the reliability-cost trade-off problem. We conclude with some suggestions for future research.

CHAPTER II

ASSESSMENT OF MECHANICAL SYSTEM RELIABILITY MODELS

Introduction

In order to determine the appropriate method for the prediction of mechanical system reliability, we must first define the existing methodologies in use. We will begin by outlining common statistical concepts used in reliability estimation which will be referred to throughout this document. Next, alternative reliability models based on differing system component arrangements will be examined. The uniform failure rate model based on the exponential distribution will be examined. The assumptions and limitations that are inherent in the application of uniform failure rate models to reliability estimation practice are detailed. Finally, the implications of the limitations of uniform failure rate models and their application to mechanical systems is discussed.

Analytical Reliability Models

Any component subject to failure has a random time to failure, t , and the time to failure of the component has a failure probability density function, (PDF), $f(t)$, defined as

$$f(t) = P(t = t) \quad t \geq 0 \quad (2.1)$$

The failure probability density function is the probability that the component will fail at a time $t=t$. The probability that component will fail by a given time t , is the failure cumulative distribution function, (CDF), $F(t)$, and is defined as

$$F(t) = P(t \leq t) \quad t \geq 0 \quad (2.2)$$

The failure probability density and cumulative density functions are related by

$$F(t) = \int_0^t f(\tau) d\tau \quad (2.3)$$

The reliability of a component is the probability that it will continue to operate, or the probability that it will not fail by time t , or

$$R(t) = P(t > t) = 1 - F(t) \quad (2.4)$$

The mean of a probability density function is a measure of its central tendency, or a parameter describing the location of the PDF. The expected life of a component is defined as its mean life, or

$$\mu = E(t) = \int_0^{\infty} \tau f(\tau) d\tau = \int_0^{\infty} R(t) dt \quad (2.5)$$

The mean time to failure (MTTF) for the i^{th} failure mode ($i=1, \dots, N$ where N is the number of failure modes) is

$$MTTF_i = E_i(t) \quad (2.6)$$

If the component has several different failure modes, and the failure and repair of one mode does not affect the other modes, then a MTTF can be determined for each failure mode. Although a MTTF can be found for each failure mode, a system composed of numerous components can have a system-level mean time to failure ($MTTF_s$), which is defined as the average time to first failure of the system without consideration of the

failure mode. The mean time between failure (MTBF) is the average of the mean time to failure for the system due to all failure modes and for any number of failure times. Letting μ_{Tj} represent the weighted time to the j^{th} failure of a system, then if m generations of parts are repaired or replaced, the MTBF can be determined as³⁰,

$$MTBF = \frac{1}{m} \sum_{j=1}^m \mu_{Tj} \quad (2.7)$$

When the system being considered is perfectly renewed through repair and maintenance, the expected life is equivalent to both the MTTF, and the MTBF.

The failure rate is the probability that a component will fail in a given period of time. The hazard rate is defined as the instantaneous failure rate, and is given as³¹

$$h(t) = \frac{f(t)}{R(t)} \quad (2.8)$$

The hazard rate is the probability that a component surviving to a specific time, t , will fail in the next small time interval, $t+dt$.

Quantifying the degree of dispersion of a variable is done by determining its variance. The variance of a random variable, t is defined as³²

$$Var(t) = E[(t - \mu)^2] \quad (2.9)$$

The square root of the variance is simply defined as the standard deviation, σ .

When more than one possible event may affect a component, or system, it is important to be able to determine the interaction between the various event variables as well as the individual impact of any specific variable. If the variables are independent, then changes in one variable value are independent of the other variable, that is changes in one

variable will have no effect on any other variable. When two variables are independent their joint PDF is the product of their individual PDFs, or³³

$$f_{x,y}(x,y) = f_x(x) \cdot f_y(y) \quad (2.10)$$

A measure of the linear relationship between any two variables is described by two related parameters, covariance and correlation. If X and Y are two random variables having means μ_x and μ_y , then the covariance of X and Y is defined as³⁴

$$Cov(X,Y) = E[(X - \mu_x)(Y - \mu_y)] = E(XY) - \mu_x\mu_y \quad (2.11)$$

Since covariance is not dimensionless, a dimensionless measure of the linear relationship termed the correlation coefficient is often used. The correlation coefficient is defined as³⁵

$$\rho(X,Y) = \frac{Cov(X,Y)}{\sigma_x \cdot \sigma_y} \quad (2.12)$$

The correlation coefficient has a range of values between -1 and +1, and is a measure of the linear relationship between two random variables. If $\rho = \pm 1$, then the two variables are linearly related; if $\rho = 0$, then there is no linear relationship, but this does not preclude the possibility the variables may be related in a non-linear manner. If two variables are independent, then both the covariance and the correlation are 0.

The independence of the variables does not reflect whether it is possible to have more than one event occurring at a particular time. If we denote the probability of an event A occurring as $P(A)$, and that of event B occurring as $P(B)$, then we see that the two possible outcomes involving these two event are that they are independent and have no intersection, or they are independent and have some intersection. The occurrence of

the intersection event is not related to the independence of the two events, since an intersection probability can occur even if the events are independent.

System Hazard Rates

We consider the determination of the hazard rates for a system composed of a number of components. The two alternative system configurations that will be considered are, series and parallel.

The parallel system configuration requires that only one system component be functioning in order for the system to operate. If a parallel arrangement of n components is assumed, the system reliability is³⁶

$$R_s(t) = 1 - Q_s(t) = 1 - P[t_1 < t \cap t_2 < t \cap \dots \cap t_n < t] \quad (2.13)$$

If the events are assumed to be independent, then the reliability becomes,

$$R_s(t) = 1 - P(t_1 < t) \cdot P(t_2 < t) \cdot \dots \cdot P(t_n < t) \quad (2.14)$$

Recall that the reliability of a single component is

$$R_i(t) = P(t_i > t) \quad (2.15)$$

Substituting equation (2.15) into equation (2.14) yields the following equation for the system reliability,

$$R_s(t) = 1 - \prod_{i=1}^n [1 - R_i(t)] \quad (2.16)$$

For the parallel case, the determination of the system hazard rate is not easily accomplished. This is due to the fact that no similar derivation to that outlined in equation (2.16) can be found for the parallel configuration case.

The series configuration requires that all system components be functioning in order for the system to operate. If a series arrangement of n components is assumed, and the time histories of the components are assumed to be independent, then the hazard rate for the system can be determined. Initially, let the assumption be added that the time each elements of the system has been operating is the same. If t represents the time to failure of the i^{th} component, then the reliability for n components is³⁷

$$R_S(t) = P(t_1 > t) \cap P(t_2 > t) \cap \dots \cap P(t_n > t) \quad (2.17)$$

$$R_S(t) = P[t_1 > t \cap t_2 > t \cap \dots \cap t_n > t] \quad (2.18)$$

If the events are assumed to be independent, then the system reliability becomes

$$R_S(t) = P(t_1 > t) \cdot P(t_2 > t) \cdot \dots \cdot P(t_n > t) \quad (2.19)$$

Recall that the reliability of a single component is

$$R_i(t) = P(t_i > t) \quad (2.20)$$

Hence the system reliability is

$$R_S(t) = \prod_{i=1}^n R_i(t) \quad (2.21)$$

Now taking the logarithms of equation (2.21) gives

$$\ln R_S(t) = \sum_{i=1}^n \ln R_i(t) \quad (2.22)$$

For any component the reliability can be expressed as

$$R_i(t) = \exp\left[-\int_0^t h(\tau) d\tau\right] \quad (2.23)$$

Or alternatively

$$\int_0^t h(\tau) d\tau = -\ln R_i(t) \quad (2.24)$$

$$h(t) = -\frac{d}{dt} \ln R_i(t) \quad (2.25)$$

Substituting equations (2.24) and (2.25) into equation (2.22) yields

$$-\frac{d}{dt} \ln R_S(t) = \sum_{i=1}^n -\frac{d}{dt} \ln R_i(t) \quad (2.26)$$

This yields a system hazard rate

$$h_S(t) = \sum_{i=1}^n h_i(t) \quad (2.27)$$

Therefore, the system hazard rate is the sum of the component hazard rates if the following assumptions are made:

1. a series system configuration is used
2. the components are assumed to have independent event histories
3. the components are assumed to have the same initial starting time.

If the assumption that the components have the same starting time is not valid and the replacement or starting time of component i is t_{i0} , the relationship given in equation (2.27) becomes,

$$h_S(t) = \sum_{i=1}^n h_i(t - t_{i0}) \quad (2.28)$$

The system hazard rate relationships derived in equations (2.27) and (2.28) are usually difficult to apply since the hazard functions are complex. However, most of the difficulties encountered in applying the relationships for the system hazard rate can be

avoided if the underlying component time to failure distribution is assumed to be exponential.

The Uniform Failure Rate Model

We will now examine system hazard rates when the underlying time to failure distribution is assumed to be exponential and then define the uniform failure rate model.

The form of the exponential PDF is given by³⁸

$$f(t) = \frac{1}{\lambda} e^{-\frac{t}{\lambda}} \quad t \geq 0 \quad \lambda > 0 \quad (2.29)$$

If the exponential PDF is assumed for the time to failure of the components, then the results from equations (2.8), (2.23), and (2.29) can be used to determine the individual hazard function for a component to be,

$$h_i(t) = \frac{1}{MTTF_i} = \frac{1}{\lambda_i} \quad (2.30)$$

where the failure rate of the exponential distribution is defined as λ . If we assume a series system configuration, independent component event histories, common component starting times, and all components exhibiting exponential time-to-failure PDF's, we can use the results of equation (2.27) to determine the system hazard rate to be,

$$h_S(t) = \sum_{i=1}^n h_i(t) = \frac{1}{\lambda_S} = \sum_{i=1}^n \frac{1}{\lambda_i} \quad (2.31)$$

From equations (2.30) and (2.31), the system MTTF can be defined as

$$MTTF_S = \sum_{i=1}^n MTTF_i \quad (2.32)$$

The application of system hazard rate relationships under the assumption of an exponential component time to failure distribution is defined as the uniform failure rate model approach to system reliability estimation.

Dependent and Independent Failure Modes

The results for the system hazard rate and MTTF apply to cases where the system is composed of a number of units, each unit possessing its own time-to-failure PDF. Multiple failure modes can result in a different system reliability depending on the interaction of the failure modes. Two alternative failure mode interactions are possible:

1. **The failure modes are independent.** Under this condition, the failure and repair of the system with respect to one failure mode renews the time history of the corresponding failure mechanism. The time histories of the remaining failure modes acting remain unchanged.
2. **The failure modes are dependent.** Under this condition, the failure and repair of the system with respect to one failure mode renews the time history of all active failure mechanisms. If the time history is reset, the effect is one of perfect renewal of the system, however the repair of a failure typically does not result in perfect renewal of the system.

For the case of dependent failure modes, repairing the system due to any failure results in the entire system being renewed. For example, a sealed ball bearing used to support a heavy rotating shaft. The two failure modes which affect the bearing would be

spalling of the ball bearings and failure of the bearing seal. A failure of the bearing due to either of these two failure mechanism results in replacement of the entire bearing assembly. Upon replacement, the time histories of both the spalling and seal failure mechanisms are reset.

Dependency of failure modes does not imply either correlation between the failure mechanism, or common random variables. The dependency of the failure modes is not determined by the interaction effects of the random variables, but is a specification of the type of replacement/repair policy employed and the physical limitations of the systems. In the case cited of the ball bearing, the failure of the bearing seal or due to spalling may be due to separate and independent failure mechanisms involving stochastically and physically independent random variables. The failure of the bearing due to either failure mechanism would physically necessitate the replacement of the entire bearing assembly, thereby resetting the failure time histories for all active failure modes.

Determining the conditions under which either of the two cases of failure mode dependency hold is necessary in order to correctly apply reliability prediction methods. Specifically, we seek to determine the restrictions inherent in the application of reliability techniques based on uniform failure rate models. Simulation models were developed for both the dependent and independent failure mode conditions. Two different failure modes were assumed to affect the hypothetical system under consideration.

First, we will examine the case of the independent failure modes. Second, we will examine the case of dependent failure modes. Finally, we will examine the impact of

changes in the failure probability density function distribution parameters on system failure rate and MTBF.

First, consider a system subject to two different failure modes. If the system could be operated in such a way that only one failure mode could occur, it would be observed that each failure mode has its own failure probability density function. Each failure probability density function would be characterized by a unique mean and variance. The total number of failures experienced by the system during any time would be the sum of the failures due to each failure mode independently. Consider a system composed of a number of identical components, each component being subject to two time history independent failure modes is considered, and use of the system is initiated, then the hazard rates for the failure modes are shown in Figure 1.

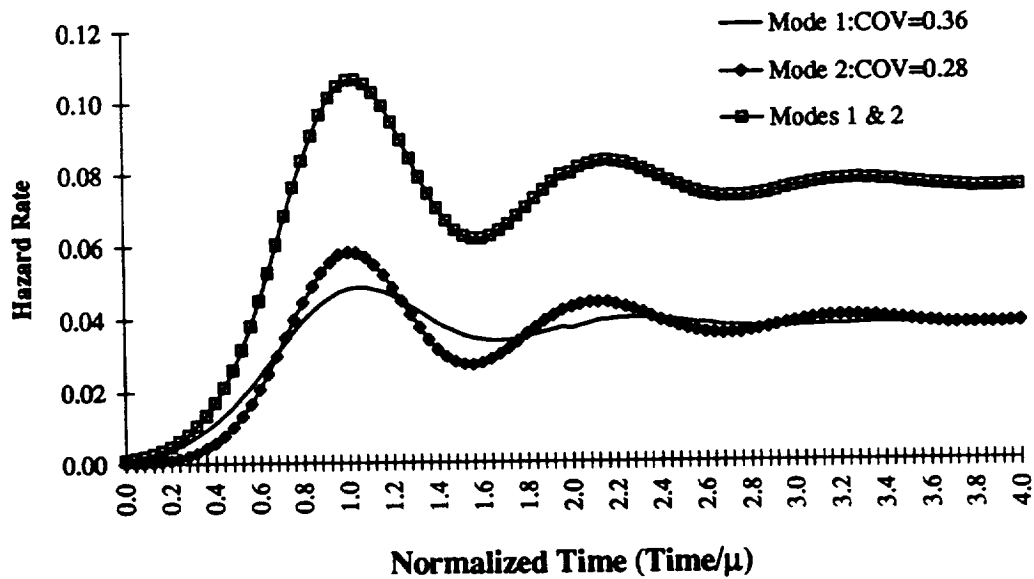


Figure 1: Two Failure Modes with Separate Aging Mechanisms

The individual failure density functions were assumed to have the same mean value, μ , but different coefficients of variation. Given that each failure density function has the same mean, the hazard rate of the system due to each individual failure mechanism should eventually stabilize at its failure rate, or $1/\mu$. Since the repair of a component due to a single failure mechanism does not affect the time history of the remaining failure mechanism, the expected number of units failing due to both failure modes at any time is the sum of the individual failure rates. Once the system has reached a steady-state failure rate, its behavior can be approximated by an exponential failure density function. Under the assumptions of independent failure modes and approximation of steady-state behavior by the exponential density function, the system hazard rate is

$$h_s(t) = h_1(t) + h_2(t) = \frac{1}{\mu} + \frac{1}{\mu} = \frac{2}{\mu} \quad (2.33)$$

From equation (2.32) system MTBF is

$$MTBF_s = \frac{1}{h_s(t)} = \frac{2}{\mu} \quad (2.34)$$

Note in Figure 1, that there is a transient period following start-up of the system during which time the individual and system failure rates are not constant. This transient behavior was noted by Kapur and Lamberson³⁹. Since the MTBF of a system is a constant, it can be concluded that the use of MTBF for estimating system reliability behavior is valid, a long time following start-up, for series systems with independent failure modes, but is not appropriate for predicting system behavior during the transient period of operation.

Now consider a system where the failure modes are dependent; the failure and repair of the system due to either failure mode results in the time histories of both failure mechanisms being reset. Each failure mechanism has its own time-to-failure distribution described by a unique mean and variance. However, when considered as system subjected to two failure mechanisms simultaneously, the system behavior is characterized by the time to first failure resulting from the failure of either of the two possible failure mechanisms. The resulting failure rate for the system cannot be determined by the application of the results for series systems which were derived earlier, equations (2.27) through (2.32), since the relative contribution to the overall system failure rate is dependent on the mean and standard deviation of each failure mode. This case represents a situation of conditional reliability, since the probability of failure due to a failure mode is dependent on the system having not previously failed.

Consider two cases, the first where the area of intersection of the two failure mode probability density functions is $\delta(1)$, the second where the area of intersection of the two failure mode probability density functions is $\delta(0.1)$. Note that δ denotes the order measure of the area of intersection of the two time-to-failure PDF's. Thus $\delta(0.1)$ would signify that the area of intersect was in the range of 0-1% of the total PDF area. Complete intersection of the PDF's would be denoted as $\delta(10)$.

When the area of intersection of the two failure mode PDF's is $\delta(1)$ both failure mechanisms contribute to the system behavior. Consider the following $\delta(1)$ PDF area of

intersection case. Monte Carlo simulation was used to determine the two failure mechanisms PDF's as well as the resulting system PDF's shown in Figure 2.

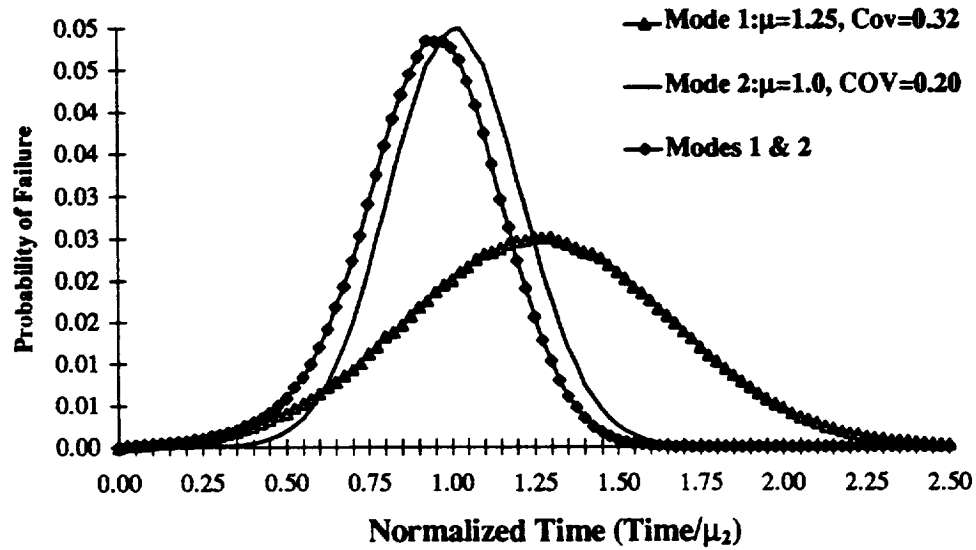


Figure 2: Combined and Individual Failure Mode PDF's

Note that the system failure PDF is different from both failure PDF's due to the fact that the system can exhibit failures from each of the two failure mechanisms. The resulting hazard rate for a system comprised of numerous identical components, each of which subjected to the two dependent failure modes is depicted in Figure 3.

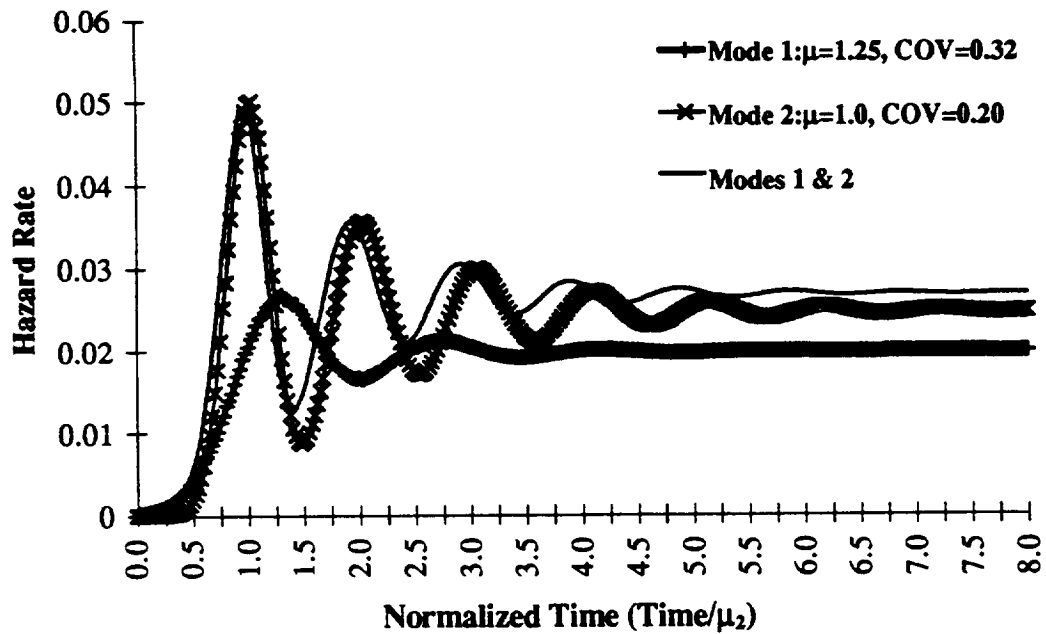


Figure 3: Hazard Rate for Individual and System Failure When Failure Resets All Failure Modes

The resulting system hazard rate is higher than that of either failure mode when considered alone, yet the system hazard rate is not the sum of the individual failure mode hazard rates. The conclusion to be drawn is that the approximation of the series system hazard rate derived earlier, equation (2.27), is not exact for systems subjected to dependent failure modes in which system failure resets all failure mode time histories. Note that the failure of the system is dominated by the earlier time-to-failure PDF.

When the area of intersection of the two failure mode PDF's is $\theta(0.1)$, no statistically significant difference is observed between the PDF with lower mean and the system PDF. Consider the following $\theta(0.1)$ PDF area of intersection case. Monte Carlo

simulation was used to determine the PDF's for each failure mode and the resulting system PDF shown in Figure 4.

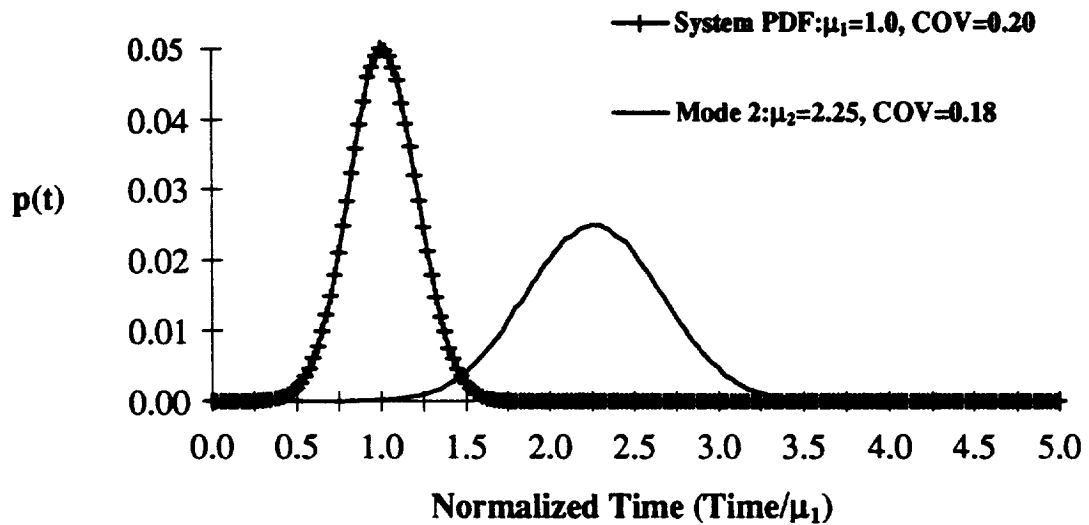


Figure 4: Combined and Individual Failure Mode PDF's-O(0.1) Case

The statistically insignificant difference between the system behavior and that of the lower mean failure mode PDF is due to the fact that the majority of failures experienced by the system will be due to the failure mode with the lowest mean life. The dominance of the system behavior by one failure mode indicates that the system is not likely to experience many failures due to the higher life failure mode. The majority of components will never survive long enough to experience failure resulting from this higher life failure mode.

The resulting system hazard rate for a system comprised of numerous identical components, where the intersection area of the failure mode PDF's is $\theta(0.1)$ is depicted in Figure 5.

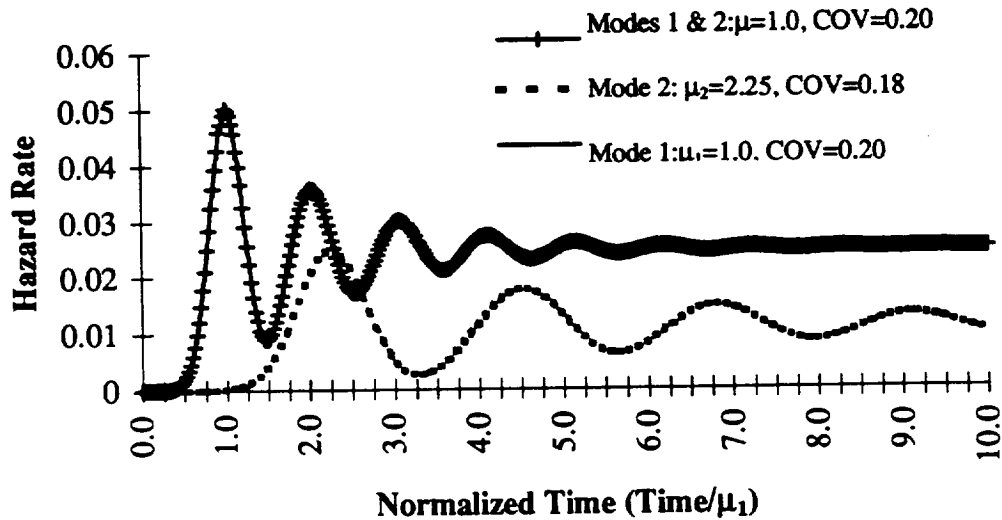


Figure 5: Combined and Individual Failure Mode Hazard Rates- $\theta(0.1)$ Case

Note that the resulting system hazard rate is not distinguishable from that exhibited by the lower life failure mode. As a result, the system hazard rate is not the sum of the individual hazard rates. The implication of this result is that the MTBF values quoted in databases represents replaceable units and not units that are repaired and renewed for individual failures.

The implications of the dependent failure mode simulation results are twofold. First, in systems subjected to dependent failure modes, the series system relationship

defining the system hazard rate (equation (2.27)) is not applicable. Second, in cases of multiple failure modes, the overall system hazard rate closely approximates the behavior of the failure mode with the lowest MTTF.

From these simulation results, the following conclusions can be drawn:

1. Use of MTBF for estimates of system reliability based on the summation of component MTBF values is only valid for series systems in which the failure modes are independent.
2. Use of MTBF for predicting the system behavior during the transient period of system start-up and operation is not appropriate.
3. Use of the lowest MTBF values are appropriate for estimating system reliability.

Limitations on the Application of Uniform Failure Rate Models to System Reliability Estimation.

In the simulation results presented, once the system was activated, a transient period during which the system did not display steady-state hazard rate behavior occurred. Eventually the system attained a steady-state hazard rate, at which point the behavior of the system could be reasonably approximated by the uniform failure rate model. Since we concluded that the transient period of system behavior could not be estimated using MTBF, we would like to determine the transient response behavior of the system. If the transient period were found to be of extremely short duration when compared with the component MTTF, then it may be argued that the overall system behavior can be

reasonable approximated by using the uniform failure rate model. If the duration of the transient period is not substantially shorter than the component MTTF, then we would like to determine if it is possible to estimate system reliability using MTBF estimation methods.

We will now examine the impact of changes in the failure probability density function distribution parameters on the system failure rate and system MTBF. We will examine how the system transient response behavior is affected by the underlying failure probability density function, and whether or not the system will ever approach steady-state conditions. The assumptions underlying this analysis are:

1. The system behavior can be described by a single PDF.
2. There are several identical components in operation.
3. All components are activated at the same time.
4. Failed units are replaced or perfectly renewed instantaneously.
5. The time the system operates is much greater than the component MTTF.

We will examine the impact of the time to failure PDF coefficient of variation and mean on both the time required to reach a steady-state hazard rate, and the maximum hazard rate experienced by the system. We will define the time to reach steady-state as the time required by the system to exhibit a $\pm 5\%$ deviation in peak-to-peak hazard rate.

First, consider the impact of changes in the coefficient of variation of the component time to failure distribution on the time to attain steady-state hazard rate conditions. A normal failure distribution will be assumed. Initially, the impact of increasing the coefficient of variation is examined. The MTTF of the system is assumed to

be constant. The impact of changing the coefficient of variation is shown in Figures 6, 7 and 8.

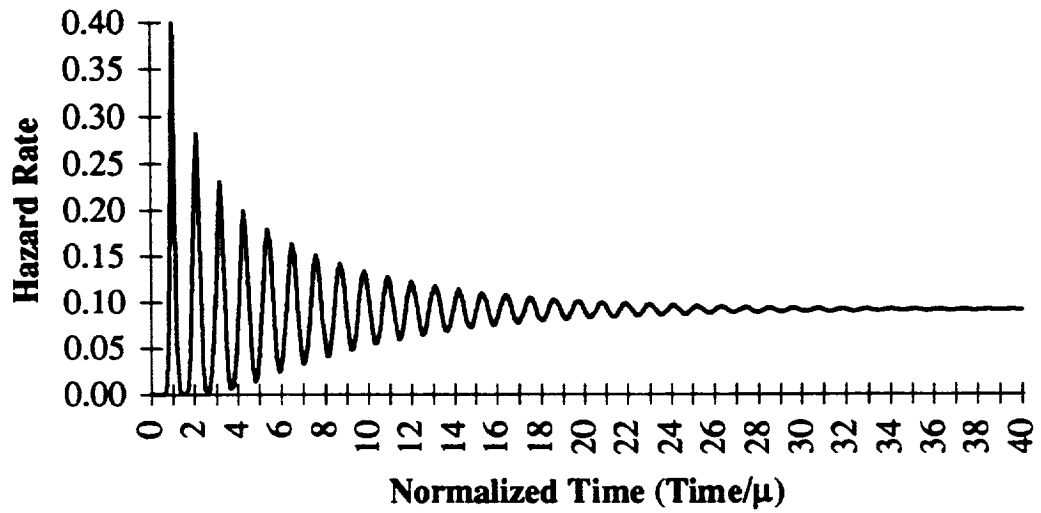


Figure 6: System Hazard Rate-Normal Distribution (COV=0.10)

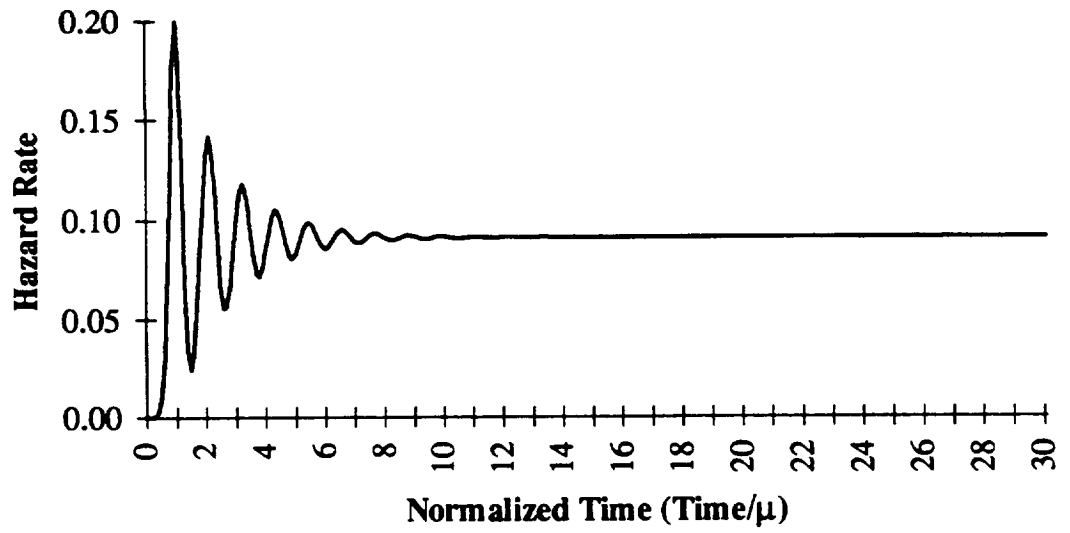


Figure 7: System Hazard Rate-Normal Distribution (COV=0.20)

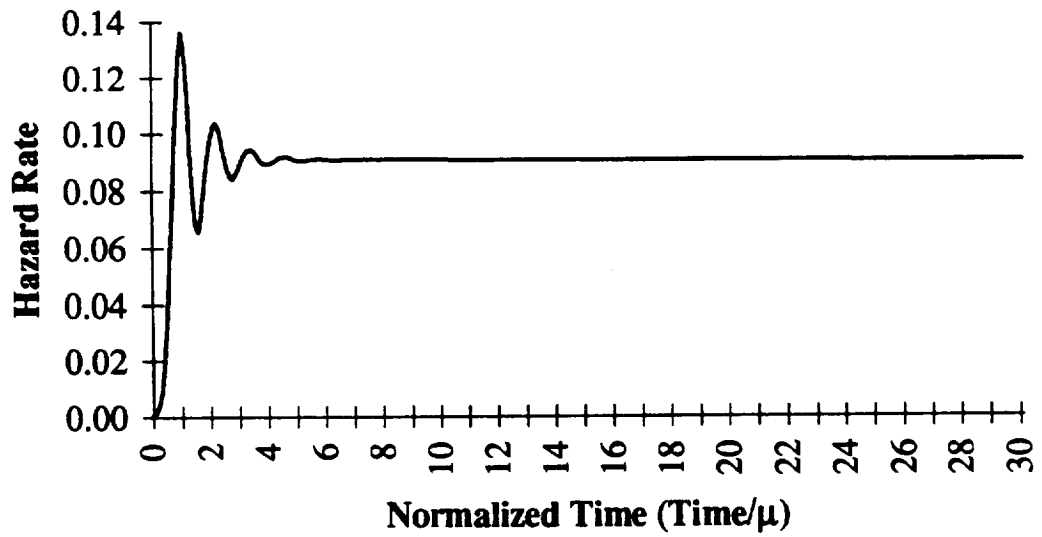


Figure 8: System Hazard Rate-Normal Distribution (COV=0.30)

Note that decreasing the coefficient of variation by a factor of 2 from 0.2 to 0.1, results in higher maximum failure rate (40% .vs. 20% of the population). Decreasing the coefficient of variation by a factor of 2 resulted in an increase in the time to reach steady state by a factor of 3.

If all units are started at the same time, it is possible that by sufficiently reducing the coefficient of variation of the component time to failure distribution the system will never reach a steady-state behavior and will exhibit a regular spike pattern of failures. In most real mechanical systems, units are started at different times, reducing the impact of such transient spike failure rates.

As the coefficient of variation is decreased, a threshold value is reached below which further reductions in the coefficient of variation results in the system never attaining a steady-state failure rate. For components exhibiting small deviations in life from their MTTF values, predicting system performance using the uniform failure rate model is not appropriate.

Second, consider the impact of changes in the component MTTF on the time to attain steady-state hazard rate conditions. A Gaussian time to failure distribution is assumed. The impact of increasing the MTTF is examined. The coefficient of variation of the time to failure distribution is held constant. Compare the system response for the two different MTTF's shown in Figure 9.

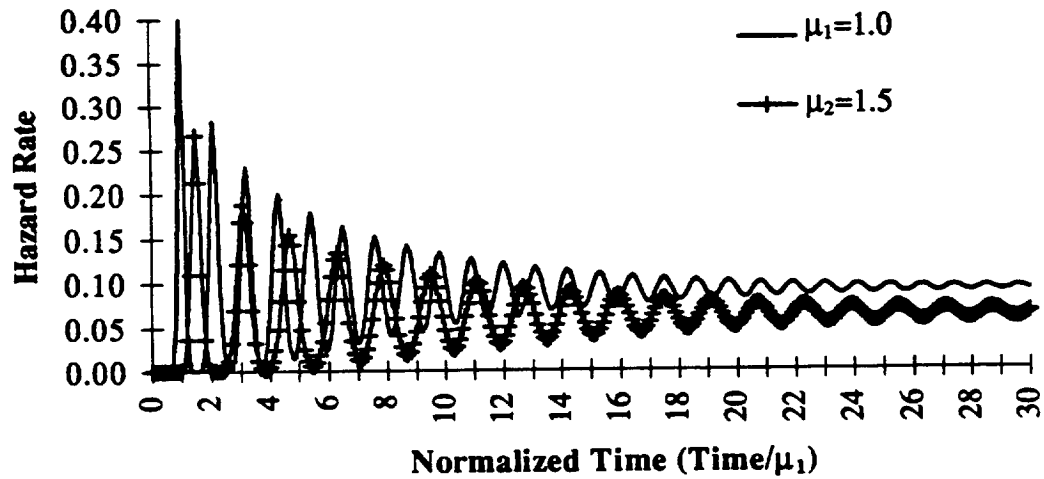


Figure 9: Influence of Changes in Mean on Hazard Rates

Increasing the MTTF by 50%, and keeping the coefficient of variation constant, requires 65% more time to reach steady-state. In addition, the failure rate peaks at multiples of the component MTTF. The simulation results demonstrated that in no case was the time to attain steady-state hazard rate conditions less than 5 times the component MTTF. The time required to reach steady-state is significant, since in many real applications involving a component MTTF of several years, the period of transient system response may often exceed the useful life of the system. The impact of increasing the MTTF on the time to reach steady-state hazard rate conditions is important if we are to assume that the uniform failure rate model can be applied, because the period of transient system behavior is of short duration when compared with the system life. If the period of

transient system response accounts for much of the useful life of the system, then clearly the application of uniform failure rate reliability prediction techniques cannot be justified.

From these simulation results we can conclude that the mean of the failure distribution is positively correlated with the time required to reach steady-state, while coefficient of variation is negatively correlated with the time required to reach steady-state.

Whether the system will attain steady-state hazard rate conditions is not dependent on the failure PDF being unimodal. The ability of the system to reach steady-state failure rate behavior is not related to the symmetry or number of modes describing the time to failure PDF. Consider the following bi-modal PDF shown in Figure 10.

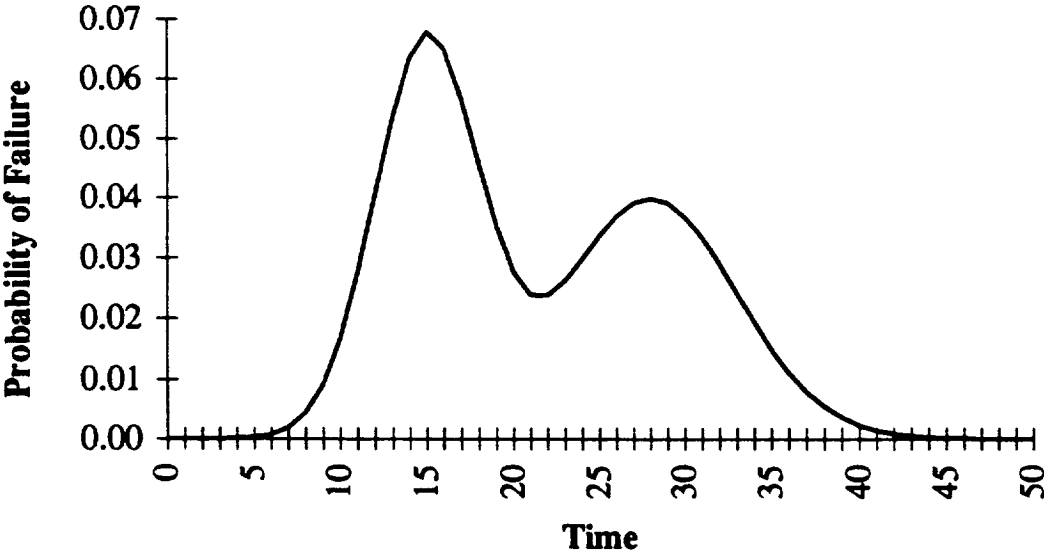


Figure 10: Bi-Modal Time to Failure Distribution

The PDF has modes at $t=15$ and $t=28$. The resulting system hazard rate, shown below in Figure 11, demonstrates that unimodality is not a requirement for the system to attain steady-state conditions.

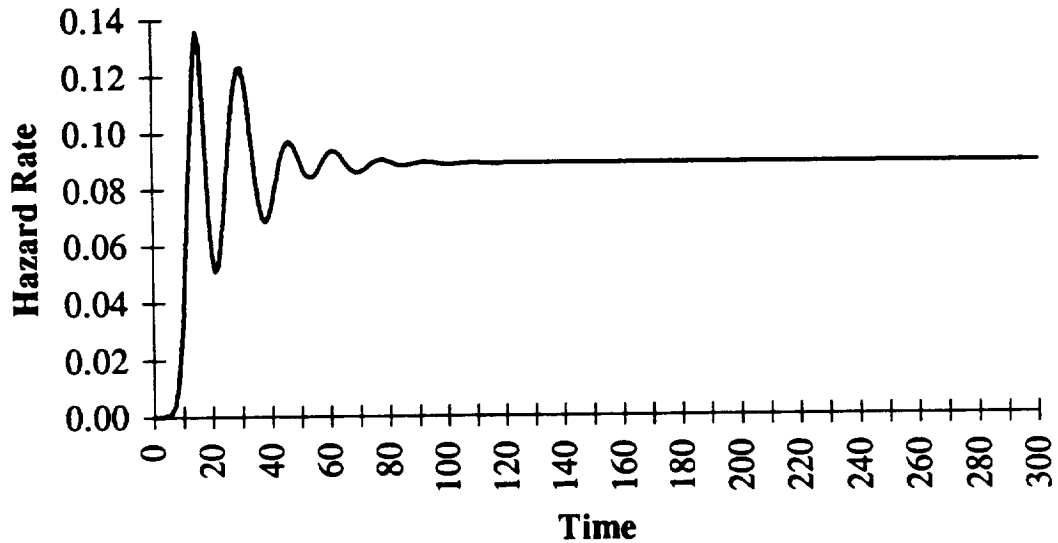


Figure 11: Bi-Modal Distribution Hazard Rate

The steady-state hazard rate was found to be 0.0889. This value of the steady-state hazard rate would correspond to an exponential distribution with mean of 11.25, a result substantially lower than the first mode of the bi-modal distribution. Figure 11 does demonstrate, however, that for the multi-modal PDF, the transient response can be seen to behave in a manner similar to that demonstrated in unimodal cases.

From these simulation results the following observations have been made regarding the transient behavior of a system:

1. Increasing the component MTTF leads to the system requiring a greater period of time to attain steady-state conditions.
2. Decreasing the coefficient of variation of the component time to failure results in a higher maximum failure rate. In addition, the system requires a greater period of time to attain steady-state conditions if the coefficient of variation is decreased.
3. In order for a system to attain steady-state conditions, there exists a lower limit on the coefficient of variation of the component time-to failure distribution.
4. Unimodal and multi-modal PDF's result in the system reaching steady-state.
5. Peaks in the transient failure rates coincide with multiples of the component MTTF.
6. The time required to reach steady state conditions is significantly greater than the MTTF for the system. The time required to reach $\pm 5\%$ of the steady-state failure rate was never less than 5 times the MTTF.

Implications of Analytical Reliability Methods on the Reliability-Cost Trade-Off Methodology

Having demonstrated the limitations inherent in the application of analytical reliability methods several implications are evident. We have shown that analytical reliability methods do not consider the physical variables that define either the failure modes or operating environment that the component experiences. If we consider equations (2.6) and (2.32) which define MTTF and the system failure rate, it is clear that

the uniform failure rate model does not include physical variables. The inability of the uniform failure rate model to include physical variables prevents its use to estimate component reliability resulting from changes in either primitive variables or operating environment. This is due to the inability to determine the reliability sensitivity to changes in the physical variables. Without a means of estimating the impact of changes in variables on reliability, analytical methods cannot be integrated into a methodology to explore reliability-cost trade-offs that result from variable changes.

The absence of physical random variables in the analytical reliability method precludes their use in determining the impact of variance reduction on reliability and cost. Reduction of variance or truncation of physical variable distributions can affect the component reliability. Methods, such as Taguchi methods and statistical process control, focus on variance reduction or control as a means of reducing cost and improving reliability. Without distributional information of physical variables in analytical methods, the cost of variance cannot be determined.

We have demonstrated that analytical reliability methods can only be used to estimate the behavior of systems that have attained a steady-state failure rate. Also we determined that the time to attain steady-state failure rates is significantly greater than the component MTTF. The fact that the time to achieve steady-state conditions is so long indicates that most mechanical systems operate in the transient failure rate regime. Assessing component reliability in the transient failure rate regime cannot be accomplished with analytical reliability methods, requiring the application of alternative reliability estimation methods in these cases.

Where analytical reliability methods can be used in reliability-cost trade-offs is when examining alternative existing components versus costs directly related to MTTF. Analytical methods could then be used to examine different available component reliabilities as compared to an estimated replacement or warranty cost. In this case, the reliability-cost trade-off does not consider the configuration or design of the component, but rather the selection of one of many alternative designs.

Having demonstrated the assumptions and limitations of analytical reliability methods and their unsuitability for use in a reliability-cost trade-off methodology, we now examine physics-based reliability methods.

CHAPTER III

EXTENSION OF FIRST-ORDER RELIABILITY METHODS TO MECHANICAL SYSTEM DESIGN

Introduction

We have examined analytical reliability models, and have demonstrated their inherent limitations and underlying assumptions. These analytical methods are not physics-based approaches to reliability estimation. The absence of physical variables in analytical reliability models creates several weaknesses. First, analytical reliability models are unable to model specific operating conditions affecting a system. Second, analytical reliability models are unable to specify the mode of failure for a system. Third, analytical reliability models are unable to determine the relative importance that individual physical variables play in specific failure modes.

To counter the shortcomings involved in using analytical reliability models, we consider the application of physics-based reliability methods to mechanical systems. First, we will outline the basic concepts of physics-based reliability methods. Second, we will determine the linkages that exist between physics-based reliability methods, primitive variables, and the uniform failure rate model. Third, we will briefly outline the physics-based failure models that affect mechanical systems, and define limit states for the failure models. Fourth, we will examine the validity of alternative modeling strategies for physics-based limit state models. We seek to demonstrate the applicability of physics-

based reliability methods to mechanical systems as well as their relationship to analytical reliability models.

First-Order Reliability Method Concepts

We will consider the fundamental principles which define physics-based reliability models, in particular first-order reliability methods (FORM). The reliability of system components is defined by the limit states that affect the system. A limit state is a characteristic of the system component which can be observed, and is defined to represent the failure of the component due to a specific failure mechanism. The failure of the component need not be represented by the catastrophic failure of the component, but may be defined as a measurable degree of degradation in one or more properties of the component.

The response function relates a limit state of the system component to the primitive variables that characterizes the system performance. The primitive variables are defined as being both statistically as well as physically independent variables. The response function is defined as:

$$\begin{aligned} g(\vec{X}) &= g(X_1, X_2, \dots, X_n) \\ \text{where } \vec{X} &= X_1, X_2, \dots, X_n = \text{vector of primitive variables} \\ g(\vec{X}) &= \text{response function} \end{aligned} \tag{3.1}$$

The limit state of the system is defined as:

$$\begin{aligned} g(\vec{X}) &= 0 \\ \text{where } g(\vec{X}) &> 0 = \text{Safe State} \\ g(\vec{X}) &< 0 = \text{Failure State} \end{aligned} \tag{3.2}$$

The limit state relationship given by equation (3.2), is an n-dimensional surface. One side of the surface is the failure region, on the other side is the safe region. The joint probability density function of the variables is

$$\begin{aligned}
 p_f &= \text{probability of failure} \\
 &= \int_{g(\bar{X}) < 0} \cdots \int f_{X_1, X_2, \dots, X_n}(x_1, x_2, \dots, x_n) dx_1, dx_2, \dots, dx_n \\
 &= \int_{g(\bar{X}) < 0} f_x(\bar{x}) dx
 \end{aligned} \tag{3.3}$$

Note that the probability of the failure state is the volume integral over the failure region.

The reliability index, β , represents the minimum distance from the origin to the limit state function. In order for the reliability index to be invariant, it is necessary for the primitive variables to be transformed to uncorrelated standard normal variables. If the variables are correlated they must first be transformed into equivalent uncorrelated variables. If the variables are nonnormal, then they must first be transformed into equivalent normal variables using either a two or three parameter fit. Once transformed into standard normal variables, the limit state function becomes,

$$g(\bar{Y}) = f(y_1, y_2, \dots, y_n) \tag{3.4}$$

The reliability index, β , is the minimum distance to the linearized limit state surface. The point on the linearized limit surface that is closest to the origin is called the most probable point, y^* , and satisfies the following relationship,

$$\beta = \min(y^{*T} \cdot y^*)^{1/2} \tag{3.5}$$

Determining the relationship between the most probable point and the reliability index involves the gradient vector of the limit state function in standard normal space, defined as,

$$\bar{G} = \left(\frac{\partial g}{\partial y_1}, \frac{\partial g}{\partial y_2}, \dots, \frac{\partial g}{\partial y_n} \right) \quad (3.6)$$

where $\frac{\partial g}{\partial y_i} = \sigma_{xi} \frac{\partial g}{\partial x_i}$

Then the reliability index and the most probable point are given as:⁴⁰

$$\beta = \frac{-\bar{G}^{*T} y^*}{(\bar{G}^{*T} \bar{G}^*)^{1/2}} \quad (3.7)$$

$$y^* = \frac{-\bar{G}^* \beta}{(\bar{G}^{*T} \bar{G}^*)^{1/2}}$$

If we consider only a first-order Taylor series approximation to the limit state function at the most probable point, then the direction cosines of the outward normal vector at the most probable point are:

$$\alpha_i = \frac{\frac{\partial g}{\partial y_i}}{\left(\sum_i \left(\frac{\partial g}{\partial y_i} \right)^2 \right)^{1/2}} \quad (3.8)$$

The direction cosines, α_i , represent the sensitivity of the reliability index, β , to changes in y_i , at the most probable point. This sensitivity measure assumes that the distribution parameters of the variable concerned remains the same. The direction cosine, α_i , relates the i^{th} component of the most probable point, y_i , to the reliability index, as shown in equation (3.9).

$$y_i^* = -\alpha_i^* \beta \quad i = 1, 2, \dots, n \quad (3.9)$$

In addition to being the minimum distance from the limit state to the origin, the most probable point is used as the expansion point for the Taylor series expansion used to linearize the limit state function.

The most probable point is found by minimizing the reliability index subject to the constraint that the point lie on the limit state function, or $g(\mathbf{Y})=0$. If a linearized approximation to the limit state function is used, then the direction cosines are constant along the function making the determination of the most probable point easy. Amongst the most useful methods used for the linearized limit state case, it that proposed by Rackwitz and Fiessler⁴¹. If a non-linear approximation to the limit state function is used, if the limit state constraint is satisfied, then it is possible to use either Lagrangian multipliers or gradient projection methods to determine the most probable point.

Linking FORM, Primitive Variables and Analytical Reliability Models

We now examine the relationship between first-order reliability methods, the limit state primitive variables, and analytical reliability models. Specifically, we will examine the relationship between changes in first-order reliability results, changes in limit state primitive variables, and MTTF measures of reliability.

We begin by considering the sensitivity of reliability index to changes in the parameters of the primitive variables. Although it would be possible to determine the sensitivity of the reliability index to changes in the primitive variables using numerical methods, we desire a closed-form solution. A closed-form result for the reliability index

sensitivity would avoid repeated application of FORM necessary for estimation of reliability sensitivities. Let the parameters of the primitive variables be denoted by \mathbf{p} .

Previously in equation (3.5) the reliability index was defined as

$$\beta(\mathbf{p}_i) = |\bar{\mathbf{y}}^*| = (\bar{\mathbf{y}}^{*T} \cdot \bar{\mathbf{y}}^*)^{1/2} \quad (3.10)$$

The sensitivity of the reliability index to changes in the distribution parameters of a primitive variable was demonstrated by Madsen et al.⁴² to be,

$$\frac{\partial}{\partial p_i} \beta(\mathbf{p}_o) = \frac{\partial}{\partial p_i} \left[(\bar{\mathbf{y}}^{*T} \cdot \bar{\mathbf{y}}^*)^{1/2} \right] = \frac{\partial}{\partial p_i} \left[\left((y_1^*)^2 + (y_2^*)^2 + \dots + (y_n^*)^2 \right)^{1/2} \right] \quad (3.11)$$

This can be rewritten as:

$$\frac{\partial}{\partial p_i} \beta(\mathbf{p}_o) = \frac{\bar{\mathbf{y}}^{*T} \cdot \frac{\partial}{\partial p_i} \bar{\mathbf{y}}^*}{(\bar{\mathbf{y}}^{*T} \cdot \bar{\mathbf{y}}^*)^{1/2}} = \frac{1}{\beta} \bar{\mathbf{y}}^{*T} \cdot \frac{\partial}{\partial p_i} \bar{\mathbf{y}}^* = \frac{1}{\beta} \mathbf{y}^{*T} \cdot \frac{\partial}{\partial p_i} \mathbf{T}(z^*, \mathbf{p}_o) \quad (3.12)$$

Note that \mathbf{y}^* is the most probable point on the limit state function. In addition \mathbf{T} is defined as the Rosenblatt transformation, which is used to transform correlated non-normal variables into equivalent uncorrelated normal variables. Finally, we define z as,

$$z^* = \mathbf{T}^{-1}(\bar{\mathbf{y}}^*, \mathbf{p}_o) \quad (3.13)$$

Madsen et al. also demonstrated the sensitivity of the probability of failure with respect to the sensitivity factors for the reliability index, given as,

$$\frac{\partial}{\partial p_i} P(F(\bar{\mathbf{y}}, \mathbf{p}_o)) = \frac{\partial}{\partial p_i} \Phi(-\beta(\mathbf{p}_o)) = \phi(-\beta(\mathbf{p}_o)) \cdot \frac{\partial}{\partial p_i} \beta(\mathbf{p}_o) \quad (3.14)$$

where $P(F(\bar{\mathbf{y}}, \mathbf{p}_o)) =$ probability of failure

$\Phi =$ normal cumulative distribution function

$\phi =$ normal probability density function

We will now use the results enumerated in equations (3.10) through (3.14) to determine the sensitivity of the MTTF to changes in the primitive variables distribution parameters.

The MTTF of any component is defined as ⁴³,

$$MTTF = \int_0^{\infty} \tau f(\tau) d\tau = \int_0^{\infty} R(t) dt = \int_0^{\infty} [1 - F(t)] dt \quad (3.15)$$

We seek to determine the sensitivity of MTTF to changes in the distribution parameters of one of the primitive variables, p_i . The partial derivative of the MTTF with respect to the primitive variable p_i is given by ,

$$\frac{\partial}{\partial p_i} MTTF(\mathbf{p}_o) = \frac{\partial}{\partial p_i} \int_0^{\infty} [1 - F(\tau)] d\tau \quad (3.16)$$

Now recall that the probability of failure of failure for the system evaluated at any point y and dependent on the primitive variable parameter \mathbf{p}_o is,

$$\text{Probability of Failure} = P(F(\bar{y}, \mathbf{p}_o)) \quad (3.17)$$

Substituting equation (3.17) into equation (3.16) yields,

$$\frac{\partial}{\partial p_i} MTTF(\mathbf{p}_o) = \frac{\partial}{\partial p_i} \int_0^{\infty} [1 - P[F(\bar{y}^*, \mathbf{p}_o)]] d\tau \quad (3.18)$$

We now apply Liebnitz's rule to equation (3.18) to give,

$$\frac{\partial}{\partial p_i} MTTF(\mathbf{p}_o) = \frac{\partial}{\partial p_i} \int_0^{\infty} 1 d\tau - \frac{\partial}{\partial p_i} \int_0^{\infty} P[F(\bar{y}^*, \mathbf{p}_o)] d\tau \quad (3.19)$$

But the partial derivative of 1 with respect to the primitive variable parameter p_i is zero, so we are left with,

$$\frac{\partial}{\partial p_i} MTTF(\mathbf{p}_o) = \int_0^{\infty} \frac{\partial}{\partial p_i} P[F(\bar{y}^*, \mathbf{p}_o)] d\tau \quad (3.20)$$

Now substituting the results of equation (3.14) into equation (3.20) gives,

$$\frac{\partial}{\partial p_i} MTTF(\mathbf{p}_o) = \int_0^{\infty} \frac{\partial}{\partial p_i} \Phi(-\beta(\mathbf{p}_o)) d\tau \quad (3.21)$$

$$\frac{\partial}{\partial p_i} MTTF(\mathbf{p}_o) = \int_0^{\infty} \phi(-\beta(\mathbf{p}_o)) \frac{\partial}{\partial p_i} \beta(\mathbf{p}_o) d\tau \quad (3.22)$$

By way of equation (3.22) we have demonstrated the sensitivity of the MTTF to changes in the primitive variables parameters. The linkage of MTTF to both changes in the primitive variables and the reliability index provides as means of comparing FORM and analytical reliability methods. In addition, by way of equation (3.22), we have means of estimating the MTTF sensitivity to changes in the primitive variable distributional parameters. This MTTF sensitivity estimate could be used in the reliability-cost trade-off methodology to incorporate MTTF related costs such as warranty and replacement costs.

First-Order Reliability Method Modeling Strategies for Mechanical Limit States

Having examined the theoretical basis for first-order reliability methods as well as the linkage between FORM and analytical reliability methods, we examine appropriate methods of modeling mechanical limit states to be employed when conducting FORM reliability estimates. Specifically, we seek to identify the relationships that can be used to model the failure modes the define mechanical limit states.

To determine the best modeling approach for first-order reliability methods applied to mechanical limit states several of the limit states, identified in the compendium of limit states (see Appendix), were selected and tested. The majority of the limit states that were deemed relevant to mechanical systems were found to be power law relationships. Two

limit states were found to follow Arrhenius relationships, namely, uniform corrosion and thermal degradation. The limit states that were modeled included:

1. wear
2. fretting wear
3. pitting
4. erosion-corrosion
5. galvanic corrosion
6. low-cycle fatigue

With the exception of low-cycle fatigue, all the noted limit-states were considered to have a response function of the form:

$$g(R,S) = R - S \quad (3.23)$$

In this case R represents either the resistance of the system to the specific degradation effect being modeled, or some maximum allowable degree of system deterioration. Similarly, S represents the actual degree of material stress induced on the system, or the actual degree of degradation of the system due to the degradation process under consideration.

When R represented the maximum allowable degree of system deterioration, it was assumed to be a random variable with a specified distribution and parameters. In all limit states modeled, the actual deterioration experienced by the system, S , was a function of several random variables. The functional form taken by S was dependent on the particular mechanical limit state being considered. The exact nature the mechanical limit states considered is outlined in Appendices A and B.

In the case of low-cycle fatigue, the response function was of the form:

$$g(N_{MIN}, N_{ACTUAL}) = -N_{MIN} + N_{ACTUAL} \quad (3.24)$$

Here N_{MIN} is the minimum number of cycles the system must operate while in service, and N_{ACTUAL} is the number of cycles to failure. N_{MIN} was assumed to be randomly distributed variable, and N_{ACTUAL} was a function of several primitive variables.

After extensive examination of the available scientific literature, little information on the distribution of specific limit state primitive variables was found. In the majority of cases where information on primitive variables distribution parameters could not be found, the variables were assumed to be either normal or log-normally distributed. The primitive variables defined in each limit state were assumed to be independent.

The first-order reliability method applied to each response function included both the mean value first-order method (MVFO) and the advanced mean value first-order method (AMVFO). If the response function (or Z function) is assumed to be smooth, then we can take a Taylor's series expansion of the response function at the mean value⁴⁴. The mean and variance of the response function can be determined if we consider only the first-order terms.⁴⁵ If the distributions of the primitive variables and their parameters are defined, and if we consider only first-order terms in the Taylor series approximation, then the cumulative density function (CDF) of the response function is also defined. The estimation of the response function CDF by linear function is referred to mean value first-order (MVFO) approach.

If the response function is non-linear, then its approximation by a first-order Taylor series will result in some error. The inclusion of higher order terms in the Taylor series

will improve the accuracy of the analysis, although the approach is more difficult. The advanced mean value first-order (AMVFO) method includes a simple function, $H(Z_1)$, to approximate the higher order terms of the Taylor series.

The application of first-order reliability methods to each response functions was conducted using the NESSUS/FPI software developed by Southwest Research Institute under funding by the NASA Lewis Research Center⁴⁶. The NESSUS/FPI software allows for the response function to be incorporated in several alternative formats. The two approaches that were used are:

1. The user defined subroutine of the form:

$$g(X) = f(X_1, X_2, \dots, X_n, Z_0) \quad (3.25)$$

In this case the response function can have any specified form.

2. A response function of the form:

$$X_1 = f(X_2, X_3, \dots, X_n, Z_0) \quad (3.26)$$

In the second approach defined in equation (3.26) one primitive variable must be separable from the others, and the response function written with the separable variable on the left-hand side. In some cases this is not feasible given the functional form of the limit state relationship. The various modeling techniques used and the validation of the techniques used for each limit state are now discussed.

Validation of First-Order Reliability Method Modeling Strategies

The accuracy of the first-order reliability method modeling strategies were validated using Monte Carlo simulation. In all cases conventional Monte Carlo analysis

was used, and no effort was undertaken to use importance sampling approaches. For each limit state a Monte Carlo simulations using 50,000 samples was employed.

Since many primitive variables distribution parameters were unknown, FORM was applied assuming normally distributed variables and again assuming log-normally distributed variables. Additional FORM analyses were conducted assuming different coefficients of variation (COV) for the primitive variables. The different coefficients of variation were used to examine the effect of primitive variable variance on limit state modeling validity.

A comparison was made between those results obtained using Monte Carlo simulation and first-order reliability methods. The cumulative density functions for each response function modeled were obtained and plotted for both the first-order reliability method and Monte Carlo simulation.

A Kolmogorov-Smirnov test was applied to each limit-state modeled to determine if the CDF found using first-order reliability methods differed from that obtained using Monte Carlo. The Kolmogorov-Smirnov test considers the maximum difference between the two cumulative density functions to determine if they are the same,⁴⁷ or:

$$D_n = \max|F_n(x) - S_n(x)| \quad (3.27)$$

Here $F(x)$ represents the theoretical or assumed value of the CDF, and $S(x)$ the observed or experimentally determined value of the CDF.

For the seven limit states considered, the results of the Kolmogorov-Smirnov tests are given below.

Table 1: Limit State Kolmogorov-Smirnov Test Results

Limit State	Distribution	COV	Sample Size	$D_{crit}:\alpha=0.10$	D_{MAX}	Significant
Pitting	Normal	0.10	20	0.26	0.011	No
	Lognormal	0.25	20	0.26	0.004	No
	Lognormal	0.50	20	0.26	0.021	No
	Lognormal	1.00	20	0.26	0.024	No
Low-Cycle	Normal	0.10	16	0.29	0.011	No
Fatigue	Lognormal	0.25	20	0.26	0.020	No
	Lognormal	0.50	20	0.26	0.019	No
	Lognormal	1.00	20	0.26	0.020	No
Fretting	Normal	0.10	17	0.28	0.010	No
	Lognormal	0.25	20	0.26	0.019	No
	Lognormal	0.50	20	0.26	0.026	No
	Lognormal	1.00	20	0.26	0.027	No
Erosion-	Normal	0.10	10	0.37	0.021	No
Corrosion	Lognormal	0.25	20	0.26	0.052	No
	Lognormal	0.50	20	0.26	0.080	No
	Lognormal	1.00	20	0.26	0.096	No
Wear	Normal	0.10	20	0.26	0.012	No
	Lognormal	0.25	20	0.26	0.011	No
	Lognormal	0.50	20	0.26	0.037	No
	Lognormal	1.00	20	0.26	0.016	No
Galvanic-	Normal	0.10	15	0.30	0.016	No
Corrosion	Lognormal	0.25	20	0.26	0.002	No
	Lognormal	0.50	20	0.26	0.002	No
	Lognormal	1.00	20	0.26	0.002	No

From these results, we conclude that there is no statistically significant difference between the cumulative density functions obtained using first-order and Monte Carlo methods for each limit state. However, this statistical comparison of first-order and Monte Carlo methods using the Kolmogorov-Smirnov test is based on the maximum difference in the CDF of the failure distribution, which would occur about the center of the distribution. We would like to determine the validity of FORM methods when the probability of failure is very low. This involves examination of the behavior of FORM methods in the tail of the probability of failure distribution, and its comparison with Monte Carlo results.

Since no statistical test exists to compare two CDF's at low probability values, we will show the probability of failure results obtained for both FORM and Monte Carlo. In each case a specific probability of failure was selected from the Monte Carlo results, the corresponding performance function value (referred to as a Z-level) was noted, and the corresponding FORM-based probability of failure at the specific performance function value was found. The two probabilities of failure for the various limit states, and the percentage difference between them is shown below.

Table 2: Monte Carlo and FORM Failure Probability Differences

Limit State	Distribution	COV	MC P(F)	FORM P(F)	Difference
Pitting	Normal	0.10	0.520%	0.555%	-6.73%
	Lognormal	0.25	1.000%	1.013%	-1.33%
	Lognormal	0.50	1.000%	1.036%	-3.67%
	Lognormal	1.00	1.000%	1.062%	-6.24%
Low-Cycle	Normal	0.10	0.604%	0.682%	-12.96%
Fatigue	Lognormal	0.25	0.268%	0.317%	-18.45%
	Lognormal	0.50	0.300%	0.448%	-49.50%
	Lognormal	1.00	0.300%	0.521%	-73.71%
Fretting	Normal	0.10	0.340%	0.320%	5.97%
	Lognormal	0.25	0.700%	0.698%	0.24%
	Lognormal	0.50	0.700%	0.684%	2.19%
	Lognormal	1.00	0.700%	0.661%	5.57%
Erosion-	Normal	0.10	0.546%	0.719%	-31.68%
Corrosion	Lognormal	0.25	0.032%	0.021%	-34.38%
	Lognormal	0.50	0.162%	0.152%	-6.17%
	Lognormal	1.00	0.032%	0.021%	-34.38%
Wear	Normal	0.10	0.452%	0.457%	-1.11%
	Lognormal	0.25	0.902%	0.920%	-1.94%
	Lognormal	0.50	1.000%	1.039%	-3.91%
	Lognormal	1.00	1.000%	0.983%	1.68%
Galvanic-	Normal	0.10	0.396%	0.421%	-6.31%
Corrosion	Lognormal	0.25	0.074%	0.073%	1.55%
	Lognormal	0.50	0.075%	0.075%	0.003%
	Lognormal	1.00	0.100%	0.100%	-0.14%

From these results, it can be seen that with the exception of low-cycle fatigue and erosion-corrosion the failure probabilities obtained from FORM and Monte Carlo are similar. Low-cycle fatigue and erosion-corrosion did display marked differences in their resulting probabilities of failure. It should be noted that in every case the difference between FORM and Monte Carlo results was less than an order of magnitude despite the fact that the results were compared at low probability of failure values.

Implications of FORM for the Reliability-Cost Trade-Off Methodology

Having demonstrated a relationship for the sensitivity of the MTTF to changes in the distributional parameters of primitive variables, as well as identifying and validating modeling strategies for various mechanical limit states, several implications are evident. We have extended the first-order reliability method to mechanical systems by demonstrating and validating specific modeling strategies for a number of mechanical limit states. The validation of FORM for mechanical systems provides reliability engineers with a viable alternative to analytical reliability methods.

The sensitivity of component reliability to changes in the distributional parameters that can be estimated from FORM results provides one of two principle elements required for the proposed design paradigm. FORM, by providing a means to determine the reliability sensitivity, provides a means of estimating the impact on component reliability of changes in the distributional parameters of the primitive variables.

Being a physics-based estimation method, FORM is a less restrictive means of assessing component reliability. The less restrictive nature of FORM permits its

application to both existing and neoteric designs, as well as for systems subjected to unique operating conditions. FORM can also be used to estimate the reliability of components at any time in their economic life. This allows FORM to be used to estimate reliability during the transient failure rate regime of operation. Reliability estimations for components in the transient failure regime would provide more accurate measures of anticipated unit failures, and permit better estimation of maintenance requirements. The ability to estimate component behavior in the transient failure rate period is in marked contrast to other reliability methods.

In equation (3.22) we derived a relationship to estimate the sensitivity of the MTTF to changes in the distributional parameters of the primitive variables using FORM results. This relationship can be used in the reliability-cost trade-off method to incorporate MTTF related costs, such as warranty and liability costs. The inclusion of such costs in a trade-off methodology would permit engineers to approximate the impact of design modifications on non-manufacturing costs. This ability to estimate non-manufacturing costs provides unique information to engineering and management regarding the relationship between product design and cost.

Having extended and validated FORM to mechanical systems, and having demonstrated its principle contributions to the reliability-cost trade-off methodology, we will now examine physics-based failure rate estimations methods.

CHAPTER IV

PHYSICS-BASED RELIABILITY MODELING

Introduction

We have examined analytical reliability methods which focus on mean time to failure and mean time between failure. Analytical method reliability predictions based on MTTF/MTBF do not consider the impact of changes in operating conditions or design specifications. Consequently, it is difficult for the engineer to use results from analytical methods to improve a product's design. Using first-order reliability methods does provide the engineer with information needed to determine design improvements.

The drawbacks of using FORM techniques are the computational time and effort required to conduct an assessment of component reliability. A simple computational approach to measure the impact of primitive variables on component reliability would provide the engineer with a simple guide to product improvement. Physics-based failure rate reliability prediction techniques are a likely candidate for such approximate assessments of component reliability.

To assess the validity of physics-based failure rate reliability prediction techniques we will examine the assumptions required for their successful application to mechanical systems. First, we will outline the basic concepts of physics-based failure rate reliability prediction techniques. Second, we will establish linkages between physics-based failure rate reliability prediction techniques and analytical reliability models by way of example.

Third, we will outline the assumptions that must hold in order to apply physics-based reliability prediction techniques to mechanical systems.

Review of Physics-Based Failure Rate Reliability Prediction Techniques

Previously we examined analytical reliability models. We demonstrated that the analytical reliability models were linked to the component time to failure PDF, and were directly influenced by its distribution parameters. Analytical reliability models do not incorporate primitive variables accounting for differing component designs or operating environments. A methodology that incorporates design and environment primitive variables is physics-based failure rate reliability prediction techniques, hereafter referred to as physics failure rate techniques.

Analytical reliability techniques depend on measures of component and system MTTF to assess reliability. Physics failure rate techniques use failure rates as a measure of component reliability. Unlike analytical reliability techniques, physics failure rate techniques derive a component failure rate by modifying a base failure rate by a number of correction factors. Each correction factor represents the anticipated deviation of a specific design or environmental primitive variable from the conditions under which the base failure rate was determined. The physics failure rate is that outlined in the Handbook of Reliability Prediction Procedures for Mechanical Equipment⁴⁸.

The failure rate models are typically of the form:

$$\lambda_{Comp} = \lambda_{Comp, B} \cdot \prod_{i=1}^n C_i \quad (4.1)$$

where: λ_{Comp} =failure rate of component

$\lambda_{\text{Comp,B}}$ =base failure rate of component

C_i =correction factor i .

In order to predict the component failure rate, λ_{Comp} , it is necessary for the engineer to know:

1. The component base failure rate, $\lambda_{\text{Comp,B}}$
2. The values of the design and environment primitive variables for the component base failure rate
3. The values of the design and environment primitive variables under which the component will operate.

The consideration of changes in component primitive variables allows the engineer to measure the impact of changes in variable values on component reliability.

To use physics failure rate techniques it is apparent that some form of empirical data on component failure rates is required. In addition to empirical data on component failure rates, information regarding the service or experimental conditions under which the data was gathered is also needed.

Linking Physics Failure Rate Methods and Traditional Reliability Techniques

We now determine the relationship between physics failure rate methods and analytical reliability methods. Specifically, we seek to determine the assumptions and limitations that must hold in order for physics failure rate methods to be valid. We will first determine the general form that the physics failure rate models must follow in order to

be valid, and then we will demonstrate the development of a specific physics failure rate model.

The relationship between the MTTF as a function of a primitive variable, p , and the probability density function is,

$$MTTF(p) = E(\tau, p) = \int_0^{\infty} \tau \cdot f(\tau, p) d\tau \quad (4.2)$$

The relationship between the MTTF and the failure rate, assuming a constant failure rate, is given by ⁴⁹,

$$\lambda(p) = \frac{1}{MTTF(p)} \quad (4.3)$$

If we consider a component operating at some anticipated value of the primitive variable, denoted p_1 , then the anticipated failure rate can be related to the base failure rate by combining equations (4.1) and (4.3) to yield,

$$\lambda(p_1) = \frac{1}{MTTF(p_1)} = \frac{1}{MTTF(p_0)} \frac{MTTF(p_0)}{MTTF(p_1)} = \frac{1}{MTTF(p_0)} \frac{\frac{1}{MTTF(p_1)}}{\frac{1}{MTTF(p_0)}} \quad (4.4)$$

where: $MTTF(p_0) = MTTF$ at reference value p_0

$MTTF(p_1) = MTTF$ at operating value p_1

From equation (4.4) we can see that the base failure rate and the correction factor are defined as,

$$\begin{aligned} \lambda(p_0) &= \frac{1}{MTTF(p_0)} = \text{base failure rate} \\ C_1 &= \frac{MTTF(p_0)}{MTTF(p_1)} = \frac{E(\tau, p_0)}{E(\tau, p_1)} = \text{correction factor accounting for } p_1 \end{aligned} \quad (4.5)$$

Equation (4.5) demonstrates that the correction factors used to modify the base failure rate are simply the ratio of the base to anticipated component MTTFs.

We will now examine the assumptions and limitations of the physics failure rate method by consideration of the failure rate relationship for a specific system. We will consider the failure rate relationship for helical springs. We seek to determine a relationship for the failure rate of helical springs of the form,

$$\lambda_{SP} = \lambda_{SP,B} \cdot \prod_{i=1}^n C_i$$

where: λ_{SP} = helical spring failure rate (4.6)

$\lambda_{SP,B}$ = helical spring base failure rate

C_i = correction factor for anticipated operating condition i

The load in the spring is a function of the spring deflection and is given as⁵⁰,

$$P_L = \frac{G_M (D_M)^4 (L_1 - L_2)}{8 (D_C)^3 N_a}$$

where: P_L = Load, lbs

G_M = Modulus of rigidity, lbs / in²

D_M = Wire diameter, in (4.7)

L_1 = Free length of spring, in

L_2 = Final deflection of spring, in

D_C = Mean diameter of spring, in

N_a = Number of active coils

The stress in the spring is affected by the loading and is given as⁵¹,

$$S_G = \frac{8 \cdot P_L \cdot D_C}{\pi (D_w)^3} K_w$$

where: S_G = Spring stress (4.8)

K_w = Wahl correction factor

The Wahl factor is determined as⁵²,

$$K_w = \frac{4r-1}{4r-4} + \frac{0.615}{r} \quad (4.9)$$

where: $r = \text{spring index} = D_c/D_w$

If the assumption is made that the reliability of the spring is determined by the ratio of the spring stress at some anticipated operating condition, S_{G_1} , to the tensile strength of the spring, S_{G_0} , then,

$$\frac{S_{G_1}}{S_{G_0}} = \frac{\left(\frac{G_{M_1} \cdot D_{w_1} \cdot \Delta L_1 \cdot K_{w_1}}{\pi \cdot D_{C_1}^2 \cdot N_{a_1}} \right)}{\left(\frac{G_{M_0} \cdot D_{w_0} \cdot \Delta L_0 \cdot K_{w_0}}{\pi \cdot D_{C_0}^2 \cdot N_{a_0}} \right)}$$

where: G_{M_1} = Modulus of rigidity for operating conditions

G_{M_0} = Modulus of rigidity for reference conditions

D_{w_1} = Wire diameter for operating conditions

D_{w_0} = Wire diameter for reference conditions

ΔL_1 = Deflection of spring for operating conditions

ΔL_0 = Deflection of spring for reference conditions (4.10)

K_{w_1} = Wahl factor for operating conditions

K_{w_0} = Wahl factor for reference conditions

D_{C_1} = Mean diameter of spring for operating conditions

D_{C_0} = Mean diameter of spring for reference conditions

N_{a_1} = Number of active coils for operating conditions

N_{a_0} = Number of active coils for reference conditions

By rearranging terms and canceling the constant, π , equation (4.10) can be rewritten as,

$$\frac{S_{G_1}}{S_{G_0}} = \frac{G_{M_1}}{G_{M_0}} \cdot \frac{D_{w_1}}{D_{w_0}} \cdot \frac{\Delta L_1}{\Delta L_0} \cdot \frac{K_{w_1}}{K_{w_0}} \cdot \frac{N_{a_0}}{N_{a_1}} \cdot \frac{D_{C_0}^2}{D_{C_1}^2} \quad (4.11)$$

Equation (4.11) does not provide a direct estimation of the spring failure rate, so some means of relating the spring life to stress must be used. If the life of the system is

measured in cycles to failure, N , then the life can be related to material stress, S , using the fatigue relationship,

$$N = a \cdot S^b \quad (4.12)$$

where a and b are constants

The constant, b , represents the slope of the S - N curve which defines the fatigue failure of materials. For metals, the slope of the S - N curve varies between -2 and -6, with a value of -3 being typically used⁵³.

The two measures of component life, the failure rate, λ , measured in failures/million cycles, and the cycles to failure, N , are related as,

$$\lambda = \frac{1}{MTTF} = \frac{1}{E(N)} \quad (4.13)$$

If Y is a function of several random variables, X_1, X_2, \dots, X_n , that is,

$$Y = g(X_1, X_2, \dots, X_n) \quad (4.14)$$

we can find the mean of Y . If a Taylor series expansion of the function, $g(X_1, X_2, \dots, X_n)$, is taken about the mean values of the random variables, X_1, X_2, \dots, X_n , and truncated at the first-order terms, then the expected value of Y can be shown to be approximated by⁵⁴,

$$E(Y) \cong g(\mu_{x_1}, \mu_{x_2}, \dots, \mu_{x_n}) \quad (4.15)$$

Equation (4.15) demonstrates that first-order approximation of the mean of the function is simply the function of the means of the random variables.

Using equations (4.4), (4.13), and (4.15) and assuming a S - N curve slope of -3, we can determine,

$$\begin{aligned}
\frac{\frac{1}{MTTF(S_1)}}{\frac{1}{MTTF(S_0)}} &= \frac{\frac{1}{E(N_1)}}{\frac{1}{E(N_0)}} = \frac{E(N_0)}{E(N_1)} \\
&\equiv \frac{E(a \cdot S_0^{-3})}{E(a \cdot S_1^{-3})} \equiv \frac{a \cdot E(S_0^{-3})}{a \cdot E(S_1^{-3})} \equiv \frac{E(S_1^3)}{E(S_0^3)} \\
&\equiv \frac{[E(S_1)]^3}{[E(S_0)]^3} \equiv \left[\frac{E(S_1)}{E(S_0)} \right]^3 \equiv \left[\frac{\mu_{S_1}}{\mu_{S_0}} \right]^3
\end{aligned} \tag{4.16}$$

Equation (4.16) demonstrates the cubic dependence of the failure rate on the ratio of mean spring stresses. Utilizing equations (4.11) and (4.16), we can rewrite equation (4.4) as,

$$\begin{aligned}
\lambda(\bar{p}_1) &\equiv \lambda(\bar{p}_0) \cdot \left[\frac{\mu_{S_1}}{\mu_{S_0}} \right]^3 \\
&\equiv \lambda(\bar{p}_0) \cdot \left[\frac{\mu_{G_{M_1}}}{\mu_{G_{M_0}}} \cdot \frac{\mu_{D_{W_1}}}{\mu_{D_{W_0}}} \cdot \frac{\mu_{\Delta L_1}}{\mu_{\Delta L_0}} \cdot \frac{\mu_{K_{W_1}}}{\mu_{K_{W_0}}} \cdot \frac{\mu_{N_{a_1}}}{\mu_{N_{a_0}}} \cdot \frac{\mu_{D_{C_1}}^2}{\mu_{D_{C_0}}^2} \right]^3 \\
&\equiv \lambda(\bar{p}_0) \cdot \left(\frac{\mu_{G_{M_1}}}{\mu_{G_{M_0}}} \right)^3 \left(\frac{\mu_{D_{W_1}}}{\mu_{D_{W_0}}} \right)^3 \left(\frac{\mu_{\Delta L_1}}{\mu_{\Delta L_0}} \right)^3 \left(\frac{\mu_{K_{W_1}}}{\mu_{K_{W_0}}} \right)^3 \left(\frac{\mu_{N_{a_1}}}{\mu_{N_{a_0}}} \right)^3 \left(\frac{\mu_{D_{C_1}}}{\mu_{D_{C_0}}} \right)^6
\end{aligned} \tag{4.17}$$

where: $\bar{p}_0 = (G_{M_0}, D_{W_0}, \Delta L_0, K_{W_0}, N_{a_0}, D_{C_0})$
= vector of primitive variables at reference conditions

$\bar{p}_1 = (G_{M_1}, D_{W_1}, \Delta L_1, K_{W_1}, N_{a_1}, D_{C_1})$
= vector of primitive variables at operating conditions

The physics failure rate model derived in equation (4.17) agrees with the models obtained in the Handbook of Reliability Prediction Procedures for Mechanical Equipment⁵⁵.

Thus, we have demonstrated the relationship between analytical reliability measures such as MTTF and the physics failure rate method. In addition, we have related

the correction factors employed by the physics failure rate method to the changes in the primitive variables and the mean of the component probability density function.

Assumptions Made in Deriving Physics Failure Rate Techniques

We have outlined the basic concepts of the physics failure rate technique as well as linking it to analytical reliability models. We now examine the assumptions and conditions that must hold in order for the physics failure rate techniques to yield valid results.

First, the base failure rate and the primitive variable values at the reference condition must be known. A consequence of this is that generic database failure rates cannot be used to establish the base failure rates of components since they do not include information on the primitive variable values at the reference condition.

Second, in order to estimate the expected life of a component, the physics failure rate models use a first-order Taylor series approximation of the performance function defining component life. For highly non-linear performance functions, the expected value of the component life based on a Taylor series approximation should include higher order terms.

Third, the models use a life relationship which defines the component life as a function of several primitive variables. The utilization of a life relationship allows for the incorporation of primitive variables into the failure rate model.

Fourth, as demonstrated in equation (4.17), each correction factor represents the ratio of a primitive variable mean value at the reference condition to its mean value at the operating conditions. Hence, the physics failure rate models do not incorporate any

measure of primitive variable variance. The dependence of physics failure rate models on the mean values of the primitive variables prevents any estimation of the percentage of the component population that is expected to failure prior to the predicted failure rate unless the underlying primitive variable distribution is either Gaussian or a one parameter distribution.

Finally, the degree of uncertainty in the failure rate estimates is likely to be large. The base failure rates used in the Handbook of Reliability Prediction Procedures for Mechanical Equipment⁵⁶ were determined from experimental observation. In a number of cases, the number of experimental samples used to determine the base failure rate was small. In some cases only 1 sample was used⁵⁷. The small sample sizes introduce considerable uncertainty in the estimate of the base failure rates. If the sample size is 1 and the underlying population time-to-failure distribution is exponentially distributed, then the confidence interval for the mean time to failure is given as⁵⁸:

$$\frac{2 \sum_{i=1}^n x_i}{\chi_{\alpha/2, 2n}^2} \leq MTTF \leq \frac{2 \sum_{i=1}^n x_i}{\chi_{1-\alpha/2, 2n}^2}$$

where: $x_i = i^{th}$ failure time (4.18)
 $n =$ number of observed failure times
 $\chi^2 =$ chi - squared distribution

If we consider a sample size of 1, then using equation (4.18), the 95% confidence interval of the population MTTF:

$$\frac{2 \cdot 1}{7.378} \leq MTTF \leq \frac{2 \cdot 1}{0.0506}$$

$$0.27108 \leq MTTF \leq 39.526 \quad (4.19)$$

where: $\chi_{0.025,2}^2 = 7.378$
 $\chi_{0.975,2}^2 = 0.0506$

This result indicates that when the sample size is 1, the actual population MTTF value is anywhere between 27.11% and 3952.6% of the sample value. Given that the component failure rate is the reciprocal its MTTF, the magnitude of the uncertainty in the base failure rate estimates are the same as those for the MTTF. Investigating the relationship between confidence limits and sample size indicates that even large sample sizes of 100 are unlikely to be sufficient to establish small 95% confidence limits on the failure rate. In order for physics failure rate models to be valid, the uncertainty in the base failure rates used in the models must be substantially less than the magnitude of range of the primitive variables employed in the models. The time and expense required to establish sufficient accuracy in physics failure rate models is substantial, and represents a major obstacle to more widespread application of physics failure rate models.

Implications of Physics-Based Methods for the Reliability-Cost Trade-Off Methodology

We have demonstrated the relationship between analytical and physics-based reliability estimation methods, as well as the assumptions that must hold in order for the physics failure rate reliability method to be valid. From these analyses, several

implications for the applicability of physics failure rate methods to product design are evident.

Although the physics-based failure rate methods incorporates primitive variables in its reliability estimates, equation (4.17) demonstrates that the method is only applicable for changes in the mean value of the primitive variables. As such, physics-based failure rate methods do not consider the impact of changes in variance or truncation of the variables on component reliability. The inability to determine the effect of variance reduction or truncation on component reliability is a limitation on the use of physics-based methods in any trade-off methodology.

The changes in primitive variables are with respect to an established base component configuration, which are obtained from available historical databases of component failure rates. The reliance on historical databases for the base failure rate values imposes two limitations on physics-based methods. First, neoteric component designs cannot be analyzed since no historical failure data exists. Second, reliability estimates cannot be made for systems with anticipated operating conditions that differ from those reflected in the base failure values. These limitations preclude the incorporation of physics-based methods in the trade-off methodology.

As we have demonstrated, the physics-based failure rate method suffers from a large degree of uncertainty in the estimated base failure rates. The large degree of uncertainty in the estimated base failure rates is the result of the small sample sizes used. In order to ensure that the magnitude of the uncertainty in the estimated base failure rates are substantially less than the allowable range of primitive variables, the number of

samples required will be several orders of magnitude larger than those comprising existing failure rate databases. The uncertainty in the physics-based failure rate method is larger than the range of feasible change in the primitive variables. Hence any estimation of the impact of changes in the primitive variables cannot be statistically distinguished from the random error in the methodology. Such large estimating errors precludes the inclusion of the physics-based failure rate method in a trade-off methodology.

We have examined the validity of analytical, physics failure rate, and first-order reliability methods. Having demonstrated the assumptions and restrictions of each method, we will now examine how engineers and managers can incorporate reliability estimation methods into the product design.

CHAPTER V

INTEGRATED PRODUCT DESIGN: A SEQUENTIAL LINEAR APPROXIMATION METHOD

Introduction

We have examined both analytical and physics-based reliability techniques from the perspective of usefulness to the designer/engineer. These methods allow the engineer to improve the performance of a proposed product, yet the impact of design changes motivated by performance criteria that include product cost has not been addressed. Considered in isolation, methodologies based solely on engineering evaluations of performance are unlikely to yield a product that represents an acceptable compromise between cost and performance.

We begin by defining the cost/reliability problem encountered in product design. Second, we outline the various means of improving product reliability. Third, a methodological approach to rationally explore product reliability/cost trade-offs and determine the product configuration is presented. Fourth, an example problem demonstrating the application of the design methodology is presented. Finally, we outline the implications of the use of the suggested methodology on design, manufacturing, and product management.

Defining Product Cost and Reliability Trade-Off Issues

We examine the nature of the reliability and cost trade-off problem that confronts engineers and management. In Chapter 1, a number of alternative methods have been suggested to incorporate cost considerations in the product design process. Most methods focus on product simplification or target costing as the fundamental means of controlling product cost.^{59 60} Yet these approaches do not consider the interaction between product performance and cost, and offer no systematic approach to assessing the impact of product configuration changes on cost.

There are three current approaches to product configuration management. First, design based methods, such as design for manufacture, focus on restricting product design to a subset of feasible product configurations. The underlying premise of design based techniques is that the restriction of acceptable product configurations to a subset composed of simplified component designs results in lower manufacturing costs. Several shortcomings of this approach have been pointed out, most importantly, that focusing on reducing product assembly may yield designs requiring longer development lead times, thereby lowering net present values for the future income stream from the product.⁶¹

Second, time-based methods, such as concurrent engineering, focus on coordinating and paralleling design activities in order to minimize the time needed to introduce a product. The assumption of time-based methods is that product market share is determined by the rapidity with which new products are introduced, and the time a product may have an effective monopoly due to the absence of competitors. Concentrating on development time can result in poor product design due to inadequate

testing. Evidence on time-based product development indicates market advantages accrue to the firms introducing neoteric products.⁶² By contrast, many products are evolved from previous designs, conditions wherein improved product performance would confer marketing advantages. The inability of time-based development techniques to assess and improve the design configuration of a product is an obstacle to its implementation as an engineering-management tool.

Third, cost-based methods, such as target costing, focus on restricting overall product cost and allocating component cost as a portion of the total product cost. Target costing requires management to identify the appropriate selling price and the resulting manufacturing cost of the product prior to the initiation of the design process.^{63 64} The overall manufacturing cost is then allocated among the component parts. The problem in applying cost-based approaches to product design is the preference it places on reducing manufacturing costs without considering product performance.

The difficulty confronting engineers is that no existing techniques provide guidelines to enhancing product performance and assessing the impact of design changes on product cost. In order to undertake the rational design of a product, engineers and management require a design methodology that provides a consistent, technically valid means of assessing a product design configuration, and to rationally explore trade-offs between product reliability and cost. In assessing component reliability the designer would like to address two fundamental questions. First, determine the minimum cost required to attain a desired level of product reliability. Second, the maximum reliability

that can be attained for a given cost. These two issues are related, and form the basis of the reliability/cost problem.

Improving Product Reliability

We now examine alternative methods to increase product reliability. Specifically, we seek to determine how design changes can be made to improve product reliability.

If we assess product reliability using first-order reliability methods, the reliability estimate is based on an examination of the applicable limit state that defines the failure mode of interest. The general form of the limit states used by FORM is

$$g(R, S) = R - S$$

where: R = resistance or strength (5.1)
 S = stress

The stress and strength variables are not deterministic, but random variables. Both the stress and strength elements of the general limit state can be rewritten to represent any particular phenomena of interest. There are three alternative means of modifying the reliability of a product subjected to a limit state failure mechanism. These three alternatives are:

1. change the mean value of a variable;
2. reduce the variance of the variables that the failure mode is most sensitive to;
3. truncate the distribution of variables that the failure mode is most sensitive to.

In many cases it will not be practical to apply all three methods of improving reliability to each variable identified in the governing limit-state relationship. As an example, we may not be able to identify a methods to change the mean value of a physical

constant, but reducing its variance through testing may be practical. Thus, knowledge of the behavior and limitations on limit state primitive variables is needed in order to select the appropriate means of improving the system reliability.

Modifying the variable mean values will often result in unique changes to the product design and hence its manufacturing costs. Employing techniques to reduce variance or truncate the distributions of variables will not require redesign of the product, but will result in changes to product manufacturing processes thereby affecting product cost.

Product Design Using Sequential Linear Approximation

We have examined the three means of altering product reliability. We now define a methodology to undertake the rational exploration of reliability and cost trade-offs for a product. Specifically, we wish to determine an optimal means of improving the product reliability, subject to both physical and cost constraints.

We begin by determining the sensitivity of the probability of failure to changes in the parameters of the primitive variables. These sensitivities can be determined from either numerical methods or closed-form solutions. Utilization of closed-form sensitivity estimation methods would eliminate the need for repeated application of FORM or Monte Carlo simulation. Madsen et al.⁶⁵ demonstrated the sensitivity of the reliability index to changes in the distributional parameters of a primitive variable to be,

$$\frac{\partial}{\partial p_i} \beta(\mathbf{p}_o) = \frac{1}{\beta} \bar{y}^{*T} \cdot \frac{\partial}{\partial p_i} \bar{y}^* = \frac{1}{\beta} \bar{y}^{*T} \cdot \frac{\partial}{\partial p_i} T(z^*, \mathbf{p}_o) \quad (5.2)$$

Note that z^* is taken to be the inverse of the Rosenblatt transformation and y^* is the most probable point determined by the FORM analysis. In addition, Madsen et al.⁶⁶ also demonstrated the sensitivity of the probability of failure to the changes in the reliability index, which was demonstrated to be,

$$\frac{\partial}{\partial p_i} P(F(\bar{y}, \mathbf{p}_o)) \approx \phi(-\beta(\mathbf{p}_o)) \cdot \frac{\partial}{\partial p_i} \beta(\mathbf{p}_o) \quad (5.3)$$

If we combine equations (5.2) and (5.3), we can define the sensitivity of the probability of failure in terms of the elements of the most probable point, y^* , to be,

$$\frac{\partial}{\partial p_i} P(F(\bar{y}, \mathbf{p}_o)) \approx \phi(-\beta(\mathbf{p}_o)) \cdot \frac{1}{\beta} \bar{y}^{*T} \cdot \frac{\partial}{\partial p_i} T(z^*, \mathbf{p}_o) \quad (5.4)$$

Since the Rosenblatt transformation is known for many common distribution types, equation (5.4) can be evaluated in closed form. Thus, the sensitivity of the probability of failure to changes in the distribution parameters of the primitive variables can be found once a FORM analysis has been conducted on the proposed design configuration.

Determining the probability of failure sensitivity to truncation of a primitive variable is not possible in closed form. Evaluation of the failure sensitivity to truncation must therefore depend on either estimation using numerical techniques or approximation by finding the equivalent sensitivity by reduction of the distribution variance. Numerical estimation of the failure sensitivity can be computed using either Monte Carlo simulation or by repetition of the FORM analysis with a single variable truncated. The failure sensitivity can also be approximated by determining the equivalent distribution obtained by reduction of variance.

Having found the sensitivities of the probability of failure, we need to determine the cost sensitivities corresponding to each possible change in the primitive variables. Since we are interested in changes from a proposed design, we do not need to assess the total cost of the product, merely the differential costs associated with specific changes in the product configuration. The determination of such costs will be dependent on the specific means used to affect each primitive variable characteristic. Some costs can be determined from proprietary manufacturing information, others can be estimated by examining changes in production processes and approximating the reduction or increase in processing costs. Sources for such standard manufacturing process information include Designing for Economical Production⁶⁷, and the Machining Data Handbook⁶⁸.

Once the sensitivities of the probability of failure and cost have been determined for changes in the distributional characteristics of the primitive variables, the overall change in product cost and reliability for a set of modifications to the primitive variables can be estimated. The change in the product reliability can be estimated as,

$$\Delta P(F(\bar{y}^*, \mathbf{p}_o)) \approx \sum_{i=1}^n \left(\frac{\partial}{\partial p_i} P(F(\bar{y}^*, \mathbf{p}_o)) \cdot \Delta p_i \right)$$

(5.5)

where: Δp_i = change in parameter i

n = number of changes in primitive variable distribution characteristics

The change in the product cost can be estimated as,

$$\Delta C(\mathbf{p}_o) \approx \sum_{i=1}^n \left(\frac{\partial}{\partial p_i} C(\mathbf{p}_o) \cdot \Delta p_i \right)$$

where: $\frac{\partial}{\partial p_i} C(\mathbf{p}_o)$ = cost sensitivity due to changes in distribution characteristic i . (5.6)

With a means of estimating the impact of design modifications on product reliability and cost, it is now possible to formulate a constrained optimization problem to determine the optimal design change. As noted earlier, the designer may consider assessing a design in terms of the minimum cost required to attain a desired level of reliability, or the maximum reliability that can be attained for a given cost. Either of these approaches can be explored by the construction of a linear programming model.

Sequential Linear Approximation Method-Overview

Consider the problem of assessing the minimum cost required to achieve a specified level of reliability. In this case the objective function is one of minimizing the change in product cost subject to a number of constraints. Among the constraints is a requirement for the estimated change in probability to exceed a specified amount, as well as constraints on the feasible range for each change in a primitive variable. Thus the linear programming formulation would be of the form,

$$\text{MIN Cost} = \sum_{i=1}^n \left(\frac{\partial}{\partial p_i} C(\mathbf{p}_o) \cdot \Delta p_i \right)$$

Subject to:

$$\sum_{i=1}^n \left(\frac{\partial}{\partial p_i} P(F(\bar{y}^*, \mathbf{p}_o)) \right) \cdot \Delta p_i \geq Q$$

(5.7)

$$\forall \Delta p_i \leq L_i$$

$$\forall \Delta p_i \geq 0$$

where: Q = Required Change in Probability of Failure

L_i = Maximum Allowable Change in Distribution Characteristic i

In addressing the problem of determining the maximum reliability that can be attained for a given cost, the objective function and the first constraint are exchanged. The other constraints on the allowable change in individual distribution characteristics are unaltered. This yields a linear program of the form:

$$\begin{aligned} \text{MAX Reliability} &= \sum_{i=1}^n \left(\frac{\partial}{\partial p_i} P(F(\bar{y}^*, \mathbf{p}_o)) \cdot \Delta p_i \right) \\ \text{Subject to:} \\ \sum_{i=1}^n \left(\frac{\partial}{\partial p_i} C(\mathbf{p}_o) \cdot \Delta p_i \right) &\leq MC \\ \forall \Delta p_i &\leq L_i \\ \forall \Delta p_i &\geq 0 \end{aligned} \tag{5.8}$$

where: MC = Maximum Allowable Cost Change

Once the appropriate linear programming model had been formulated a feasible solution to the problem can be found. The feasible solution to the problem indicates the required changes in initial primitive variable characteristics that yield the optimal objective function value. The product primitive variable characteristics are then modified according to the results of the linear program feasible solution, and based on these revised variable values, an updated FORM estimate of the product reliability is generated.

With these results, the procedure to undertake the sequential linear approximation method (SLAM) can be summarized in the following steps:

Step 1 Define the initial product design configuration.

Step 2 Define the appropriate limit states that are likely to affect the proposed design.

- Step 3** Construct a permissibility matrix which identifies the feasible changes in the distribution characteristics of every primitive variable in the limit state.
- Step 4** Use FORM to estimate the probability of failure, $P(F)$, and the most probable point, y^* . If the probability of failure meets performance specifications, stop; otherwise continue to step 5.
- Step 5** Calculate the probability of failure sensitivities, $\partial P(F)/\partial p_i$, for the feasible changes in distribution characteristics of every primitive variable.
- Step 6** Calculate the cost sensitivities, $\partial C/\partial p_i$, for the feasible changes in distribution characteristics of every primitive variable.
- Step 7** Formulate the linear programming model required.
- Step 8** Use the linear program to determine the required changes in primitive variable distribution characteristics, Δp_i . Using the estimated changes in distribution characteristics found in step 8, return to step 4, and update the estimated product reliability.

A flowchart detailing the methodology enumerated above is presented in Figure 12.

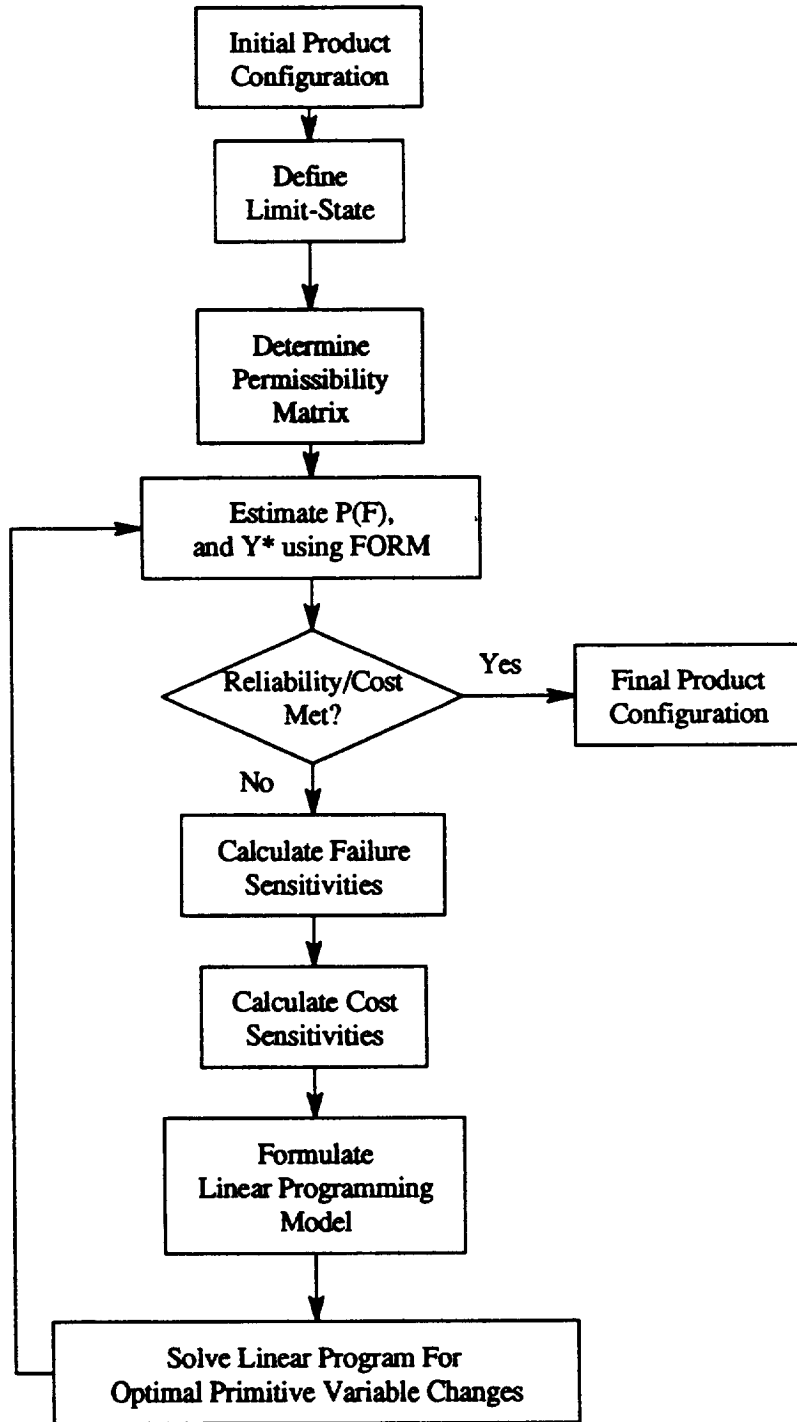


Figure 12: Sequential Linear Approximation Method

Applying the Sequential Linear Approximation Method

We now demonstrate the application of the sequential linear approximation method by way of example. Consider the design of a water pump for a large stationary emergency diesel generator. The unit is an 8 cylinder, 4-cycle diesel engine rated at 3500 kW, operating at 450 rpm. From analysis of the engine cooling needs, approximately 800 gpm of coolant water will be required during engine operation. Based on shear stress and allowable torsional twist, the water pump shaft should be at least 1.5 inches in diameter and 12 inches long. The pump rotates at 300 rpm and drives an 8 inch diameter steel impeller. The shaft rotates in a solid bushing bearing. The allowable wear on the shaft after 2 years of operation must not exceed 0.007 inches in order to maintain acceptable alignment of the drive gear train. We are interested in examining the pump design to demonstrate how to attain a desired reliability for minimum cost, as well as how much improvement in reliability can be attained for a fixed cost level.

The initial pump shaft design parameters are presented below.

Table 3: Pump Shaft Initial Variable Parameters

Variable	Mean	Standard Deviation	Distribution Type
Allowable Wear	0.007	0.0005	Normal
Coefficient of Wear	3.0E-7	1.0E-7	Lognormal
Shaft Diameter	1.500	0.001	Normal
Bushing Length	2.00	0.10	Normal
Applied Load	10.0	2.00	Normal
RPM	300.0	60.0	Normal
Brinell Hardness	235.0	25.0	Normal
Operating Hours	17520.0	1500.0	Normal

We will now consider the case of minimizing the product cost required to attain a desired degree of reliability.

Step 1 Define the initial product design configuration.

The initial values of the primitive variables have already been stated.

Step 2 Define the appropriate limit states that affect the shaft.

We are interested in the reliability of the pump shaft with respect to wearing of the shaft due to the bearing. This form of wear can be characterized as adhesive wear, with a limit state of the form,

$$g(C_k, Al, D, Bl, RPM, HRS, HB, W_{all}) = W_{all} - \frac{C_k \cdot \left[\frac{Al}{D \cdot Bl} \right] \cdot RPM \cdot 60 \cdot HRS \cdot \pi \cdot D}{HB \cdot 1422}$$

where: W_{all} = Allowable Wear

C_k = Coefficient of Wear

Al = Applied Load

D = Shaft Diameter

Bl = Bushing Length

RPM = Revolutions per Minute

HRS = Hours of Operation

HB = Brinell Hardness Number

(5.9)

Step 3 Construct a permissibility matrix.

We seek to determine the feasible changes that could be made in each of the limit state primitive variables. Changes in the allowable wear are not considered feasible, since modifying the allowable wear would negatively affect the performance of the drive gear train, which is outside the consideration of this problem.

The coefficient of wear, C_k , can be changed. The mean of the coefficient of wear can be reduced through the addition of lubrication delivery systems to the pump assembly. The standard deviation of the coefficient of wear can be reduced through experimentation to obtain better estimates of its value. A method of truncating the coefficient of wear is not known, and hence was not considered.

The mean and standard deviation of the bushing length, Bl , can be changed to 2.25 inches and 0.01 inch respectively. In addition, bushings could be inspected

to select bushings that exceed 2.00 inches. This inspection process would be equivalent to a 50% truncation of the bushing length distribution.

The applied load on the shaft, Al , could be reduced from 10.00 lbs to 6.40 lbs by the removal of material from the shaft and impeller attained through additional machining. The primary weight saving would be the result of hollowing out the shaft. The standard deviation in the shaft cannot be reduced, since the primary source of fluctuations in the applied load results from fluid pressure variations. Truncation of the fluid pressure fluctuations can be achieved by incorporating a pressure relief valve. Such truncation would allow truncation of the applied load either above 15 lb. or 11 lb.

The shaft speed of rotation, RPM , can be reduced by using a different impeller configuration. Reduction in the standard deviation of the shaft speed could be achieved by powering the pump from an electric motor in place of the current mechanical drive. Truncation of the shaft RPM can be achieved by incorporating a fluid coupling and governor in the mechanical drive assembly.

The mean of the Brinell hardness of the shaft, HB , can be increased by flame hardening the shaft after machining. The Brinell hardness could be increased from 235 to 450 Hb. Reducing the standard deviation of the Brinell hardness requires implementation of process controls and designed experiments. Truncation of the Brinell hardness could be achieved by inspection of pump shafts and rejection of those with unacceptable low values. The degree of truncation of

Brinell hardness was assumed to be feasible over 0 to 50% of the variable distribution.

Both the shaft diameter, D , and the operating hours, HRS , distribution characteristics cannot be modified.

Given these restrictions, the feasible changes in the primitive variables are outlined in the following permissibility matrix.

Table 4: Pump Shaft Permissibility Matrix

Variable	Initial μ	New μ	Initial σ	New σ	Initial Truncation	Possible Truncation
W_{all}	0.007	N/A	0.0005	N/A	0%	N/A
C_k	3.0E-7	1.0E-8	1.0E-7	10E-8	0%	N/A
D	1.500	N/A	0.001	N/A	0%	N/A
$B1$	2.00	2.25	0.10	0.01	0%	0-50%
$A1$	10.00	6.40	2.00	N/A	0%	6% or 30%
RPM	300.0	200.0	60.0	10.0	0%	2.3%,16%,50%
HB	235.0	450	25.0	10.0	0%	0-50%
HRS	17520.0	N/A	1500.0	N/A	0%	N/A

Step 4 Use FORM to estimate the probability of failure, $P(F)$, and the most probable point.

Applying FORM techniques to the wear limit state results in an initial estimation of the probability of failure for the shaft to be 13.17%. The value of the reliability index, β , is 1.1182. The most probable point vector values are shown below.

Table 5: Most Probable Point Vector Values

Variable	y^*
W_{all}	-0.1813
C_k	0.8128
D	0.0000
Bl	-0.1261
Al	0.4589
RPM	0.4589
HB	-0.2746
HRS	0.2107

Since the probability of failure of 13% exceeds our design goal of a probability of failure below 4 %, we must determine how to improve the reliability of the pump assembly.

Step 5 Calculate the failure sensitivities.

The relationship to determine the failure sensitivities for changes in the mean and standard deviation of the primitive variables are given in equation (5.4) . This relationship requires knowledge of the Rosenblatt transformation for the specific distribution of each primitive variable. In our case all the variables are either normally, or lognormally distributed, distributions for which the Rosenblatt transformations are well known.

If the variable is normally distributed then the transformation is given by,

$$U_1 = \frac{Z_1 - \mu_1}{\sigma_1} \quad (5.10)$$

The sensitivities of the reliability index to changes in the mean and standard deviation of normally distributed variables are ⁶⁹,

$$\begin{aligned} \frac{\partial \beta}{\partial \mu_1} &= -\frac{u_1^*}{\beta \cdot \sigma_1} \\ \frac{\partial \beta}{\partial \sigma_1} &= -\frac{(u_1^*)^2}{\beta \cdot \sigma_1} \end{aligned} \quad (5.11)$$

If the variable is lognormally distributed, then the transformation is given by ⁷⁰,

$$U_2 = \frac{\log Z_2 - E[\log Z_2]}{D[\log Z_2]}$$

$$\text{where: } E[\log Z_2] = \text{mean} = \log \mu_2 - \frac{1}{2} \log(1 + COV_2^2) \quad (5.12)$$

$$D[\log Z_2] = \text{standard deviation} = \sqrt{\log(1 + COV_2^2)}$$

The sensitivities of the reliability index to changes in the mean and standard deviation of lognormally distributed variables are ⁷¹,

$$\frac{\partial \beta}{\partial \mu_2} = -\frac{u_2^*}{\beta \cdot \mu_2 \cdot \sqrt{\log(1 + COV_2^2)}}$$

$$\frac{\partial \beta}{\partial COV_2} = -u_2^* \frac{COV_2}{\beta \cdot \sqrt{\log(1 + COV_2^2)} \cdot (1 + COV_2^2)} \left(\frac{u_2^*}{\sqrt{\log(1 + COV_2^2)}} - 1 \right) \quad (5.13)$$

Using equations (5.11), (5.13), and (5.4) the sensitivity of the probability of failure to changes in the mean and standard deviation of every primitive variable can be found. The sensitivity of the probability of failure to truncation of the primitive variable distributions must be found. The probability of failure sensitivities to variable truncation were determined in two ways. First, FORM analysis was conducted assuming truncation of the random variable and the change in the probability of failure was noted. Subsequently a probability of failure sensitivity measure was determined. Second, a probability of failure sensitivity was found by finding the reduction in the standard deviation required to ensure that less than 0.1-1.0% of the tail of the distribution exceeded a Z value corresponding to the truncation Z value. The two sensitivity measure were then compared, and it was found that in the case of normally distributed variables, the two methods exhibited less than 3% variation.

Using these methods, the probability of failure sensitivities can be determined and are shown below.

Table 6: Probability of Failure Sensitivities-First Iteration Results

Variable	$\partial P(F)/\partial \mu$	$\Delta \mu$	$\partial P(F)/\partial \sigma$	$\Delta \sigma$	$\partial P(F)/\partial tr.$	% truncation
C_k	0.1089	0-2.9E-7	0.06034	9.0E-8	N/A	N/A
Bl	0.2403	0-0.25	0.00273	0.09	0.00325	0-50%
Al	0.04373	0-3.6	N/A	N/A	0.00102/ 0.04397	6%/ 30%
RPM	0.00146	0-100	0.03345	50	0.0037 0.0024 0.0675	2.3% 16% 50%
HB	0.00209	215	0.00863	15	0.00701	0-50%

Step 6 Calculate the cost sensitivities for feasible changes in the distribution characteristics.

Determining the cost sensitivities for changes in the distribution characteristics is found by specifying how such changes can be achieved. For example, reducing the applied load from 10 to 6.4 lbs can be achieved by making the shaft hollow. In this case, the machining time required to bore out can be estimated to be 15 minutes plus 5 minutes for set-up, assuming lot production practices⁷². Assuming an hourly cost of \$60, the hole costs \$5.57/lbm removed, and a fixed charge of \$1 for tooling is incurred. Thus, the cost incurred for each

possible change in the primitive variable characteristics can be fixed, variable or a combination of fixed and variables charges.

It was assumed that 500 unit were to be produced. The cost sensitivities of each primitive variable change were determined to be:

Table 7: Cost Sensitivities-First Iteration Results

Variable	Type of Change	Fixed Cost	Variable Cost
C_k	shift μ	0	1.5
C_k	reduce σ	50	0
B1	shift μ	1	8
B1	reduce σ	2	0
B1	truncation 0-50%	0.40	0.25
A1	shift μ	1	5.57
A1	truncation 6%	20	0
A1	truncation 30%	35	0
RPM	shift μ	0	2
RPM	reduce σ	400	0
RPM	truncation 2.3%	30	0
RPM	truncation 16%	80	0
RPM	truncation 50%	110	0
HB	shift μ	3	0.14
HB	reduce σ	50	0
HB	truncation 0-50%	1	2.4

Step 7 Formulate the linear program.

Since we wish to determine the minimum cost that will result in a probability of failure of 4%, the linear program model should be of the form outlined in equation (5.7). Using the information contained in the permissibility matrix, the probability of failure sensitivities, and the cost sensitivities, the formulated linear program is given below.

$$\begin{aligned} \text{MIN Cost} = & 1.5x_1 + 50x_2 + 8x_3 + 1x_4 + 2x_5 + 0.25x_6 + 0.40x_7 + 5.57x_8 \\ & + 1x_9 + 20x_{10} + 35x_{11} + 2x_{12} + 400x_{13} + 30x_{14} + 80x_{15} \\ & + 110x_{16} + 0.14x_{17} + 3x_{18} + 50x_{19} + 2.4x_{20} + 1x_{21} \end{aligned}$$

Subject to:

$$\begin{aligned} & 0.001089x_1 + 0.06034x_2 + 0.2403x_3 + 0.00273x_5 + 0.00324x_6 + 0.04373x_8 \\ & + 0.00102x_{10} + 0.04397x_{11} + 0.00146x_{12} + 0.00335x_{13} + 0.00037x_{14} + 0.00240x_{15} \\ & + 0.06746x_{16} + 0.002093x_{17} + 0.00863x_{19} + 0.00701x_{20} \geq 0.09174 \end{aligned}$$

$x_1 \leq 100$	maximum allowable change in mean of C_k
$x_3 \leq 0.25$	maximum allowable change in B1
$x_3 - 10000x_4 \leq 0$	assess fixed charge if $x_3 > 0$
$x_6 \leq 50$	maximum allowable truncation of B1
$x_6 - 10000x_7 \leq 0$	assess fixed charge if $x_6 > 0$
$x_8 \leq 3.6$	maximum allowable change in A1
$x_8 - 10000x_9 \leq 0$	assess fixed charge if $x_8 > 0$
$x_{12} \leq 100$	maximum allowable change in RPM
$x_{17} \leq 215$	maximum allowable change in HB
$x_{17} - 10000x_{18} \leq 0$	assess fixed charge if $x_{17} > 0$
$x_{20} \leq 50$	maximum allowable truncation of HB
$x_{20} - 10000x_{21} \leq 0$	assess fixed charge if $x_{21} > 0$

The additional constraints for the binary variables are:

$$\begin{aligned}
 x_2 &= \begin{cases} 1 & \text{if } \sigma_{C_k} \text{ is reduced} \\ 0 & \text{otherwise} \end{cases} \\
 x_5 &= \begin{cases} 1 & \text{if } \sigma_{Bl} \text{ is reduced} \\ 0 & \text{otherwise} \end{cases} \\
 x_{10} &= \begin{cases} 1 & \text{if Al is truncated less than 15} \\ 0 & \text{otherwise} \end{cases} \\
 x_{11} &= \begin{cases} 1 & \text{if Al is truncated less than 11} \\ 0 & \text{otherwise} \end{cases} \\
 x_{13} &= \begin{cases} 1 & \text{if } \sigma_{RPM} \text{ is reduced} \\ 0 & \text{otherwise} \end{cases} \\
 x_{14} &= \begin{cases} 1 & \text{if RPM is truncated less than 420} \\ 0 & \text{otherwise} \end{cases} \\
 x_{15} &= \begin{cases} 1 & \text{if RPM is truncated less than 360} \\ 0 & \text{otherwise} \end{cases} \\
 x_{16} &= \begin{cases} 1 & \text{if RPM is truncated less than 300} \\ 0 & \text{otherwise} \end{cases} \\
 x_{19} &= \begin{cases} 1 & \text{if } \sigma_{HB} \text{ is reduced} \\ 0 & \text{otherwise} \end{cases} \\
 x_{10} + x_{11} &\leq 1 && \text{only 1 truncation of Al permitted} \\
 x_{14} + x_{15} + x_{16} &\leq 1 && \text{only 1 truncation of RPM permitted} \\
 \forall x_i &\geq 0 && \text{for } i = 1, 2, \dots, 21
 \end{aligned}$$

Step 8 Estimate the required changes in primitive variable values.

Solving the linear program using available computer software yields the following estimated changes in the primitive variable distribution characteristics required to achieve 4% probability of failure.

Incremental product cost = \$7.6195/unit

Shift $\mu_{BL} = +0.25 \rightarrow \mu_{BL}=2.25$ "

Shift $\mu_{AL} = -0.35359 \rightarrow \mu_{AL} = 9.64641$ lbs

Truncate distribution of the bushing length by 50% \rightarrow lower limit on bushing length is 2.25".

We now return to step 4 and update the reliability estimate of the component using the revised primitive variable values.

Using the results obtained by the linear program the primitive variable values were changed, and an updated FORM analysis was conducted to determine the reliability of the pump assembly. The updated estimation of the probability of failure is 6.3179% and a reliability index value of 1.5286. The updated most probable point vector values are shown below.

Table 8: Updated Most Probable Point Vector Values

Variable	y^*
W_{all}	-0.2512
C_k	1.1208
D	0.0000
BI	-0.0901
AI	0.6331
RPM	0.6151
HB	-0.3831
HRS	0.2886

Since the probability of failure of 6.3% still exceeds the goal of a probability of failure of 4%, we now repeat the process by updating the probability of failure sensitivities and proceed through the process until the desired reliability is attained.

Repeating the process completely yields an estimated probability of failure of 4.3%, and a reliability index of 1.7125. In order to attain this probability of failure, the Brinell hardness is increased from 235 to 254. The resulting primitive variable parameter values were determined and are shown below.

Table 9: Updated Pump Shaft Variable Parameters

Variables	Mean	Standard Deviation	
W_{all}	0.007	0.0005	
C_k	3.0E-7	1.0E-7	
D	1.500	0.001	
Bl	2.25	0.10	Lower limit=2.25
Al	9.646	2.0	
RPM	300	60	
HB	254	25	
HRS	17520	1500	

The overall cost associated with these changes in the primitive variables is estimated to be \$13.232/unit. Additional repetition of the process would yield a probability of failure less than 4%.

In considering the case of the maximizing the product reliability for a given increase in cost, the procedure is identical with the exception of the formulation of the linear programming model. In this case, the reliability constraint becomes the objective function, and the previous cost minimization objective function becomes a constraint. The determination of the coefficients for reliability maximization is accomplished in the same manner as outlined.

When the reliability maximization problem is considered for the pump shaft problem restricted to a maximum allowable cost increment of \$7.62, the resulting changes in the primitive variable distributional characteristics are identical to those found for the cost minimization case.

Implications of the Sequential Linear Approximation Methodology

Having defined and demonstrated the sequential linear approximation methodology, two implications are evident. First, the application of the proposed methodology will permit the designer/engineer to rationally explore the trade-off between component reliability and cost. More importantly, the designer will be provided with information as to the optimal means of improving a proposed design, with respect to either cost or reliability. The ability to directly link reliability and cost of proposed product

designs provides management with the ability to directly measure the impact of changes in a design on product costs.

The second implication of the methodology is that it provides designers and management with a rapid means of assessing the potential reliability of competing designs. By investigating a proposed design and focusing on the maximum reliability attainable for a specified cost increase, management can evaluate differing alternative designs to determine those designs that offer the greatest potential for improvement.

These two benefits provide managers and engineers with more useful information regarding product cost and reliability than alternative design methodologies.

CHAPTER VI

CONCLUSIONS AND FUTURE RESEARCH

Conclusions

We have developed a design methodology that allows engineers to undertake reliability and cost trade-off analysis. We have shown how current analytical reliability methods cannot be incorporated into the design methodology due to four limitations on their use. First, the absence of physical variables in analytical methods was shown to prevent their use in the assessment of variable changes on reliability. Second, analytical reliability methods were shown not to include the unique operating conditions experience by the component in the reliability estimates. Third, the restriction of analytical reliability methods to the estimation of systems that have attained steady-state failure rate conditions was demonstrated. The time to attain steady state failure rates was shown to be several time greater than the component MTTF, indicating the need to be able to estimate component reliability during this operating time. Fourth, analytical reliability methods were shown not to consider the impact of variance reduction on reliability and cost. These four limitations precluded the use of analytical methods in reliability-cost trade-off methodology.

We have demonstrated the feasibility and validity of extending FORM to mechanical system design. We demonstrated that even at low probabilities of failure FORM and Monte Carlo yield markedly similar results. We detailed how FORM provides

one of two major elements needed in the design paradigm by providing a means of estimating reliability sensitivity to primitive variable distributional changes. We examined how FORM represents a less restrictive reliability methodology since it can be applied to systems that are unique, as well as being valid for the reliability assessment of a system in either steady-state or transient failure rate regimes.

We showed that although the physics-based failure rate reliability method provides for the assessment of the impact of changes in the primitive variable on component reliability, it has several limitations. Physics-based failure rate methods were demonstrated to involve changes in the mean of primitive variables, and consequently, does not allow for the estimation of the impact of variance reduction on component reliability. The reliance of physics-based methods on base failure rates was shown to restrict its application to components with design and operating conditions similar to existing components.

We proved that the base failure rates used by the physics-based failure rate method have a large degree of uncertainty, and that such uncertainty will result in inaccurate reliability estimates. We demonstrated that the uncertainty in the base failure rates exceeds the allowable range of change for the primitive variables, making reliability estimates indistinguishable from the random error of the method. For these reason, the physics-based failure rate method could not be incorporated in the design trade-off method.

Finally, we developed the sequential linear approximation method for assessing component design. We outlined how the method uses reliability and cost to evaluate a component design. Using the sequential linear approximation method, we have

demonstrated how FORM estimates can be incorporated into the methodology to optimize product design. The determination of cost sensitivities to changes in primitive variable distributional parameters, and how such sensitivities are employed by the methodology was developed. The sequential linear approximation method (SLAM) was demonstrated to be an effective means of optimizing the product design with respect to either product reliability or cost. Using the SLAM approach engineers can determine the optimal means to improve product design or to assess the ultimate attainable reliability of a proposed design.

Future Research

The examination of the existing reliability methods has identified several areas for future research. First, determination of a mathematical relationship for the transient period following system commissioning would provide an assessment tool for new systems.

Second, the lack of information on primitive variable distributions and parameter values requires substantial basic research. Additional information on the primitive variable distribution and parameter values would significantly increase the utility of FORM techniques.

APPENDIX A

COMPENDIUM OF MECHANICAL LIMIT STATES

1. Compendium of Mechanical Limit States

1.1 Purpose

The creation of a compendium of mechanical limit states was undertaken in order to provide a reference base for the application of First-Order Reliability Methods to mechanical systems in the context of the development of a system level design methodology. The compendium was conceived as a reference source, specific to the problem of developing the noted design methodology, and not an exhaustive or exclusive compilation of mechanical limit states. The compendium is not intended to be a handbook of mechanical limit states for general use.

1.2 Proposed Use of Compendium

The compendium provides a diverse set of limit-state relationships for use in demonstrating the application of probabilistic reliability methods to mechanical systems. The different limit-state relationships will be used to analyze the reliability of a candidate mechanical system.

1.3 Selection of Limit-States

In determining the limit-states to be included in the compendium, a comprehensive listing of the possible failure modes that could affect mechanical systems was generated. Previous literature defining mechanical modes of failure was studied, and cited failure modes were included. From this, the following classifications for failure modes were derived:

- Wear
- Corrosion
- Fatigue
- Material Degradation

With the definition of the different failure modes, a literature search for each was conducted, with the aim of establishing relationships for each failure mechanism to be used in formulating mechanical limit-states.

The individual failure modes that were determined for each classification are:

Wear

- Adhesive wear
- Abrasive wear
- Lubricated wear
- Fretting wear
- Surface fatigue wear
- Liquid impact erosion

Fatigue

- Low-cycle fatigue
- High-cycle fatigue
- Crack growth

Corrosion

- Erosion-corrosion
- Galvanic corrosion
- Uniform attack
- Pitting corrosion
- Cavitation
- Crevice corrosion
- Stress corrosion cracking
- Selective leaching
- Inter-granular corrosion

Material Degradation

- Thermal degradation
- Radiation damage

Although it was possible to determine the different failure modes that could affect a mechanical system, the identification of relationships for all noted failure modes was not possible. The difficulty in identifying some of the limit-state relationships is due to a lack of accurate analytical models. Consequently, the compendium consists of relationships for those failure modes for which reasonably robust relationships exist.

1.4 Distribution Properties

The compendium does not contain information on the distribution properties of the individual primitive variables. With the exception of fatigue and wear related primitive variables, little research was uncovered that dealt with the distribution properties of limit-state primitive variables. There is significant research available on the best estimates of variables values, and when appropriate some of these values have been included in the relevant sections. The lack of much information on the distribution properties of many primitive variables indicates the need for additional research efforts in this area.

1.5 Form of Limit-State Relationships

The result of the investigation into mechanical limit-states indicate that the vast majority of identified relationships are of the form of a power law. All the limit states cited within the compendium, with the exception of those for uniform attack and thermal degradation, take a power law form.

2. Wear

Wear is the removal of material from solid surfaces as a result of mechanical action. In most cases the amount of the material removed from the surfaces is small in relation to the overall material mass of the components involved.

Wear processes have been identified to conform to four different forms. The four major forms of wear enumerate by Rabinowicz (1965) are:

- 1. Adhesive wear;**
- 2. Abrasive wear;**
- 3. Corrosive wear;**
- 4. Surface fatigue wear.**

In addition to these four major wear processes, there are a number of minor processes that are often categorized as being a wear process.

Models for the following wear processes are presented in sub-sections 1 through 5:

- 1. Adhesive wear**
- 2. Abrasive wear**
- 3. Lubricated wear**
- 4. Fretting wear**
- 5. Liquid impact erosion.**

References

Rabinowicz, E., Friction and Wear of Material, J. Wiley, 1965.

2.1 Adhesive Wear

Definition

"Adhesive wear occurs when two smooth bodies are slid over each other, and fragments are pulled off one surface to adhere to the other" (Rabinowicz, 1965). Once the fragments have been torn from their original surface and attached to the opposing surface, they may reattach to their original surface, or become loose fragments.

Limit-State Formulation

Experimental data indicates that there are three laws of adhesive wear, namely;

1. The amount of wear is generally directly proportional to the load L ;
2. The amount of wear is generally proportional to the distance slid, x ;
3. The amount of wear is generally inversely proportional to the hardness, p , of the surface being worn away.

Holm (1946) proposed that the volume worn away could be described by:

$$V = \frac{cLx}{p}$$

where c = material dependent nondimensional constant

Evidence for this relationship is mixed, with some result being very close to the predicted volumes and other being widely different. Archard (1953) presented a model of sliding which allows for the derivation of the above equation, while providing insight into the meaning of the constant, c . From his model we get the following model for the volume of material worn away through adhesive wear;

$$V = \frac{kLx}{3p}$$

*where k = coefficient of wear
= probability of any junction
forming a fragment*

p = flow pressure of softer metal

As can be seen the difference in these equations is that we have replaced *c* with *k/3*. The only important requirement for the second equation to hold is that the volume of the fragment should be proportional to the cube of the junction diameter.

An alternative form of the second equation is:

$$V = \frac{kA_r x}{3}$$

where A_r = actual area of contact

Although knowledge of the volume worn is important, typically we are more interested in the depth of material worn away. The extension of the above relations to yield the depth of material worn away is given in the Wear Control Handbook (ASME, 1980);

$$\frac{d}{L} = \frac{K P}{H}$$

where d = depth of wear

P = nominal pressure

L = sliding distance

H = material hardness

This form of the wear relationship now permits the estimation of the life of the surface. If we let the sliding distance, L , be expressed as the velocity, v , and the time, t , the relationship becomes:

$$t = \frac{dH}{K P v}$$

The authors go on to demonstrate that the coefficient of wear, K is the proportional of volume worn away to the theoretical worn volume that would have resulted if every asperity contact produced a worn particle.

Model Assumptions

The assumptions of the model are:

1. k =probability of any junction forming a fragment
2. Each junction is in existence throughout the sliding distance, d .

Notes

Values for k can be found in Proceedings of the Conference on Lubrication and Wear (1957 on), and the Transactions of the American Society of Lubrications Engineers (1958-1963).

References

Rabinowicz, E., Friction and Wear of Materials, J. Wiley, New York, 1965.

Holm, R., Electric Contacts, Almquist and Wiksells, Stockholm, 1946.

Archard, J.F., Contact and Rubbing of Flat Surfaces, Journal of Applied Physics, vol. 24, pp. 981-988.

M.B. Peterson and W.O. Winer, eds., Wear Control Handbook, ASME, New York, 1980.

2.2 Abrasive Wear

Definition

Abrasive wear occurs when a rough hard surface, or a soft surface containing hard particles, slides on a softer surface. As a result of the sliding action, the softer surface has a series of grooves ploughed into its surface. The material removed in the creation of the grooves is typically found to be loose particles.

Limit-State Formulation

Rabinowicz (1965), assuming that the hard surface was composed of conical asperities, derived the following relationship:

$$\frac{\partial V}{\partial L} = \frac{L \tan \theta}{\Pi \rho}$$

This equation has the same form as the equation derived for adhesive wear. Thus we can use the same relationship as that for adhesive wear with the following value of the coefficient of wear:

$$k_{abr} = 0.96 \tan \theta$$

References

Avient, B.W.E., J. Goddard, and M. Wilman, *An Experimental Study of Friction and Wear During Abrasion of Metals*, Proceedings of Royal Society, Vol. A-258, pp. 159-180, 1960.

Kruchov, M.M., and M.A. Babichev, *Resistance to Abrasive Wear of Structurally Inhomogeneous Materials*, Friction and Wear in Machinery, Vol. 12, pp. 5-23, ASME, New York, 1958.

Rabinowicz, E., L.A. Dunn, and P.G. Russell, *The Abrasive Wear Resistance of Some Bearing Steels*, Lubrication Engineering, Vol. 17, pp.587-593, 1961.

Rabinowicz, E., Friction and Wear of Materials, J. Wiley, New York, 1965.

2.3 Lubricated Wear

Definition

Lubricated wear occurs when two smooth surfaces are slid over each other in the presence of a lubricating media. The lubricating media serves to partially or completely separate the surface asperities of the opposing surfaces, thereby reducing or eliminating the formation of worn particles.

Failure Mechanism

Lubricated wear occurs when the degree of lubricant separating the two surfaces is insufficient to prevent asperity contact. If asperity contact occurs, then other wear mechanisms can be used to determine the wear.

Even under dry conditions, absorbed gas molecules act as a lubricant, thereby yielding less wear than predicted by theoretical relationships. A more accurate form of the standard wear relationship is (see: Rowe , C.N., *Lubricated Wear*, Wear Control Handbook, eds., M.B. Peterson and W.O. Winer, ASMe, New York, 1980.):

$$\frac{V}{d} = k_m A_m = k_m \alpha A = k_m \alpha \frac{L}{H}$$

where k_m = adhesive wear coefficient free of contaminants

A_m = area of metallic contact

α = fraction of true area which is metal to metal

Rowe then demonstrated:

$$\alpha = \frac{X}{U t_o} e^{-\frac{E}{RT_s}}$$

where X = diameter of area of absorbed lubricant molecule

t_o = fundamental time of vibration of molecule in absorbed state

U = sliding velocity

E = energy of absorption

T_s = surface temperature

The temperature rise in the contact surface can be approximated by:

$$\Delta T = \frac{gfWU}{8JK_{tc}r}$$

where g = gravitational constant

J = mechanical equivalent of heat

K_{tc} = thermal conductivity

f = coefficient of friction

r = radius of contact area

When wear particles begin to interact they breakdown the lubricant film and increase lubricant temperature. The result is collapse of lubricant film and catastrophic wear. This transition is marked by the end of mild wear processes, and the move to insufficient lubrication and catastrophic wear.

$$\frac{L}{U} = \frac{H t_o V}{K_m X d} e^{\frac{E}{RT_s}}$$

If it is assumed that,

$$\frac{V}{d} = \text{Constant at onset of transition}$$

Then,

$$\left(\frac{L}{U}\right)_T = C e^{\frac{B}{TT}}$$

where:

C, B are constants

T = transition load - speed ratio and temperature

2.4 Fretting Wear

Definition

Fretting wear is the removal of material at a component interface that is the result of relative movement of the components, usually of such small magnitude that the movement is not detected by visual inspection.

Failure Mechanism

Fretting wear involves 3 possible basic processes (Waterhouse, 1972):

1. Mechanical action disrupts oxide films on the surface exposing clean and possibly strained metal, which would be reactive and in atmosphere would oxidize rapidly during the cold cycle after disruption.
2. Removal of metal particles from the surface in a finely divided form by a mechanical grinding action or by formation of welds at points of contact which are broken at a surface other than the original interface by shearing or fatigue.
3. Oxide debris resulting from either process 1, or 2 is an abrasive powder that damages the surfaces.

In observation of fretting behavior, research has found that (Waterhouse, 1972):

1. Fretting damage is reduced in a vacuum or inert atmosphere.
2. Debris formed by fretting of iron is largely composed of Fe_2O_3 .
3. Greater damage occurs at low frequencies for a given number of cycles compared with high frequencies.
4. Metal loss increases with load and relative slip.
5. Greater damage occurs below room temperature compared with above room temperature.
6. Damage is greater in dry atmospheric conditions than humid atmospheric conditions.

Uhlig (1954) proposed a model of a regular array of asperities removed by successive cycles. It is assumed that the asperities plough in the metal surfaces. From this a model for the weight loss per cycle due to scraping of the oxide film layer was determined as:

$$W_{CORR} = 2nlck \ln\left(\frac{s}{2lf\tau} + 1\right)$$

where: n = number of circular asperities / unit area

l = distance moved by an asperity in 1/2 cycle

= amplitude of slip

c = diameter of asperity

s = spacing of asperity

f = frequency

τ, k = constants

The weight loss per cycle due to the ploughing action is:

$$W_{MECH} = \frac{2k'lp}{p_o} = k_2lP$$

where: P = normal load

p_o = yield pressure

k', k_2 = constants

Uhlig assumes a linear oxidation rate, so:

$$W_{CORR} = \frac{ncks}{f\tau}$$

Note that:

$$\begin{aligned} \text{asperity spacing} &= n^{0.5} \\ \text{total area of contact} &= np (c/2)^2 \end{aligned}$$

Thus,

$$W_{CORR} = k_o \frac{P^{0.5}}{f} - k_1 \frac{P}{f}$$

$$\text{where: } k_o = \frac{2k}{\tau \sqrt{p_o \pi}}$$

$$k_1 = \frac{4k}{\tau p_o \pi}$$

Combining these results yields,

$$W_{TOTAL} = \frac{(k_o P^{0.5} - k_1 P)N}{f} + k_2 l P N$$

where: N = total number of cycles

The previous relationships apply to the initial fretting which causes a fatigue crack and ultimately causes a fretting fatigue failure. The following notation will be used:

- S_{MAX} = maximum shear stress on asperities of bridge
- p = normal pressure on asperities
- m = coefficient of friction
- p_o = yield pressure of weaker material
- H = hardness of bridge material
- S_{alt} = alternating shear stress in material due to alternating bending stress and frictional shear stress
- s_{alt} = alternating bending stress in material
- s_y = yield strength of weaker material

Assuming that:

- i. $p_o = 3s_y$
- ii. $s_y = k H$

Assuming that the asperity contact is subjected to a shear stress, μp , then the maximum pressure that the asperity on the bridge can sustain is:

$$p = \frac{k_1 H^2}{k_2 + 4\mu^2}$$

Small elements of the material experience alternating shear stress as a result of the alternating motion, the maximum value of which is :

$$S_{alt} = 0.5(4\mu^2 p^2 + \sigma_{alt}^2)^{0.5}$$

When the alternating shear stress, S_{alt} , reaches the fatigue strength of the material in shear, a fatigue crack will be initiated. The bending stress that will yield this critical value of the alternating shear stress is:

$$\sigma_{alt} = \left(4S_{alt}^2 - \frac{4k_1 H^2}{k_2 + 4\mu^2} \right)^{0.5}$$

References

Uhlig, H.H., *Mechanism of Fretting Corrosion*, Journal of Applied Mechanics, ASME Transactions, Vol. 76, 1954, pp.401-407.

Waterhouse, R.B., Fretting Corrosion, Pergammon Press, London, 1972.

2.5 Liquid Impact Erosion

Definition

Liquid impact erosion occurs when the action of a liquid striking a solid object results in the removal of the surface material.

Failure Mechanism

There are several models for liquid impact erosion, namely:

- Thiruvengadam's Theory
- Springer's Theory
- Hertzian Theory
- Evan's Elastic Plastic Theory

Each of these theories is discussed below.

Thiruvengadam's Theory of Liquid Impact Erosion

Thiruvengadam (1967) developed the notion of erosion strength, S_e .

S_e = energy absorbing capacity of material per unit volume under erosive forces.

The erosion process is controlled by 2 opposing phenomena:

1. time-dependent efficiency of absorption of impact energy by the material;
2. attenuation of impact pressure due to changing surface topography as the surface material is eroded.

The intensity of a single drop impact is defined as,

$$I_c = \frac{P_w^2}{\rho_w C_w}$$

where I_c = intensity of impact

P_w = pressure imparted to surface by liquid impact

ρ_w = density of liquid

C_w = compressional wave velocity for liquid

The attenuation of the intensity of impact, I_i , is assumed to be:

$$I_i = \left(\frac{A}{R + R_f} \right)^m I_e$$

where: I_i = attenuated intensity

A = proportionality constant

R = mean depth of erosion from original surface

R_f = thickness of liquid layer on surface

The intensity of erosion, defined as the power absorbed by a unit eroded area of material, is designated, I_e :

$$I_e = S_e \frac{dR}{dT}$$

and

$$I_e = n I_i$$

where $n + n(t)$ is time dependent property governing energy absorption efficiency

This can be constructed into a normalized differential equation, the solution to which is;

$$\bar{\tau} = \frac{n}{\left(1 + k \frac{n+1}{n} \int_1^{\bar{\tau}} \bar{n} d\bar{\tau} \right)^{\frac{n}{n+1}}}$$

This approach has 2 weaknesses:

1. The dependence on the presence of a liquid layer on the surface to attenuate the loading pulses.
2. The parameter, n , is related to the theory, but has no physical meaning in most liquid drop situations, since the liquid layer is either thin or nonexistent.

Springer's Theory of Liquid Impact Erosion

Springer's (1976) theory is based on concepts involving metal fatigue. The model assumes that the incubation period, the acceleration period and the maximum rate period of the characteristic erosion curve can be represented by:

$$M^* = \alpha^* (N^* - N_i^*)$$

where: M^* = erosion mass loss

α^* = rate of mass loss

N^* = number of impacts per site

N_i^* = number of impacts corresponding to the incubation period

Based on Miner's rule in torsion and bending fatigue, Springer derives the expression for impacts in the incubation model:

$$N_i^* = a_1 \left(\frac{S}{P} \right)^{a_2}$$

where: a_1, a_2 = constants

P = avg. interfacial pressure due to water drop impact

and

$$S = \frac{4 \sigma_u (b-1)}{(1-2\nu) [1 - (\sigma_l / \sigma_u)^{b-1}]}$$

where: ν = Poisson's ratio

σ_u = ultimate tensile strength

σ_l = endurance limit

$$b = \frac{b_2}{\log_{10} \left(\frac{\sigma_u}{\sigma_l} \right)} = \text{derived from } S - N \text{ curve}$$

From a least square fits of the data, $a_1 = 7 \times 10^{-6}$, and $a_2 = 5.7$. The weakness of this approach is the arbitrary selection of a constant, b , which is applied to all materials.

Hertzian Impact Theory

Hertzian impact theory (1886) has been employed in the study of body impact. In a collision of a deformable sphere and target, the time dependent radius of contact area is:

$$a(t) = a_1 \sin \frac{1}{2} \left(\frac{\pi t}{T} \right)$$

where: $a_1 = K^{0.2} r v_0^{0.4} = \text{maximum contact radius}$

$T = 2.943 K^{0.4} r v_0 = \text{duration of bodies in contact}$

$$K = 1.25\pi \rho_1 \left[\frac{1}{\rho_1 C_1^2} \right] = \text{elastic properties of impacting bodies}$$

$\rho_1, \rho_2 = \text{density of sphere and target}$

$C_1, C_2 = \text{elastic wave velocity of sphere and target}$

$$C_i^2 = \frac{1}{\rho_i} \frac{E}{(1-\nu^2)}$$

If the liquid is assumed to be a deformable sphere impacting a rigid body, then when the relative velocity between the 2 bodies is 0,

$$a(t) = a_1 = \frac{5}{4} \pi^{0.2} r \left(\frac{V_o}{C_1} \right)^{0.4}$$

Zero relative velocity between the 2 bodies occurs at $t=T/2$.

The magnitude of the liquid impact pressure differs from those of solids, so the following results from the case of water hammer are used:

$$P_w = \rho_w C_w V_0$$

where: ρ_w = density of liquid

C_w = acoustic wave velocity in liquid

V_0 = liquid impact velocity

Accounting for the compressibility of the liquid,

$$P_w = \frac{\rho_w C_w V_0}{1 + \frac{\rho_w C_w}{\rho_t C_t}}$$

where the subscript t , denotes the properties of the target.

The impact of a water drop on a rigid surface was found to be:

$$P_w = \frac{\alpha}{2} \rho_w C_w v_0$$

Evans' Elastic-Plastic Theory

Evans (1976) proposed that the predicted erosion rate is:

$$V = v_0^{19} r^{11} \rho^{19} Ke^{-4} H^{-1}$$

where: V = volume lost / impact

v_0 = impact velocity

r = particle radius

ρ = particle density

Ke = stress intensity factor

H = dynamic hardness

Empirical Models

Due to the complex nature of the processes involved in impact erosion, the traditional approach has been the utilization of models fitted to empirical data. Schmitt (1970) has proposed that impact erosion be modelled using equations of the form:

$$MDPR = KV^\alpha \sin^\beta \theta$$

where: MDPR = mean depth of penetration rate

K = constant

V = velocity

θ = impact angle

α, β = empirically determined exponents

Schmitt notes that uncoated 2-dimensionally reinforced composite materials, beta of 2 is a best fit for velocities between 450 and 1700 m/sec.

References

Evans, A.G., et al., Impact Damage in Brittle Materials in the Plastic Response Regime, Contract No. 00014-75-C-0069, Report No. SC5023.9TR, Rockwell International Center, Thousand Oaks, CA., 1976.

Hertz, H., Miscellaneous Papers, Macmillan and Company, London, 1886.

Schmitt, G.F., Erosion Rate-Velocity Dependence for Materials at Supersonic Speeds, Characterization and Determination of Erosion Resistance, ASTM-STP-474, American Society for Testing and Materials, 1970.

Springer, G.S., Erosion by Liquid Impact, Scripta Publishing Co, J. Wiley, Washington, D.C., 1976.

Thiruvengadam, A., The Concept of Erosion Strength, Erosion by Cavitation or Impingement, ASTM-STP-408, American Society for Testing and Materials, 1967.

3. Corrosion

Corrosion is the destructive attack of a metal by chemical or electrochemical reaction with its environment (Uhlig, 1971). The destruction of a metal surface by physical causes is not classified as corrosion.

The major classifications of corrosion given by Fontana (1986) are:

1. Erosion-corrosion
2. Galvanic corrosion
3. Uniform attack
4. Pitting corrosion
5. Cavitation
6. Crevice corrosion
7. Stress corrosion cracking
8. Selective leaching
9. Intergranular corrosion

Models for the first six forms of corrosion were found, and are presented in sub-sections 1 through 6 that follow. At this time no deterministic relationships were found that accurately predict stress corrosion cracking, selective leaching, or intergranular corrosion.

References

Fontana, M., Corrosion Engineering, 3rd Edition, McGraw-Hill Book Co., San Francisco, 1986.

Uhlig, H., Corrosion and Corrosion Control, 2nd Edition, J. Wiley & Sons, New York, 1971.

3.1 Erosion-Corrosion

Definition

Erosion-corrosion is defined as the accelerated corrosion of a metal as a result of a flowing fluid disrupting or thinning a protective film of corrosion products.

Failure Mechanism

The transition from laminar to turbulent flow occurs over a velocity range and is dependent on the geometry, surface roughness, and liquid viscosity. The conditions of fluid flow and the transition to turbulent flow is predicted using the Reynolds number:

$$Re = \frac{V d}{\gamma}$$

where: V = velocity (m / s)

d = characteristic specimen length (m)

γ = kinematic viscosity (m^2 / s)

When a liquid exhibits predominantly turbulent flow, a thin laminar sublayer, of thickness δ_h , exists near the metal surface as a result of viscous drag. If material is being removed from the metal surface there will be a diffusional boundary layer of thickness δ_d , (Poulson, 1983). The Schmidt number describes the relationship between these two boundary layers:

$$Sc = \frac{\gamma}{D}$$

where: D = diffusivity of the relevant species (m / s)

As the value of the Schmidt number increases the diffusion layer will become thinner, and its formation occur more rapidly (Poulson, 1983).

In most cases the resistance of the surface to mass transfer, both laminar and turbulent regions of flow, is accomplished through the definition of the mass transfer coefficient, K , as:

$$K = \frac{\text{rate of reaction}}{\text{concentration driving force}}$$

The mass transfer rate is more conveniently described by a dimensionless number, the Sherwood number,

$$Sh = \frac{K d}{D}$$

For reactions that are governed by mass transfer, the relationship between the Sherwood, Reynolds, and the Schmidt numbers is found by empirical results to be of the form,

$$Sh = \text{constant} \cdot Re^x \cdot Sc^y$$

Typical experimental results indicate that x is usually 0.3-1, and y is 0.33. These values are applicable in cases where the surface is initially smooth. The case of rough surfaces subjected to mass transfer is outlined below. In addition, the consideration of different surface configurations that may be subject to erosion-corrosion is accommodated by the constant in the above equation, a constant that is geometry dependent. The most common geometries studied, and some results are outlined in the next section.

When a metal is subjected to erosion corrosion it will develop scallop shaped ridges. The roughening due to the creation of these ridges tends to increase the mass transfer rate, and the rate of erosion corrosion. The availability of relationships defining either mass transfer or erosion corrosion from rough surfaces is extremely limited. Recent work has indicated that once a surface is roughened, the rate of mass transfer is governed by roughness, not the geometry of the surface (Poulson, 1990). More importantly, the results indicate that a universal governing relationship for mass transfer for roughened surfaces may exist, namely,

$$Sh = 0.01 Re Sc^{0.33}$$

The results indicating such a result are shown in Figure 1, taken from Poulson (Corr. Sc., 1990). Poulson does indicate that the main differences between geometries is their tendency to roughen; he cites that bends in pipes tend to roughen faster, probably as a result of their attaining a critical Reynolds number more easily. Although the smooth surface mass transfer relationships are useful for the prediction of initial rates of erosion corrosion, the roughened surface relationship will govern the erosion corrosion process once the surface is no longer smooth. The precise point at which the roughened surface relationship is applicable has yet to be established.


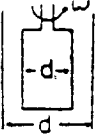
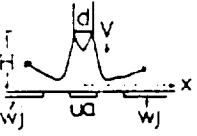
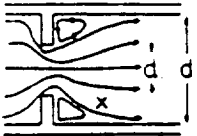
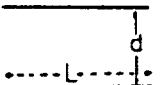
References

- Abdulsalam, M., and J.T. Stanley, *Steady-State Model for Erosion-Corrosion of Feedwater Piping*, Corrosion, Vol. 48, no. 7, pp. 587-593, 1992.
- Heitz, E., *Chemo-Mechanical Effects of Flow on Corrosion*, Corrosion Engineering, Vol. 47, no. 2, pp. 135-145, 1991.
- Kappesser, R., I. Cornet, and R. Greif, *Mass Transfer to a Rough Rotating Cylinder*, Electrochemical Science, Dec. 1971, pp. 1957-1959.
- Markin, A.N., I.S. Sivokin, and A.G. Krushodov, *Mathematical Simulation of Corrosion-Electrochemical Processes*, Corrosion, Vol. 47, no. 9, pp. 659-664, 1991.
- Nesic, S., and J. Postlethwaite, *Relationship between the Structure of Disturbed Flow and Erosion-Corrosion*, Corrosion, Vol. 46, no. 11, pp. 874-880, 1990.
- Nesic, S., and J. Postlethwaite, *A Predictive Model for Localized Erosion-Corrosion*, Corrosion, Vol. 47, no. 8, pp. 582-589, 1991.
- Nesic, S., and J. Postlethwaite, *Hydrodynamics of Disturbed Flow and Erosion-Corrosion: Part I-Single-Phase Flow Study*, Canadian Journal of Chemical Engineering, Vol. 69, pp.698-710, June 1991.
- Poulson, B., *Electrochemical Measurements in Flowing Solutions*, Corrosion Science, Vol. 23, no. 4, pp. 391-430, 1983.
- Poulson, B., *Mass Transfer from Rough Surfaces*, Corrosion Science, Vol. 30, no. 6/7, pp. 743-746, 1990.

Initial Erosion Corrosion Geometry-Dependent Relationships

The following table gives the initial smooth surface erosion corrosion rates.

(From Poulson, B., *Electrochemical Measurements in Flowing Solutions*, *Corrosion Science*, vol. 23, no. 4, pp. 391-430, 1983)

ROTATING DISC		$Re = \frac{\omega r^2}{\gamma}$ $Re_c = 17.35 \times 10^5$	$\bar{Sh}_w = 0.6205 Re^{0.5} Sc^{0.33}$ $\bar{Sh}_c = 0.0078 Re^{0.9} D_c^{0.33}$
ROTATING CYLINDER		$Re = dV = \frac{\omega d^2}{2\gamma}$ $Re_c \sim 200$	$\bar{Sh}_{rot} = 0.079 Re^7 Sc^{0.365}$ $\bar{Sh}_{rot} = (1.25 + 5.76 \log d/\lambda) Re Sc$
IMPINGING JET		$Re = \frac{dV}{\gamma}$ $Re_c \approx 2000$	$\bar{Sh}_w = 1.12 Re Sc^{1/(1+1/d)}$ $Sh_w = 0.65 Re^2 (x/d)$
NOZZLE OR ORIFICE		$Re_c = \frac{dV}{\gamma}$ $Re_c \sim 600$	$Sh_w = 0.276 Re^{0.7} Sc^{0.33}$ $\frac{Sh_c}{Sh_w} = 1 + A \left[1 + B \left(\frac{Re^{0.7}}{0.0165 Re^{0.7}} - 2 \right) \right]$
TUBE		$Re = \frac{dV}{\gamma}$ $Re_c \approx 2000$	$\bar{Sh}_c = 1614 (Re Sc d/L)^{0.5}$ $\bar{Sh}_w = 0.276 Re^{0.7} Sc^{0.33} (d/L)^{0.5}$ $\bar{Sh}_{rot} = 0.0165 Re^{0.7} Sc^{0.33}$

Symbol	Geometry	Technique	Equation	Ref
n	25d 180° bend in 226mm tube	copper in 1N HCl+4g/l Fe ³⁺	Sh=01Re ^{.98} Sc ^{.33}	16
┘	95mm impinging jet at height 95mm		Sh=065 Re ^{1.02} Sc ^{.33}	17
◻	rotating cylinder $\frac{d}{\epsilon}=87$	LCDT	Sh=016 Re ^{.95} Sc ^{.33}	10
•	90mm pipe	plaster dissolution	Sh=02 Re ^{.9} Sc ^{.33}	13

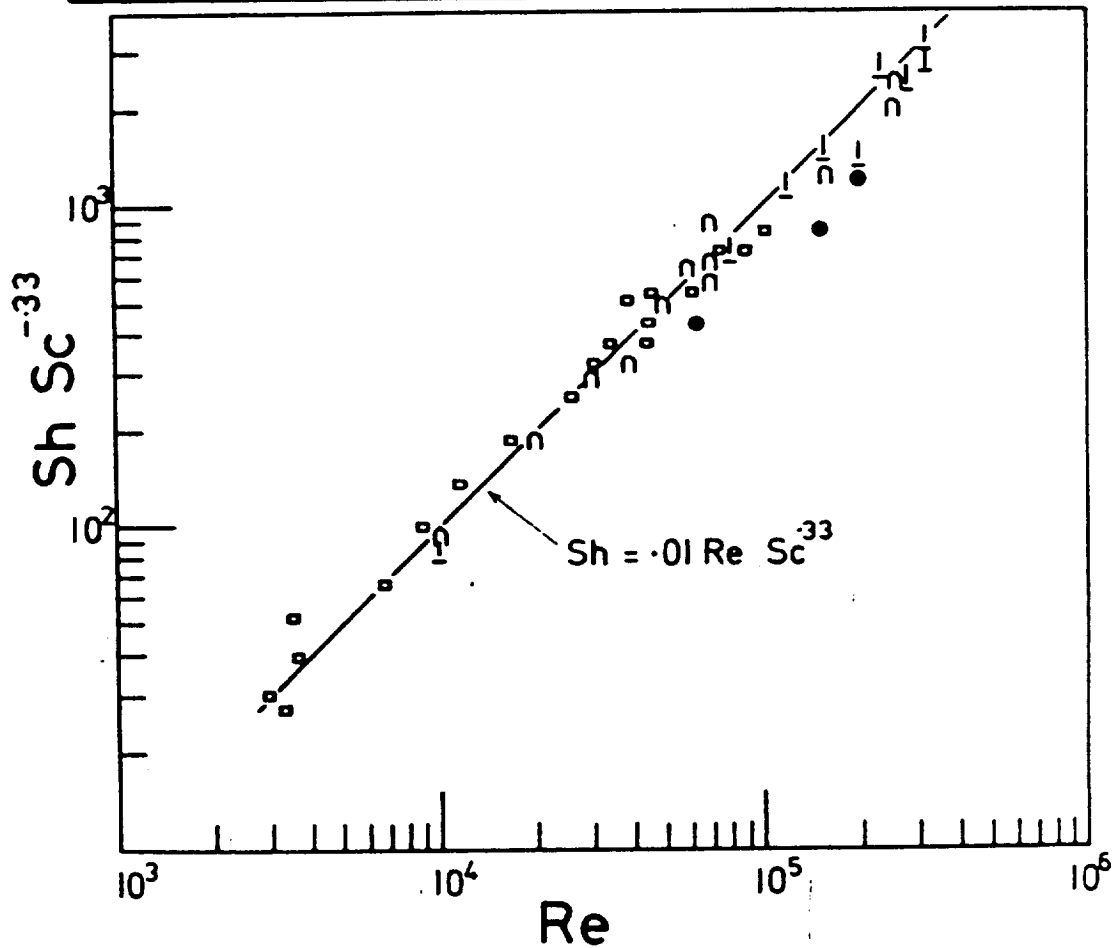


FIG 1 MASS TRANSFER FROM ROUGH SURFACES

3.2 Galvanic Corrosion

Definition

Galvanic corrosion is the corrosion associated with the current of a galvanic cell made up of dissimilar electrodes (Uhlig, 1948).

Failure Mechanism

The fundamental behavior of galvanic corrosion follows the behavior of a dry cell. The relationship between the current flow in a dry cell and the weight of material corroded is given by Faraday's law:

$$W = k I t$$

where: W = weight of metal reacting

k = electrochemical equivalent

I = current in amperes

t = time in seconds

It is important to distinguish between the open-circuit potential of a system and the corrosion potential of a system. The corrosion potential of the system is not the open-circuit potential of the system since the electrode reactions going on are continuously dissipating energy.

In determining the galvanic corrosion, the initial step is the establishment of the corrosion potential, f_{corros} . The potential difference of the polarized electrodes, f , is given by (Uhlig 1971):

$$\psi = I_1(\bar{R}_e + \bar{R}_m)$$

where: ϕ = potential difference

I_1 = current

R_e = electrolytic resistance

R_m = external metal resistance

On short circuit, the current becomes the maximum current, I_{MAX} , and R_M can be neglected, resulting in the potential difference being (Uhlig, 1971) :

$$\phi = I_{MAX} R_e$$

The measured potential of a corroding metal is the corrosion potential, f_{corros} . The value of the maximum current, I_{MAX} , is known as the corrosion current, I_{corros} . The corrosion rate of the anodic areas on a metal surface is related to I_{corros} by Faraday's Law (Uhlig, 1971). By applying Faraday's Law, the corrosion rate per unit area can be expressed as a current density.

The potential of the system changes as the reaction progresses, resulting from net current to or from the electrode, and this process is referred to as polarization. The result is the system potential does not remain constant, resulting in variable current density. The are three causes of polarization (Uhlig, 1971):

1. Concentration Polarization

Concentration polarization occurs when, as a result of the current flow, material is deposited on the electrode, decreasing the surface concentration of ions. Infinite concentration polarization is approached when the concentration of ions on the surface approaches zero. The corresponding current density is referred to the limiting current density. For conditions where concentration polarization is present, the difference in the material potentials is given by;

$$\phi_2 - \phi_1 = -\frac{RT}{nF} \ln \frac{i_L}{i_L - i}$$

where: $\phi_2 - \phi_1 =$ difference ϵ potentials

$R =$ gas constant (8.314 J / deg - mole)

$T =$ absolute temperature

$F =$ Faraday = 96500 C / eq

$n =$ number of electrons involved in the reaction

$i_L =$ limiting current density

$i =$ applied current density

The limiting current density (A/cm²) can be determined from:

$$i_L = \frac{DnF}{\delta} c \times 10^{-3}$$

where: $D =$ diffusion coefficient for reduced ion

$\delta =$ thickness of the stagnant layer of electrolyte on electrode surface

$t =$ transference number of all ions in solution except reduced ion

$c =$ concentration of diffusing ion (moles / liter)

For all ions at 25°C, with the exception of H and OH, D averages about 1×10^{-5} cm²/sec, and the limiting current density can be approximated by:

$$i_L = 0.02 \text{ nc.}$$

2. Activation Polarization

In this case, the polarization is the result of a slow electrode reaction; or equivalently, the electrode requires an activation energy in order to proceed (Uhlig, 1971). The activation polarization, h , increases with the current density according to:

$$\eta = \beta \log \frac{i}{i_o}$$

Note that both β and i_o are constant for each metal and environment, and are temperature dependent. The exchange current, i_o , is the current density equivalent to the equal forward and reverse reactions at the electrode at equilibrium (Uhlig, 1971).

3. IR Drop

The polarization includes a drop in the potential for the electrolyte surrounding the electrode.

Calculation of Corrosion Rates

In determining the corrosion rate, the anode-cathode area ratio must first be considered. If A_a is the fraction of the surface that is anode, and A_c is the fraction that is cathode, such that $A_a + A_c = 1$, then:

$$\phi_{c'} = \phi_c - \beta_c \log \frac{I_c}{A_c i_{oc}}$$

$$\phi_{a'} = \phi_a + \beta_a \log \frac{I_a}{A_a i_{oc}}$$

where: $\phi_{c'}$ = polarized potential - cathode

$\phi_{a'}$ = polarized potential - anode

ϕ_c = open - circuit potential - cathode

ϕ_a = open - circuit potential - anode

β_c = Tafel slope - cathode

β_a = Tafel slope - anode

I = current per unit metal surface area

When the system is in steady state, $f_c = f_a = f_{corros}$, and $I_a = I_c = I_{corros}$, then the maximum corrosion current occurs when:

$$\beta_c(1 - A_c) - \beta_a A_c = 0$$

$$\text{or } A_c = \frac{\beta_c}{(\beta_c + \beta_a)}$$

If $\beta_c = \beta_a$, then the maximum corrosion rate occurs when $A_c = A_a = 0.5$.

In estimating the corrosion current, if the solution is a deaerated acid, then the following relationship is a useful approximation:

$$\phi_{corros} = - \left[0.059 \text{ pH} + \beta \log \frac{i_{corros}}{i_o} \right]$$

Alternatively, Stern and Geary (1958), derived the following relationship:

$$I_{corros} = \frac{I_{applied}}{2.3 \Delta \phi} \left(\frac{\beta_c \beta_a}{\beta_c + \beta_a} \right)$$

where: β_a = Tafel constant for anodic reaction

β_c = Tafel constant for cathodic reaction

$\frac{i_{applied}}{\Delta \phi}$ = polarization slope in region near corrosion potential

Once the corrosion current has been determined, the corrosion rate can be found using Faraday's Law.

References

Bockris, J., et al. ed., Comprehensive Treatise of Electrochemistry: Volume 4 Electrochemical Materials Science, Plenum Press, New York, 1981.

Makrides, A.C., and N. Hackerman, Dissolution of Metals in Aqueous Acid Solutions, Journal of the Electrochemical Society, Vol. 105, no. 3, pp. 612-634, 1991.

Stern, M., and A. Geary, Journal of the Electrochemical Society, Vol. 104, No. 56, 1958.

Uhlig, H., The Corrosion Handbook, J. Wiley & Sons, New York, 1948.

Uhlig, H., Corrosion and Corrosion Control, Second Edition, J. Wiley & Sons, New York, 1971.

3.3 Uniform Attack

Definition

Uniform attack is the destruction of a material as a result of an electrochemical reaction with its environment, where the rate of corrosion is constant over the material surface.

Failure Mechanism

No empirical relationship exists to predict the rate of uniform attack of a material. Typically, materials are arranged into 3 categories of susceptibility to uniform attack (low, moderate, high), and little predictive work has been done.

Despite the few models available for uniform attack, the application of an Arrhenius type relationship would permit the prediction of rates of corrosion at differing temperatures and corrosive environments. The use of an Arrhenius relationship assumes that the corrosion rate is constant up to a critical temperature, T^C , and increasing rates of corrosion at temperatures in excess of T^C . In addition, the Arrhenius model assumes that the material is continually exposed to the corrosive environment, with the concentration of corrosives remaining fixed. The model is then:

$$\begin{aligned} & \text{For } T < T^C \\ & ML = C = \text{Constant} \end{aligned}$$

$$\begin{aligned} & \text{For } T \leq T^C \\ & ML = Ce^{\frac{\phi}{k} \left(\frac{1}{T^C} - \frac{1}{T} \right)} \end{aligned}$$

where: ML = rate of material loss (ipy)

C = constant corrosion rate: specific to material and environment

ϕ = activation energy for corrosion (eV)

k = Boltzmann constant (0.8617×10^{-4} eV / K)

T = absolute temperature of the environment ($^{\circ}$ K)

T^C = absolute temperature - critical ($^{\circ}$ K)

The sum of the rates of material loss for each temperature exposure multiplied by the exposure duration should yield the total material loss.

References

Uhlig, H., The Corrosion Handbook, J. Wiley & Sons, New York, 1948.

Cruse et al., Space Transportation System Life Management System Development. Phase 2, SwRI Project No. 06-2924, Report No. 06-2924-1A, Southwest Research Institute, San Antonio, TX, 1989.

Cruse et al., STS Life Management System Development, SwRI Project No. 06-2148, Report No. 06-2148-1A, Southwest Research Institute, San Antonio, TX, 1988.

3.4 Pitting Corrosion

Definition

"Pitting corrosion is the local dissolution leading to the formation of cavities in passivated metals or alloys that are exposed to aqueous, nearly neutral solution containing aggressive anions", (Szklańska-Smiałowska, 1986). Pitting corrosion is characterized by the fact that pitting will be not initiated if the anodic potential is below a critical threshold value.

Failure Mechanism

Pitting corrosion is dependent on three factors:

1. The anodic potential exceeding the critical potential for pit nucleation, E_{ap} .
2. The time required to form the first pit on a passive metal exposed to a solution containing aggressive anions, referred to as the induction time for pit initiation, τ .
3. The kinetics of pit growth.

The induction time for pit initiation is inversely related to the concentration of chloride ions, Cl^- , or the potential. The induction time for pit initiation is thought to represent the time to penetrate the passive film. Studies by Nishimura and Kudo (1981) demonstrated that τ was proportional to the thickness of the passive film barrier layer.

Pit induction time is greatly affected by the concentration of chloride ions in the solution; the relationship is given by:

$$\frac{1}{\tau} = k([Cl^-] - [Cl^-]^*)$$

where: $[Cl^-]^*$ = critical Cl^- concentration (pitting if $Cl^- > [Cl^-]^*$)

Hoar and Jacob (1967) determined t for 18Cr-8Ni stainless steel. The rate of pit initiation, τ , was found to be proportional to the n^{th} power of the Cl^- concentration, for the region where n was between 2.5 to 4.5. Other researchers have determined the values of n for different materials (see attached table from Szklańska-Smiałowska, 1986).

The determination of pit growth is easy for the potentiostatic case. Szklarska-Smialowska (1986) reported that Engell and Stolica found that the rate of pit growth was:

$$i = i^* + k_1 (t - \tau)^b$$

where: i = total current

i^* = current in passive state

t = total time

τ = induction time

k_1, b are constants

If the passive state current is disregarded and the time, t , is calculated from the beginning of the pit propagation, then the relationship becomes:

$$i = k \cdot t^b$$

In this case, k is dependent on the concentration of the chloride ion, Cl^- . If the number of pits is constant over time, then $b=2$; if the number of pits increases with time, then $b=3$. The assumptions made in this model are:

1. Pits are hemispherical in shape.
2. Current density in the pits is constant; thus the pit radii should increase linearly with time.

Szklarska-Smialowska (1986) reported that Forchhammer and Engell studied the growth of the pit radius, r , and the number of pits, N , and found:

$$r = k \cdot t^{\frac{1}{3}}$$

In addition, the research found that the coefficient b , cited above, varied from 0.6 to 1.2 for austenitic stainless steels.

Godard (1960) found that the greatest pit depth, d , in aluminum was proportional to:

$$d = k \cdot t^{\frac{1}{3}}$$

The results of numerous studies found that the relationship proposed for pit growth is not applicable in all situations. This led Szklarska-Smialowska to propose three models:

Case 1 Hemispherical Pit Model ($r=h$)

$$i = \frac{r^3}{t} N$$

Case 2 Cap Shaped Pit Model ($r>h$)

$$i \equiv \frac{h^2 R(3 - \alpha)}{t} N$$

Case 3 Cylinder Shaped Pit Model ($r<h$)

$$i = \frac{r^2 h}{t} N$$

Order of Reaction Values, n.

(From Szklarska-Smialowska, Z., Pitting Corrosion of Metals, p. 110, 1986)

Order of Reaction (n) with Respect to the Aggressive Anion for Different Materials at 25 C

Metal or Alloy	Aggressive Anion	pH	n	Potential	Reference No.
Al 1199	low Cl ⁻ conc.	0.0	11.1	0.18 V _{SCE}	23
	higher Cl ⁻ conc.		4.0		
Al 2024 (99.99% Al)	0.004-0.01M Cl ⁻	0.0	3.0	0.18 V _{SCE}	23
	0.003-0.004M Cl ⁻ (in H ₂ SO ₄)	0.0	8.8		
		3.5	4.8		
Pure, preanodized Al	0.01-1M KCl	6.1	0.1		24
	1-3M KCl	5.9-	0.9		
Al alloy 7075	Cl ⁻	0.3	8	0.18 V _{SCE}	25
	Br ⁻	0.3	4		
	I ⁻	0.3	2		
	F ⁻	5.8	3		
	Cl ⁻	5.8	2		
Al 1199	Cl ⁻	3.56	1.5	0.6 V _{Hg/Hg₂SO₄}	26
	Br ⁻	3.56	2.5		
18Cr-8Ni stainless	Cl ⁻	2.0	2.5-4.5	0.4-0.8 V _{SHE}	12
Iron	10 ⁻³ M Cl ⁻ in H ₂ SO ₄	0.0	3	0.85-1.75 V _{SHE}	3
Nickel	low Cl ⁻ conc.	2.0	4	0.5 V _{SCE}	14
	high Cl ⁻ conc. in H ₂ SO ₄		3		
18Cr-8Ni stainless	Cl ⁻ in H ₂ SO ₄	0.0	2.5	0.2 V _{SCE}	21
			4.5-5	0.6 V _{SCE}	

References

Godard, H.P., *Pitting Kinetics*, Canadian Journal of Chemical Engineering, Vol. 38, p. 167, 1960.

Nishimura, R., and K. Kudo, *Effect of Thickness and Composition of Films on the Breakdown of Passivity of Iron*, Proceedings of the 8th International Congress on Metal Corrosion, Mainz, DECHEMA, Frankfurt am Main, Vol. 1, p.6, 1981.

Szklarska-Smialowska, Z., Pitting Corrosion of Metals, NACE, Houston, TX, 1986.

3.5 Cavitation

Definition

Cavitation is a dynamic phenomena that is concerned with the growth and collapse of cavities in a liquid. Cavitation is a liquid phenomena that is the result of pressure reductions in the liquid.

It is important to note that:

1. cavitation can occur in liquids in motion or at rest.
2. cavitation is not restricted to or excluded from occurring at solid boundaries.

Failure Mechanism

At this time no comprehensive model that adequately predicts the behavior of cavitation erosion is available. Existing models of cavitation erosion have focussed on extremely simplified cases involving the collapse of single cavities on a solid surface. The agreement between such models and experimentally observed results varies. This being the case, the best guide to the designer is the avoidance of situations where cavitation can occur.

The cavitation number, σ , is a useful parameter for categorizing cavitating flows and is defined as (Knapp, 1970):

$$\sigma \equiv \frac{P_{\infty} - P_V}{0.5 \rho V_{\infty}^2}$$

where: P_{∞} = absolute pressure at some reference locality

P_V = vapor pressure (at liquid bulk temperature)

V_{∞} = reference velocity

ρ = liquid density

If the value of σ is large, then no cavitation will occur, while if σ is sufficiently small then cavitation behavior will be well developed. Limited cavitation will occur when the cavitation number is of some intermediate value. This is exhibited by a few bubbles in the flow. The limited cavitation number which describes this state is:

$$\sigma_L \equiv \frac{P_{\infty L} - P_V}{0.5 \rho V_{\infty}^2}$$

Here, $P_{\infty L}$ is the absolute pressure at the reference locality that corresponds to the state of limited cavitation.

The determination of the nature of cavitation has been studied with two different approaches:

1. *Desinent Cavitation*

In this case cavitation is established while holding the velocity constant, and then increasing the pressure until the cavitation disappears at a pressure value, referred to as the desinence pressure, $P_{\infty D}$. The desinent cavitation number is determined from the same relation as that above, with the exception that P_{∞} is replaced by $P_{\infty D}$.

2. *Incipient Cavitation*

In this case velocity is held constant, eliminating all cavitation, and then the pressure is decreased until cavitation appears at the inception pressure, $P_{\infty I}$. The incipient cavitation number is determined by replacing P_{∞} by $P_{\infty I}$ and applying the above relationships.

References

Holl, J.W., *Limited Cavitation*, Proceedings of the ASME Fluids Engineering and Applied Mechanics Conference, Northwestern University, Evanston, IL, June 16-18, 1969.

Knapp, R.T., J.W. Daily, and F.D. Hammit, Cavitation, McGraw-Hill Book Co., New York, 1970.

3.6 Crevice Corrosion

Definition

"Crevice corrosion occurs when two or more surfaces in close proximity lead to the creation of a locally occluded region where enhanced dissolution can occur", (Sharland, 1992). The rate of crevice corrosion is usually a function of the depth and width of the crevice. The distinction between crevice corrosion and pitting is that crevice corrosion proceeds at a much faster rate than pitting. This more rapid corrosion rate is a result of the restrictive crevice geometry which permits the crevice electrolytic solution to under change much more rapidly than a pit.

Failure Mechanism

The complex nature of crevice corrosion has made prediction of crevice corrosion rates difficult. At present, no accurate deterministic model of crevice corrosion exists. The current approach favored for the evaluation of crevice corrosion is the application of finite element methods. A number of packaged computer programs are available to predict crevice corrosion based on finite element methods, including:

CHEQMATE-CHEMICAL EQUILIBRIUM WITH MIGRATION AND TRANSPORT EQUATIONS developed by A. Haworth, S.M. Sharland, P.W. Tasker, and C.J. Tweed outlined in Harwell Laboratory Report, NSS-R113, 1988.

HARWELL-presented by C.P. Jackson, *The TSGL Finite-Element Subroutine Library*, AERE Report AERE-R10713, 1982.

Governing Equations

The transportation of aqueous species i is governed by the mass-balance equation. The mass-balance equation describes the diffusion under concentration gradients, electromigration under potential gradients, and chemical reaction', (Sharland, 1989). The mass-balance equation is:

$$\frac{\partial C_i}{\partial t} = D_i \Delta^2 C_i + z_i U_i F \Delta(C_i \Delta \phi) + R_i$$

where: C_i = concentration of species i

D_i = effective diffusion coefficient

z_i = charge number

R_i = rate of production / depletion of species i by chemical reaction

$$U_i = \text{mobility} = \frac{D_i}{RT}$$

For a crevice geometry that is assumed to be rectangular, the steady-state transport equations for species i is:

$$D_i \left(\frac{\partial^2 C_i}{\partial x^2} + \frac{\partial^2 C_i}{\partial y^2} \right) + \frac{z_i D_i F}{RT} \left[\frac{\partial}{\partial x} \left(C_i \frac{\partial \phi}{\partial x} \right) + \frac{\partial}{\partial y} \left(C_i \frac{\partial \phi}{\partial y} \right) \right] + R_i = 0$$

The boundary conditions are usually then determined.

References

- Sharland, S.M., and P.W. Tasker, *A Mathematical Model of Crevice and Pitting Corrosion-1. The Physical Model*, Corrosion Science, Vol. 28, no. 6, pp. 603-620, 1988.
- Sharland, S.M., and P.W. Tasker, *A Mathematical Model of Crevice and Pitting Corrosion-1. The Mathematical Solution*, Corrosion Science, Vol. 28, no. 6, pp. 621-630, 1988.
- Sharland, S.M., C.P. Jackson, and A.J. Diver, *A Finite-Element Model of the Propagation of Corrosion Crevices and Pits*, Corrosion Science, Vol. 29, no. 9, pp. 1149-1166, 1989.
- Sharland, S.M., *A Mathematical Model of the Initiation of Crevice Corrosion in Metals*, Corrosion Science, Vol. 33, no. 2, pp. 183-201, 1992.

Walton, J.C., *Mathematical Modeling of Mass Transport and Chemical Reaction in Crevice and Pitting Corrosion*, Corrosion Science, Vol. 30, no. 8/9, pp. 915-928, 1990.

Watson, M.K., and J. Postlethwaite, *Numerical Simulation of Crevice Corrosion: The Effect of the Crevice Gap Profile*, Corrosion Science, Vol. 32, no. 11, pp. 1253-1262, 1991.

Watson, M.K., and J. Postlethwaite, *Numerical Simulation of Crevice Corrosion of Stainless Steel and Nickel Alloys in Chloride Solutions*, Corrosion Science, Vol. 46, no. 7, pp. 522-530, 1990.

4. Fatigue

Definition

Fatigue failure is a general term given to the sudden and catastrophic separation of a machine part into two or more pieces as a result of the application of fluctuating loads or deformations over a period of time.

The major forms of fatigue are:

1. High-cycle fatigue
2. Low-cycle fatigue
3. Crack growth
4. Surface fatigue

Of the various types of fatigue, high-cycle fatigue, low-cycle fatigue, and crack growth.

Physical Process of Fatigue

The fatigue process consists of three stages:

1. Crack initiation phase
2. Subcritical crack propagation
3. Final fracture

Of these stages, most designers are concerned with crack initiation and subcritical crack propagation.

Probability models of fatigue life

Because many of the factors involved are random in nature, the appropriate development of analysis and design methodologies should be probabilistic. Two distributions that have been widely used in fatigue studies are the lognormal and Weibull distributions. Use of the lognormal distribution has been based primarily on arguments of mathematical expediency. However, it has been pointed out that the hazard function for the lognormal model decreases for large values of N . This does not agree with our physical understanding of progressive deterioration resulting from the fatigue process. Nevertheless, the lognormal distribution often seems to provide a "good fit" of cycles to failure data. The Weibull distribution is based on more physical convincing arguments. Moreover, the Weibull distribution is well-suited for certain procedures of statistical extrapolation to large systems.

4.1 High-Cycle Fatigue

Definition

High-cycle fatigue is associated with lower stress levels and high numbers of cycles to produce fatigue failure. It is typically associated with cycle lives greater than about 10^4 or 10^5 cycles.

Failure Mechanism

The crack initiation period consumes a substantial percentage of the usable fatigue life in high-cycle fatigue problems where stress fluctuations are low at fatigue-critical locations. The crack propagation period is very short compared with the crack growth period.

The classical model (The Basquin Equation):

$$N S^m = C$$

where:

S = stress amplitude, or stress range.

M, C = empirically determined constants which depend on the material and are significantly affected by the environment

N = fatigue life, cycles to failure.

References

Fatigue Reliability: Introduction, ASCE, Vol. 108, No. ST1, January 1982.

Collins, J.A., Failure of Materials in Mechanical Design, J. Wiley & Sons, New York, 1993.

Freudenthal, A., Reliability Analysis Based on Time to the First Failure, Pergamon Press, London, 1972.

4.2 Low-Cycle Fatigue

Definition

Low-cycle fatigue is associated with high stress levels and low number of cycles to produce fatigue failure. It is typically associated with cycle lives from one up to about 10^4 or 10^5 cycles.

Failure Mechanism

When stress fluctuations are high, fatigue cracks initiate quite early and a significant portion of the service life of the component may be spent propagating the crack to critical size. The two phases are of roughly equal importance, in terms of order of magnitude, in low cycle fatigue.

The general model

$$\epsilon_a = \frac{\sigma_{f'}}{E} (2N)^b + \epsilon_{f'} (2N)^c$$

where:

- ϵ_a = strain amplitude.
- E = modulus of elasticity.
- $\sigma_{f'}$ = fatigue strength coefficient.
- b = fatigue strength exponent.
- $\epsilon_{f'}$ = fatigue ductility coefficient.
- c = fatigue ductility exponent.

This model considers elastic strain and plastic strain life separately. The total strain life is the summation of the two.

Langer (1962) proposed an simple model for the LCF life. The model is,

$$S = \frac{E}{4\sqrt{N}} \ln\left(\frac{100}{100 - RA}\right) + S_e$$

where: $S = \frac{1}{2} E \epsilon_f$

E = modulus of elasticity

N = number of cycles to failure

RA = percent reduction in area of tensile test

S_e = endurance limit

Langer suggest assuming a RA value of 50% which is the minimum specified value. Using this RA value and rearranging the equation, we can determine the following relationship for the number of cycles to failure:

$$N = \left(\frac{0.1732868E + S_e}{S}\right)^2$$

References

Collins, J.A., Failure of Materials in Mechanical Design, J. Wiley & Sons, New York, 1993.

Langer, B.F., Design of Pressure Vessels for Low-Cycle Fatigue, Journal of Basic Engineering, ASME, Vol. 84, No. 3, Sept. 1962.

Manson, S.S., and M.H. Hirschberg, Fatigue: An Interdisciplinary Approach, Syracuse University Press, Syracuse, NY, 1964.

Low-Cycle Fatigue, H. D. Solomon et al. eds., ASTM Special Technical Publication 942, ASTM, Philadelphia, PA, 1988.

4.3 Crack growth fatigue

Failure Mechanism

The crack growth rate is given by:

$$\frac{da}{dN} = C(\Delta K)^n$$

$$K = F(a)S\sqrt{\pi a}$$

where:

a = crack depth for a surface flaw or half-width for a penetration flaw.

F(a) = finite geometry correction factor which may depend on a.

K = stress intensity factor.

S = applied stress.

n, c = experimentally determined constants which depend on the mean cycling stress.

Reference

Collins, J.A., Failure of Materials in Mechanical Design, J. Wiley & Sons, New York, 1993.

5. Thermal Degradation

Definition

Thermal degradation is the deterioration of the functionality or physical properties of a material due to the effects of temperature. The degradation is due solely to the effects of temperature and does not involve other materials.

Failure Mechanism

The interest in thermal degradation lies in materials that are non-metallic, since thermal influences on metals can result in changes in the grain structure. The material properties of metals possessing different grain structures is well documented. As a result, this examination of thermal degradation will focus primarily on polymers and insulating materials.

In the case of polymers, the two main types of degradation are (Grassie, 1985) :

1. Depolymerisation, which is the breaking of the main polymer chain backbone so that at any intermediate stage the products are similar to the parent material in that the monomer units remain distinguishable. The products of the degradation may be monomer, or they may be volatile chain fragments.
2. Substituent reactions result in the attachment of substituents to the backbone of the polymer molecules involved so that the chemical nature of the repeat unit is changed even though the chain structure may remain intact.

In the case of polystyrene, if the chain scission occurs in a polymer molecule without volatilisation, then (Grassie, 1985):

$$P_t = \frac{P_o}{(s + 1)}$$

where: P_o = initial chain length of the polymer

P_t = chain length of the polymer after time t

s = average number of scissions per molecule

From this equation the fraction of broken bonds, α , can be found. If the chain scission is random then $\alpha=kt$ where k =rate constant for chain scission. If the chain contains weak and strong links, then $\alpha=\beta+kt$, where β is the fraction of weak links in the molecule.

In practice the approach is to determine the lifetime of polymers using approaches based on Arrhenius equations. Burnay (1990) reports that a relationship that accounts for both thermal and radiation degradation on polymers is:

$$a(T,D) = \exp\left[-\frac{E}{R} \left(\frac{1}{T_{ref}} - \frac{1}{T}\right)\right] \left[1 + k \exp\left(\frac{Ex}{R} \left(\frac{1}{T_{ref}} - \frac{1}{T}\right)\right) D^x\right]$$

where: E = activation energy

R = gas constant

T = absolute temperature polymer environment

T_{ref} = reference temperature

k = radiation degradation reaction constant

D = dose rate

Note that E , k , and x are empirical constants. The parameter E can be determined from the polymer where radiation is not a problem. Thus, k and x are empirically determined from irradiation data. Burnay further reports that the majority of polymers studied have been found to have $x=1$. For cases where $x=1$, the above relation is simply:

$$a(T,D) = \exp\left[-\frac{E}{R} \left(\frac{1}{T_{ref}} - \frac{1}{T}\right)\right] + kD$$

This relationship is simply the sum of the thermal degradation described by the Arrhenius relationship plus a dose rate component, D , multiplied by a radiation degradation reaction constant, k . In cases where radiation is not significant, the relationship for simple thermal degradation results.

Note that the parameter, $a(T,D)$, is used as the constant deterioration rate in the Arrhenius equation. By using the above relationships to determine the modified the deterioration rate constant, the Arrhenius equation can consider the effects temperature and radiation on polymer degradation.

References

Burnay, S.G., *A Practical Model for Prediction of the Lifetime of Elastomeric Seals in Nuclear Environments*, Proceedings from 200th National Meeting of the American Chemical Society, Washington, August 26-31, 1990 (Published in Radiation Effects on Polymers, ACS Symposium Series #475)

Grassie, N., and G. Scott, Polymer Degradation and Stabilization, Cambridge University Press, Cambridge, U.K., 1985.

Schnabel, W., Polymer Degradation, Macmillan Publishing Co., New York, 1981.

Troitskii, B.B. and L.S. Troitskaya, *Mathematical Models of the Initial Stage of the Thermal Degradation of Poly (Vinyl Chloride)*, Journal of Polymer Science: Part A: Polymer Chemistry, Vol. 28, pp. 2695-2709, 1990.

Proceedings from 200th National Meeting of the American Chemical Society, Washington, August 26-31, 1990.

APPENDIX B

**MECHANICAL LIMIT STATES
USED
IN
FIRST-ORDER RELIABILITY MODELS**

Six mechanical limit states were analysed and compare using both Monte Carlo simulation and first-order reliability methods. The six limit states examined were:

1. Pitting
2. Low-cycle fatigue
3. Fretting
4. Erosion-corrosion
5. Wear
6. Galvanic-corrosion.

The precise form of the performance function used for each of these limit states is given below.

Pitting

The limit state for pitting is:

$$g(\bar{D}) = D_{allow} - D_{actual}$$

where: D_{allow} = maximum allowable pit depth

D_{actual} = actual pit depth

The actual pit depth is determined as:

$$D_{actual} = K \cdot T^{0.33}$$

where: K = constant dependent on
concentration of chloride ion

T = time in months

Low-Cycle Fatigue

The limit state for low-cycle fatigue is:

$$g(\bar{N}) = -(N_{Min} - N_{Actual})$$

where: N_{Min} = minimum number of cycles
required for service

N_{Actual} = predicted number of cycles
to failure

The predicted number of cycles to failure is determined as:

$$N_{Actual} = \left(\frac{0.173268 \cdot E + S_e}{S} \right)^2$$

where: E = modulus of elasticity

S_e = endurance limit

$$S = \frac{1}{2} E \cdot \epsilon_t$$

Erosion-Corrosion

The limit state for erosion-corrosion is:

$$g(E_{allow} - E_{actual})$$

where: E_{allow} = allowable erosion

E_{actual} = actual erosion

The actual erosion is determined as:

$$E_{actual} = \frac{4}{3} \cdot \frac{M}{R_f} \cdot C \cdot X \cdot \frac{D}{d} \cdot \left(\frac{V \cdot d}{\mu} \right)^Y \cdot \left(\frac{\mu}{r \cdot D} \right)^Z$$

where: M = molar mass of iron

R_f = density of iron

C = bulk oxygen concentration

D = diffusion coefficient of transferred species

d = pipe diameter

V = mean velocity

μ = fluid viscosity

X, Y, Z = constants

Fretting

The limit state for fretting is:

$$g(\bar{W}) = W_{allow} - W_{actual}$$

where: W_{allow} = maximum allowable wear

W_{actual} = actual wear

The actual wear is determined as:

$$W_{actual} = \frac{(k_0 \cdot P^{0.5} - k_1 \cdot P)N}{f} + k_2 \cdot l \cdot P \cdot N$$

where: P = normal load (psi)

N = total number of cycles

f = cycles per second

k_0 = constant

k_1 = constant

k_2 = constant

Galvanic Corrosion

The limit state for galvanic corrosion is:

$$g(\bar{W}) = W_{allow} - W_{actual}$$

where: W_{allow} = allowable galvanic corrosion

W_{actual} = actual galvanic corrosion

The actual galvanic corrosion is determined as:

$$W_{actual} = \frac{t \cdot M \cdot I}{F \cdot n}$$

where: t = time in seconds

M = atomic weight of anode metal

I = galvanic current in amperes

F = Faraday's constant (96,501 coulombs)

n = charge of metal ions formed

REFERENCES

- 1 Khintchine, A. Ya., "Mathematisches uber die Erwartung von einen offentlicher Schalter", Matemalliche Sbornik, 1932, quoted by R.E. Barlow and F. Proschan, Mathematical Theory of Reliability, J. Wiley and Sons, New York, 1965, p.1.
- 2 Palm, C., "Arbetskraftens Fordelning vid betjaning av automatskiner", Industritidningen Norden, 1947, p.75, quoted by R.E. Barlow and F. Proschan, Mathematical Theory of Reliability, J. Wiley and Sons, New York, 1965, p.1.
- 3 Lotka, A.J., "A Contribution to the Theory of Self-Renewing Aggregates with Special Reference to Industrial Replacement", Annual of Mathematical Statistics, V. 10, 1939, pp.1-25.
- 4 Campbell, N.R., "The Replacement of Perishable Members of a Continually Operating System", Journal of the Royal Statistical Society, V. 7, 1941, pp. 110-130.
- 5 Feller, W., "On the Integral Equation of Renewal Theory", Annual of Mathematical Statistics, V. 12, 1941, pp. 243-267.
- 6 Weibull, W., "A Statistical Theory of the Strength of Materials", Proceedings, Royal Swedish Institute of Engineering Research, Stockholm, Sweden, No. 151, 1939.
- 7 Weibull, W., "The Phenomenon of Rupture in Solids", Proceedings, Royal Swedish Institute of Engineering Research, Stockholm, Sweden, No. 153, 1939.
- 8 Gumbel, E.J., "Les Valeurs Extremes des Distributions Statistiques", Annales de l'Institute Henri Poincare, V. 4, Fasc. 2, 1935, p.115.
- 9 Rao, S.S., Reliability-Based Design, McGraw-Hill, New York, 1992, p. 15.
- 10 Rao, S.S., Reliability-Based Design, McGraw-Hill, New York, 1992, p. 15.
- 11 Rao, S.S., Reliability-Based Design, McGraw-Hill, New York, 1992, p.16.
- 12 Rao, S.S., Reliability-Based Design, McGraw-Hill, New York, 1992, p.16.
- 13 Rao, S.S., Reliability-Based Design, McGraw-Hill, New York, 1992, p.16.
- 14 Handbook of Reliability Prediction Procedures for Mechanical Equipment, CARDEROCKDIV, NSWC-92/L01, Carderock Division, Naval Surface Warfare Center, Bethesda, MD, 1992.
- 15 Madsen, H.O., S. Krenk, and N.C. Lind, Methods of Structural Safety, Prentice-Hall, Englewood Cliffs, NJ, 1986, p. 2.

- 16 Madsen, H.O., S. Krenk, and N.C. Lind, Methods of Structural Safety, Prentice-Hall, Englewood Cliffs, NJ, 1986, p. 3.
- 17 Cornell, C.A., "Bounds on the Reliability of Structural Systems", Journal of the Structural Division, ASCE, V. 93, 1967, pp.171-200.
- 18 Lind, N.C., "The Design of Structural Design Norms", Journal of Structural Mechanics, V. 1, No. 3, 1973, pp. 357-370.
- 19 Ditlevsen, O., "Structural Reliability and the Invariance Problem", Research Report No. 22, Solid Mechanics Division, University of Waterloo, Waterloo, Canada, 1973.
- 20 Lind, N.C., "The Design of Structural Design Norms", Journal of Structural Mechanics, V. 1, No. 3, 1973, pp. 357-370.
- 21 Hasofer, A.M., and N.C. Lind, "Exact and Invariant Second Moment Code Format", Journal of the Engineering Mechanics Division, ASCE, V. 100, 1974, pp. 111-121.
- 22 Rackwitz, R., and B. Fiessler, "Structural Reliability Under Combined Random Load Sequences", Computers and Structures, V. 9, 1978, pp. 489-494.
- 23 Ditlevsen, O., "Narrow Reliability Bounds for Structural Systems", Journal of Structural Mechanics, B. 7(4), 1979, pp. 453-472.
- 24 Cruse, T.C., Q. Huang, S. Mehta, and S. Mahadevan, "System Reliability and Risk Assessment", Paper No. AIAA-92-2345, Proceedings of the 33rd Structures, Structural Dynamics and Materials Conference, Dallas, Texas, 1992, pp. 424-432.
- 25 Boothroyd, G., and P. Dewhurst, Design for Assembly, University of Massachusetts, Department of Mechanical Engineering, Amherst, MA, 1983.
- 26 Miyakawa, S., and T. Ohashi, "The Hitachi Assemblability Evaluation Method (AEM)", Proceedings, First International Conference on Product Design for Assembly, April 1986.
- 27 Vasilash, G.S., "Simultaneous Engineering: management's new competitiveness tool.", Production, July 1987.
- 28 Hout, T.M., and G. Stalk, jr., Competing Against Time:How Timebased Competition is Reshaping Global Markets, Free Press, NY, 1990.
- 29 Sakurai, M., "Target Costing and How to Use It", Journal of Cost Management, Summer 1989, pp. 39-50.

- 30 Vinogradov, O., Introduction to Mechanical Reliability: A Designer's Approach, Hemisphere Publishing Corporation, New York, 1991, p. 102.
- 31 Kapur, K.C., and L.R. Lamberson, Reliability in Engineering Design, John Wiley & Sons, New York, 1977, p.12.
- 32 Hogg, R.V., and A.T. Craig, Introduction to Mathematical Statistics, Macmillan Publishing, New York, 1978, p.49.
- 33 Hogg, R.V., and A.T. Craig, Introduction to Mathematical Statistics, Macmillan Publishing, New York, 1978, p. 80.
- 34 Hogg, R.V., and A.T. Craig, Introduction to Mathematical Statistics, Macmillan Publishing, New York, 1978, p. 73.
- 35 Hogg, R.V., and A.T. Craig, Introduction to Mathematical Statistics, Macmillan Publishing, New York, 1978, p.73.
- 36 Kapur, K.C., and L.R. Lamberson, Reliability in Engineering Design, John Wiley & Sons, New York, 1977, p.216.
- 37 Kapur, K.C., and L.R. Lamberson, Reliability in Engineering Design, John Wiley & Sons, New York, 1977, pp. 213-213.
- 38 Kapur, K.C., and L.R. Lamberson, Reliability in Engineering Design, John Wiley & Sons, New York, 1977, p. 15.
- 39 Kapur, K.C., and L.R. Lamberson, Reliability in Engineering Design, John Wiley & Sons, New York, 1977, pp. 233-237.
- 40 Melchers, R.E., Structural Reliability: Analysis and Prediction, Ellis Horwood Ltd., West Sussex, England, 1987, pp. 108-112.
- 41 Rackwitz, R., and B. Fiessler, "Structural Reliability Under Combined Random Load Sequences", Computers and Structures, Vol. 9, pp. 489-494, 1978.
- 42 Madsen, H.O., S. Krenk, and N.C. Lind, Methods of Structural Safety, Prentice-Hall, Englewood Cliffs, New Jersey, 1986, pp.120-121.
- 43 Kapur, K.C., and L.R. Lamberson, Reliability in Engineering Design, John Wiley & Sons, New York, 1977, p.10.
- 44 Wu, Y.-T., Fast Probability Integration :Theoretical Manual, FPI Version 4.2, Southwest Research Institute, San Antonio, 1989, p. 36.

- 45 Wu, Y.-T., Fast Probability Integration :Theoretical Manual, FPI Version 4.2, Southwest Research Institute, San Antonio, 1989, p. 36.
- 46 NESSUS/FPI User's Manual, Version 1.0, Southwest Research Institute, San Antonio, TX, 1991.
- 47 Ang, A. H-S., and W.H. Tang, Probability Concepts in Engineering Planning and Design: Volume1-Basic Principles, J. Wiley, New York, 1975, pp. 277-279.
- 48 Handbook of Reliability Prediction Procedures for Mechanical Equipment, CARDEROCKDIV, NSWC-92/L01, Carderock Division, Naval Surface Warfare Center, Bethesda, MD, 1992.
- 49 Kapur, K.C., and L.R. Lamberson, Reliability in Engineering Design John Wiley & Sons, New York, 1977, p.234.
- 50 Handbook of Reliability Prediction Procedures for Mechanical Equipment, CARDEROCKDIV, NSWC-92/L01, Carderock Division, Naval Surface Warfare Center, Bethesda, MD, 1992, p. 44.
- 51 Handbook of Reliability Prediction Procedures for Mechanical Equipment, CARDEROCKDIV, NSWC-92/L01, Carderock Division, Naval Surface Warfare Center, Bethesda, MD, 1992, p.44.
- 52 Handbook of Reliability Prediction Procedures for Mechanical Equipment, CARDEROCKDIV, NSWC-92/L01, Carderock Division, Naval Surface Warfare Center, Bethesda, MD, 1992, p.44.
- 53 McClintock, F.A., and A.S. Argon, eds., Mechanical Behavior of Materials, Addison-Wesley Publishing Co., Reading, MA, 1966, p. 587.
- 54 Ang, A. H-S., and W.H. Tang, Probability Concepts in Engineering Planning and Design: Volume1-Basic Principles, J. Wiley, New York, 1975, pp. 196-201.
- 55 Handbook of Reliability Prediction Procedures for Mechanical Equipment, CARDEROCKDIV, NSWC-92/L01, Carderock Division, Naval Surface Warfare Center, Bethesda, MD, 1992, pp. 44-45.
- 56 Handbook of Reliability Prediction Procedures for Mechanical Equipment, CARDEROCKDIV, NSWC-92/L01, Carderock Division, Naval Surface Warfare Center, Bethesda, MD, 1992, p.12.
- 57 Handbook of Reliability Prediction Procedures for Mechanical Equipment, CARDEROCKDIV, NSWC-92/L01, Carderock Division, Naval Surface Warfare Center, Bethesda, MD, 1992, p.14.

- 58 Kapur, K.C., and L.R. Lamberson, Reliability in Engineering Design, John Wiley & Sons, New York, 1977, pp. 252-254.
- 59 Boothroyd, G. and P. Dewhurst, "Design for Assembly", Mechanical Engineering, February 1988, pp. 28-31.
- 60 Sakurai, M., "Target Costing and How to Use It", Journal of Cost Management, Summer 1989, pp. 39-50.
- 61 Ulrich, K, D. Sartorius, S. Pearson, and M. Jakiels, "Including the Value of Time in Design-for-Manufacturing Decision Making", Management Science, Vol. 39, No. 4, April 1993, pp. 429-447.
- 62 Hout, T.M., and G. Stalk, jr., Competing Against Time: How Timebased Competition is Reshaping Global Markets, Free Press, NY, 1990.
- 63 Sakurai, M., "Target Costing and How to Use It", Journal of Cost Management, Summer 1989, pp. 39-50.
- 64 Monden, Y. and M. Sakuari, "Target Costing and Kaizen Costing in Japanese Automobile Companies", Journal of Management Accounting Research, No. 3, Fall 1991.
- 65 Madsen, H.O., S. Krenk, and N.C. Lind, Methods of Structural Safety, Prentice-Hall, Englewood Cliffs, NJ, 1986, p.121.
- 66 Madsen, H.O., S. Krenk, and N.C. Lind, Methods of Structural Safety, Prentice-Hall, Englewood Cliffs, NJ, 1986, p. 122.
- 67 Trucks, H.E., Designing for Economical Production, Second Edition, Society of Manufacturing Engineers, Dearborn, MI, 1987.
- 68 Machining Data Handbook, 3rd ed., Machinability Data Center, Cincinnati, OH, 1980.
- 69 Madsen, H.O., S. Krenk, and N.C. Lind, Methods of Structural Safety, Prentice-Hall, Englewood Cliffs, NJ, 1986, pp. 121-122.
- 70 Madsen, H.O., S. Krenk, and N.C. Lind, Methods of Structural Safety, Prentice-Hall, Englewood Cliffs, NJ, 1986, p. 122.
- 71 Madsen, H.O., S. Krenk, and N.C. Lind, Methods of Structural Safety, Prentice-Hall, Englewood Cliffs, NJ, 1986, p. 122.

72 Machining Data Handbook, 3rd ed., Machinability Data Center, Cincinnati, OH, 1980, pp.3-28.

REPORT DOCUMENTATION PAGE

Form Approved
OMB No. 0704-0188

Public reporting burden for this collection of information is estimated to average 1 hour per response, including the time for reviewing instructions, searching existing data sources, gathering and maintaining the data needed, and completing and reviewing the collection of information. Send comments regarding this burden estimate or any other aspect of this collection of information, including suggestions for reducing this burden, to Washington Headquarters Service, Directorate for Information Operations and Reports, 1215 Jefferson Davis Highway, Suite 1204, Arlington, VA 22202-4302, and to the Office of Management and Budget, Paperwork Reduction Project (0704-0188), Washington, DC 20503.

1. AGENCY USE ONLY (Leave blank)	2. REPORT DATE <p style="text-align: center;">April 1997</p>	3. REPORT TYPE AND DATES COVERED <p style="text-align: center;">Final Contractor Report</p>	
4. TITLE AND SUBTITLE <p style="text-align: center;">Mechanical System Reliability and Cost Integration Using a Sequential Linear Approximation Method</p>		5. FUNDING NUMBERS <p style="text-align: center;">WU-523-22-13 G-NAG3-1352</p>	
6. AUTHOR(S) <p style="text-align: center;">Michael T. Kowal</p>			
7. PERFORMING ORGANIZATION NAME(S) AND ADDRESS(ES) <p style="text-align: center;">Vanderbilt University Nashville, Tennessee 37203</p>		8. PERFORMING ORGANIZATION REPORT NUMBER <p style="text-align: center;">E-10708</p>	
9. SPONSORING/MONITORING AGENCY NAME(S) AND ADDRESS(ES) <p style="text-align: center;">National Aeronautics and Space Administration Lewis Research Center Cleveland, Ohio 44135-3191</p>		10. SPONSORING/MONITORING AGENCY REPORT NUMBER <p style="text-align: center;">NASA CR-202336</p>	
11. SUPPLEMENTARY NOTES <p>Project Manager, Christos C. Chamis, NASA Lewis Research Center, Research and Technology Directorate, organization code 5000, (216) 433-3252.</p>			
12a. DISTRIBUTION/AVAILABILITY STATEMENT <p style="text-align: center;">Unclassified - Unlimited Subject Category 39</p> <p style="text-align: center;">This publication is available from the NASA Center for Aerospace Information, (301) 621-0390.</p>		12b. DISTRIBUTION CODE	
13. ABSTRACT (<i>Maximum 200 words</i>) <p>The development of new products is dependent on product designs that incorporate high levels of reliability along with a design that meets predetermined levels of system cost. Additional constraints on the product include explicit and implicit performance requirements. Existing reliability and cost prediction methods result in no direct linkage between variables affecting these two dominant product attributes. A methodology to integrate reliability and cost estimates using a sequential linear approximation method is proposed. The sequential linear approximation method utilizes probability of failure sensitivities determined from probabilistic reliability methods as well a manufacturing cost sensitivities. The application of the sequential linear approximation method to a mechanical system is demonstrated.</p>			
14. SUBJECT TERMS <p style="text-align: center;">Mechanical system; Reliability; Primitive variables; Response surface; Failure mode; Failure mechanism; Analytical reliability modes; Physics-based failure rate reliability</p>		15. NUMBER OF PAGES <p style="text-align: center;">168</p>	
		16. PRICE CODE <p style="text-align: center;">A08</p>	
17. SECURITY CLASSIFICATION OF REPORT <p style="text-align: center;">Unclassified</p>	18. SECURITY CLASSIFICATION OF THIS PAGE <p style="text-align: center;">Unclassified</p>	19. SECURITY CLASSIFICATION OF ABSTRACT <p style="text-align: center;">Unclassified</p>	20. LIMITATION OF ABSTRACT